

Investigation of novel cooling methods to enhance aerospace component manufacturing practices

By

Devan Koen



*Thesis presented in partial fulfilment of the requirements for the degree
Master of Science in Engineering
at
Stellenbosch University*

Supervisor: Mr. Nico Treurnicht
Faculty of Engineering
Department of Industrial Engineering

December 2011

Declaration

By submitting this thesis electronically, I declare that the entirety of the work contained therein is my own, original work, that I am the sole author thereof (save to the extent explicitly otherwise stated), that reproduction and publication thereof by Stellenbosch University will not infringe any third party rights and that I have not previously in its entirety or in part submitted it for obtaining any qualification.

Signature: _____

Date: _____

Abstract

The aerospace industry actively pursues innovation, especially in materials and their use in new applications, to improve their aircraft as well as their competitive position. Ti-6Al-4V has been available now for more than 50 years. Yet, in the new generation of aircraft using structural composites, a dramatic increase in the proportion of Ti-6Al-4V will be seen along with emerging application in automotive and chemical industries. This material possesses superior material properties compared to conventional materials such as steel and aluminium, although it is at the expense of machinability. Researchers are therefore actively searching for improved cutting technologies to improve production rates for Ti-6Al-4V. At higher cutting speeds than the industry norm of 60 - 90 m/min, machining becomes a challenge, resulting in low productivity on titanium parts.

The limiting factor in the machining of Ti-6Al-4V is high tool temperatures of the order of 1000°C, caused by its resistance to absorb heat and good mechanical strength at elevated temperatures. The result is extreme temperatures that are concentrated on the cutting edge of the tool. The challenge to improve the tool life is therefore focused on removing heat from the insert. Liquid nitrogen was identified as a good candidate as coolant with the additional advantage of being environmentally friendly.

The research presented investigates the use of a gravity feed enclosed liquid nitrogen cooling system to improve the tool life of the cutting inserts. The liquid nitrogen is contained on the insert rake face by means of a tool cap. To improve the effectiveness of the cooling method, a polycrystalline diamond (PCD) insert was used. This insert has a considerably higher thermal conductivity that aids in cooling the cutting edge. Tungsten carbide inserts are used for benchmark testing.

The round tungsten carbide inserts with conventional cooling performed exceptionally well for machining titanium compared to square inserts, yielding exceptional tool life improvements while significantly increasing the material removal rate.

Positive results were recorded with the liquid nitrogen cooling system when used with the polycrystalline diamond cutting insert. A number of far reaching performance issues are identified relating to the design of the tool cap that hindered clear scientific outputs. From a research perspective, the project makes a contribution to the knowledge base in this field. Additionally a new approach in cooling was investigated, resulting in clear indications of design changes required.

Opsomming

Die lugvaart industrie streef aktief innovasie na, veral op die gebied van materiale en hul gebruike, om hul vliegtuie en kompeterende posisie in die mark te verbeter. Ti-6Al-4V is al vir meer as 50 jaar beskikbaar. 'n Drastiese verhoging in die aanvraag na Ti-6Al-4V deur die lugvaart, motor en chemiese industrieë word verwag wanneer die volgende geslag vliegtuie wat koolstofvesel as strukturele materiaal begin gebruik, in produksie gaan. Die materiaal het beter materiaaleienskappe as konvensionele materiale soos staal en aluminium, maar dit kom egter teen die prys van masjieneerbaarheid. Ti-6Al-4V se masjienering bo die industrie norm van 60 – 90m/min is 'n groot uitdaging. Navorsers soek daarom deurentyd na verbeterde sny tegnologieë om die produksie tempo van Ti-6Al-4V te verbeter.

Die beperkende faktor vir Ti-6Al-4V masjienering is die temperatuur wat genereer word. Die weerstand van die materiaal om hitte te absorbeer en sy goeie meganiese eienskappe veroorsaak dat temperature in die beitel 1000°C bereik. Hierdie temperature word egter op die snykant van die beitel gekonsentreer. Die uitdaging is dus om hierdie temperature in die beitel te beheer. Vloeibare stikstof is geïdentifiseer as 'n goeie kandidaat vir verkoeling met die bykomende voordeel dat dit omgewingsvriendelik is.

Die navorsing wat hier uiteengesit word, ondersoek die gebruik van 'n geslote kamer beitelverkoelingstelsel wat deur gravitasie met vloeibare stikstof voorsien word om die beitel leeftyd te verbeter. Die oppervlak van die beitel word in hierdie konsep direk aan die vloeibare stikstof blootgestel. Om die effektiwiteit van die stelsel te verbeter word van PCD beitels gebruik gemaak. Die beitel se verbeterde hittegeleidingsvermoë help om die beitel se snykant koel te hou. Tungstenkarbied beitels word gebruik om 'n standaard te stel vir eksperimentele analise.

Die ronde tungstenkarbied beitels en konvensionele verkoeling het verstommend goed presteer vir Ti-6Al-4V masjienering in vergelyking met vierkantige beitels. Die materiaalverwyderingstempo is aansienlik verhoog sonder om die beitel se leeftyd in te boet.

Positiewe resultate is waargeneem met die vloeibare stikstof sisteem saam met die PCD beitels. 'n Aantal verreikende uitdagings is geïdentifiseer wat suiwer wetenskaplike afleidings bemoeilik. Hierdie probleme kan almal aan die ontwerp van die toerusting toegeskryf word. Die werk lewer egter steeds 'n bydrae tot die kennis in die veld. 'n Bykomende benadering vir verkoeling is ondersoek wat duidelik ontwerp-veranderings aandui.

Table of Contents

Declaration.....	ii
Abstract	iii
Opsomming.....	iv
List of Figures	viii
List of Tables	xi
Acknowledgements	xii
Glossary	xiii
1. Introduction	1
2. Problem statement and objectives.....	2
2.1. Hypothesis	2
3. Titanium, its alloys and industry.....	2
3.1. Physical properties of titanium and its alloys.....	3
3.2. Challenges of titanium machining.....	5
3.2.1. Heat generation and distribution in cutting operations.....	6
3.2.2. Adhesion and diffusion	7
3.2.3. Flank wear.....	8
3.3. Tool materials for titanium cutting	9
3.3.1. Uncoated carbide tool inserts	9
3.3.2. Tool coatings for titanium machining.....	10
3.3.3. Cubic boron nitrate (CBN).....	10
3.3.4. Polycrystalline diamond (PCD).....	10
3.4. Tool failure.....	12
3.5. Cooling approaches.....	14
3.6. Cutting fluids.....	14

3.6.1.	Liquid Nitrogen.....	15
3.7.	Surface integrity.....	16
3.8.	Effect of tool geometry and cutting strategy on tool life.....	16
3.9.	Solutions from literature	17
3.9.1.	Hot machining of work piece	17
3.9.2.	Cooling.....	17
3.10.	Design objectives	28
4.	Design Concept.....	28
4.1.1.	Tool holder modification	29
4.1.2.	Tool Cap	30
5.	Methodology.....	32
5.1.	Research design	33
5.2.	Instrumentation	36
5.2.1.	Cutting tools.....	36
5.2.2.	Experimental set-up	37
5.2.3.	LN ₂ supply	38
5.2.4.	Connecting the Reservoir with the tool cap	39
5.2.5.	Confirmation of material properties	42
5.3.	Safety with LN ₂	42
5.4.	Analysis.....	44
5.4.1.	Analysis of wear	44
5.4.2.	Calculation formulas.....	46
6.	Results.....	47
6.1.	Pilot testing.....	47
6.2.	Tungsten Carbide with Conventional Cooling	47
6.3.	PCD inserts with conventional cooling.....	52

6.4.	PCD insert with liquid nitrogen (LN ₂) cooling	58
7.	Discussion of results	62
7.1.	Tool life reporting and productivity	62
7.2.	Insert geometry and tungsten carbide tool discussion	64
7.3.	Polycrystalline diamond (PCD) insert performance	70
7.3.1.	PCD with soluble oil cooling.....	70
7.3.2.	PCD inserts with Liquid nitrogen (LN ₂) cap cooling	74
7.3.3.	Tool cap performance analysis.....	77
8.	Additional work	79
9.	Conclusion	80
	Bibliography	82
	Appendix 1:	I
	Appendix 2:	V
	Appendix 3:	VIII
	Appendix 4:	X
	Appendix 5:	XV
	Appendix 6:	XXVI

List of Figures

Figure 1: Material usage in aero-engines (1)	2
Figure 2: Titanium usage in the GE90 Aero-engine (3).....	3
Figure 3: Cutting tool temperature Distribution (14)	7
Figure 4: Typical insert Wear (2)	8
Figure 5: Change in tool hardness as a function of temperature(1,2).....	11
Figure 6: Typical PCD Insert	11
Figure 7: Phase Diagram of Diamond (25)	12
Figure 8: Graphic representation of flank wear factors	13
Figure 9: Extreme directional effects of flood cooling (14)	14
Figure 10: Modified Cutting insert; (a) Cad drawing, (b) Actual insert (16)	18
Figure 11: Average cutting forces (16)	19
Figure 12: Average feed forces (16)	19
Figure 13: Flank wear (16)	20
Figure 14: Tool wear after 5 min at 97m/min (16).....	20
Figure 15: Application Nozzle (15)	21
Figure 16: Rake face cooling using liquid Nitrogen (13)	23
Figure 17: Modified tool holder design (6)	23
Figure 18 - Schematic drawing of design (7).....	25
Figure 19 - Design of cryogenic nozzle: Auxiliary nozzle active (7)	25
Figure 20 - Design of cryogenic nozzle: Auxiliary nozzle inactive (7)	26
Figure 21 - Chip breaker position (7).....	27
Figure 22: Tool temperatures when machining Ti-6Al-4V (14).....	28
Figure 23: Tool Holder: SRSC12 04 M0	30
Figure 24: Tool Cap design 1	31
Figure 25: Tool cap design 2	32
Figure 26: Tool Movements	34
Figure 27: Rotational acceleration requirements	34
Figure 28: CNC facing cycle code.....	35
Figure 29: CNC code for longitudinal cutting.....	36
Figure 30: Experimental setup	38

Figure 31: Reservoir with PTFE Base	39
Figure 32: Ice developing on cutting edge.....	40
Figure 33: LN ₂ supply setup – Prone to forming ice plugs	40
Figure 34: Forming of an ice plug	41
Figure 35: Custom copper pipe	41
Figure 36: Use of pressure relief valve (34)	43
Figure 37: Typical dewar construction (adapted from (31)).....	44
Figure 38: Olympus GX51 Microscope	45
Figure 39: Inspection Plate	45
Figure 40: Typical tool wear curve (23)	48
Figure 41: Tool life prediction for RCMW 12 04 M0 H13A (35)	48
Figure 42: Flank wear relative to cutting time	49
Figure 43: Flank wear at 16.49 min on WC, $v_c = 120$ m/min, $f = 0.1$ mm/rev, $a_p = 0.25$ mm (50x).....	50
Figure 44: Flank wear at 13.19 min on WC, $v_c = 150$ m/min, $f = 0.1$ mm/rev, $a_p = 0.25$ mm (50x).....	50
Figure 45: Flank wear at $v_c = 150$ m/min, $f = 0.1$ mm/rev, $a_p = 0.25$ mm	51
Figure 46: Flank wear after 19.34 minutes, $v_c = 150$ m/min, $f = 0.15$ mm/rev, $a_p = 0.25$ mm	51
Figure 47: Flank wear after 29.89 minutes, $v_c = 150$ m/min, $f = 0.15$ mm/rev, $a_p = 0.25$ mm	52
Figure 48: Flank wear at $v_c = 150$ m/min, $f = 0.15$ mm/rev, $a_p = 0.25$ mm	52
Figure 49: PCD Shim	53
Figure 50: New PCD Insert edge.....	54
Figure 51: Flank wear after 45 seconds with excessive chatter.....	54
Figure 52: Chipping on rake face due to chatter.....	55
Figure 53: Flank wear of PCD insert under flood cooling after 1 minute 30 seconds (Excessive chatter) .	55
Figure 54: Flank wear of PCD insert under flood cooling after 45 seconds	56
Figure 55: Flank wear growth trend of PCD insert under Soluble cooling.....	56
Figure 56: Flank wear of PCD insert under flood cooling after 2min 57 sec.....	57
Figure 57: Flank wear of PCD insert under flood cooling after 3min 18 sec.....	57
Figure 58: Flank wear of PCD insert under flood cooling after 3min 25 sec.....	58
Figure 59: Flank wear of PCD insert under LN ₂ cooling after 46 sec	59
Figure 60: Insert cutting edge identification.....	59
Figure 61: Flank wear growth trend of PCD insert under liquid nitrogen (LN ₂) cooling.....	60
Figure 62: Flank wear of PCD insert under LN ₂ cooling after 3 min 41 sec	60

Figure 63: Flank wear of PCD insert under LN ₂ cooling after 5 min 24 sec	61
Figure 64: Separation between the rake face of the PCD and the Ti-6Al-4V chip	61
Figure 65: Flank wear of PCD insert under LN ₂ cooling after 7 min 57 sec	62
Figure 66: Flank wear of PCD insert under LN ₂ cooling after 7 min 57 sec	62
Figure 67: Tool life representations	63
Figure 68: Tool Life measured as material removed	64
Figure 69: Some insert geometries	64
Figure 70: Insert – work piece interface	65
Figure 71: Sandvik cutting recommendations	66
Figure 72: Average flank wear on WC inserts with conventional cooling	67
Figure 73: Chip thickness and chip thinning	68
Figure 74: Effect of large nose radius on end of cut	70
Figure 75: Maximum flank wear with regard to material removed.....	70
Figure 76: Build up on rake face of PCD insert.....	71
Figure 77: Chipping at 3 min 18 sec on PCD inserts, Parameter Set 3.....	72
Figure 78: Chipping at 3 min 25 sec on PCD inserts, Parameter Set 3.....	72
Figure 79: Average flank wear relative to material removed	72
Figure 80: Maximum flank wear at parameter set 3.....	75
Figure 81: Chip welded to tool cap.....	76
Figure 82: LN ₂ Supply System.....	78

List of Tables

Table 1: Tool softening temperatures (1,2)	11
Table 2 : Cutting parameters (16)	18
Table 3: Cutting Conditions for experiments by Wang et al. (13).....	22
Table 4: Tool life criteria (7).....	25
Table 5: Experimental tool life results and comparison (7).....	27
Table 6: Material Conductivity.....	29
Table 7: RCMW Insert geometry.....	37
Table 8: Ti-6Al-4V annealed only material specifications (30).....	42
Table 9: Measured hardness of Ti-6Al-4V samples	42
Table 10: Tool life criteria (7).....	46
Table 11: Round insert experimental conditions	49
Table 12: Insert geometry.....	52
Table 13: Experimental cutting conditions	52
Table 14: Round insert experimental conditions	66
Table 15: Recommended cutting data	69

Acknowledgements

The author would like to thank the following people for their contributions:

The AMTS group and TIA for their funding of the project.

Mr. Nico Treurnicht for his guidance and motivation throughout the project.

Element Six (Pty) Ltd for supplying the cutting inserts required for experimentation.

Hildegarde Mouton for her support and patience during the completion of the project.

Johan and Dalena Koen for their love, support and inspiration.

My heavenly father for granting me the talent to complete my studies.

Glossary

a_p	Depth of cut
V_c	Cutting speed
f	Feed rate
T_m	Total machining time
MRR	Material removal rate
Ti-6Al-4V	A α - β titanium alloy used widely in aerospace
HRC	Hardness measured on the Rockwell C scale
ISO	International Organisation for Standardization
LN ₂	Liquid Nitrogen
N ₂	Nitrogen gas
MQL	Minimum quantity lubrication
PCD	Poly crystalline diamond
Thermal conductivity	The ability of the material to conduct heat
Insert	Interchangeable tool tip used for machining materials. Available in a vast variety of materials and shapes
WC	Tungsten carbide
Conventional cooling	Coolant is sprayed at low pressure toward the cutting region. Coolant consists of oil diluted with water.
m/min	Meters per minute
mm/rev	Millimetres per revolution
GPa	Gigapascal
W/mK	Watts per meter Kelvin
Pre-cooling	When the work piece is cooled prior to machining
MPa	Megapascal
Dewar	A vacuum insulated container used to transport liquid nitrogen

1. Introduction

The aircraft industry is known for continuously searching for innovative methods to manufacturing challenging components. One of the methods by which this is done is the use of advanced materials. Titanium alloys are one of the material families that are valuable to the aircraft industry due to their excellent mechanical properties. They are commonly used for structural airframe components and demanding components within the aero-engines. However, titanium and its alloys are known for being a material that is difficult to machine, yielding low productivity rates. This has hampered the growth of titanium usage in areas other than the aircraft industry.

Titanium is however not only used in the aircraft industry and the demand for titanium in industries such as automotive, medical and chemical is showing promising growth. In all of these industries, the material has to be machined to produce the final product. In aircraft components, this is a challenging area as light weight components are usually made from a solid billet. This results in the majority of material being removed by some machining process. The need for an effective machining method is therefore of required.

Many researchers have pursued a number of avenues in search of a solution for titanium machining, such as pre-heating of the work piece, minimum quantity lubrication (MQL) and cooling. The most challenging problem with titanium machining is however to deal with the large amount of heat that is generated. For this reason, cooling has proven to be the most successful approach. Hence most researchers are now pursuing this route.

South Africa's manufacturing sector is attempting to penetrate the aircraft manufacturing supply chain through counter trade agreements with aircraft manufacturers. This does however require the local manufacturing standard to be on par with the strict requirements of the industry. The South African government is therefore funding research within the field of advanced material research in order to encourage knowledge growth in this sector.

The research presented is in support of this objective of the South African government to try and establish knowledge within South Africa in the field of advanced machining. The project therefore focuses design and testing of an advanced cooling system to improve the machinability of Ti-6Al-4V machining. The system is analysed to determine the effectiveness of the design to achieve the objectives stated.

2. Problem statement and objectives

2.1. Hypothesis

Localised LN₂ cooling on PCD inserts reduces wear rates when machining Ti-6Al-4V compared to PCD and WC inserts with soluble oil cooling.

3. Titanium, its alloys and industry

To be able to research titanium machining, it is important to know about the titanium alloy variants, their properties and where they are used. This sketches the important background and where titanium alloys fit into the bigger picture.

Titanium alloys are typically used in demanding airframe structures and aircraft engines. An aircraft engine can be divided into three major divisions namely the compressor, the combustor and the turbine. These are housed in a casing that is normally manufactured from combinations of aluminium and titanium. The materials that are used within the aero-engine are mostly alloys of steel, aluminium, nickel and titanium. Alloy material properties are aimed at high strength-to-weight ratios, high corrosion resistance as well as high temperature strength. Titanium and nickel based alloys are considered to be the most suitable to the requirements. Other materials such as carbon fibre and metal matrixes are becoming more popular. Figure 1 shows the change in material usage in aero-engines as a percentage of the engine weight over the last five decades.

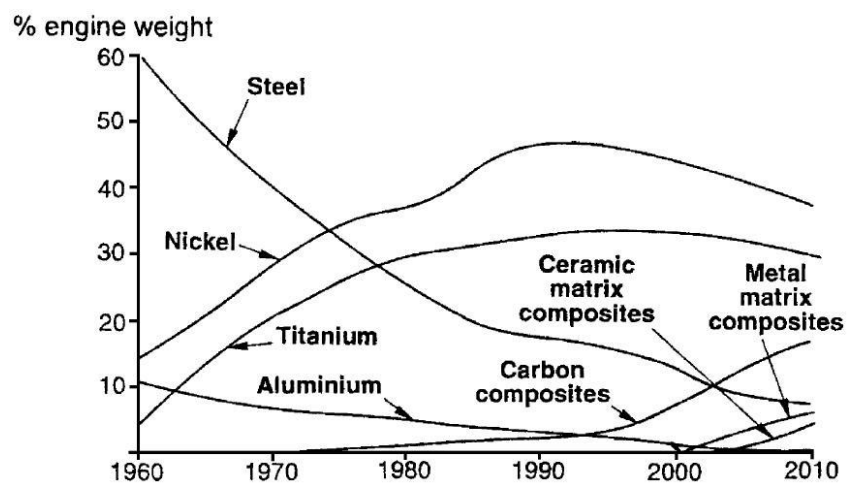


Figure 1: Material usage in aero-engines (1)

Within the aero-engine titanium alloys are used in the low and high pressure stages of compressors, parts experiencing high fatigue and parts subjected to large centrifugal forces such as disks and turbine blades (also see Figure 2). The use of titanium in aero-engines will however increase if obstacles in the machining process that result in premature part failure can be overcome. Titanium is also widely used in airframe structures, especially in areas where the operating temperature exceeds 130°C. (1,2)

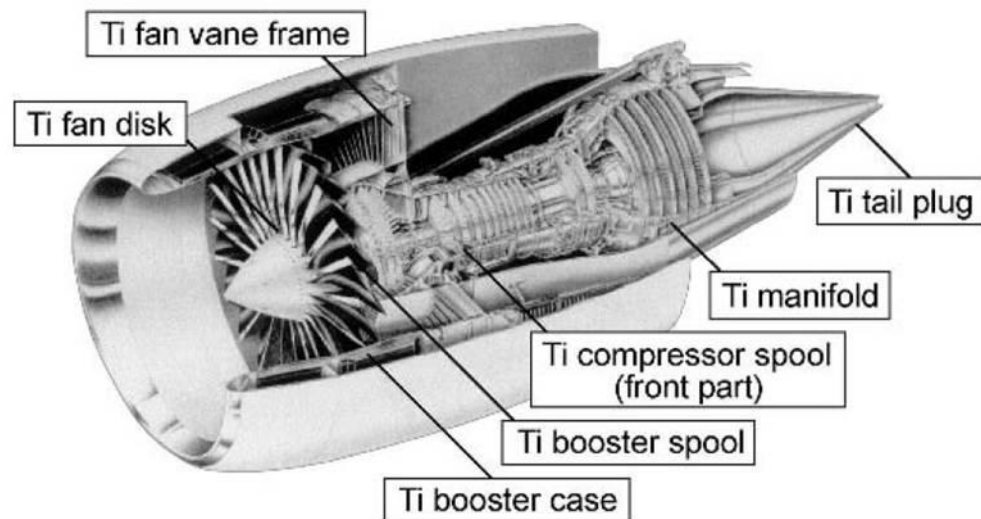


Figure 2: Titanium usage in the GE90 Aero-engine (3)

3.1. Physical properties of titanium and its alloys

Aerospace engineers are continuously searching for opportunities to reduce aircraft mass without compromising the strength and reliability of the aircraft. To achieve this objective they investigate materials that have a superior strength to weight ratio to what they are currently using. However, they also have to consider the manufacturing cost of the aircraft when choosing these materials. Titanium is one of the materials often used by aircraft design engineers to reduce the aircraft mass. This is primarily due to its high strength to weight ratio, high corrosion resistance and its ability to maintain its material properties at high temperatures (1,2,4,5,6,7,8,9). These properties are however dependent on the alloy type being used.

Titanium is subjected to a phenomenon called allotropy (4,7). Allotropy is when a material has more than one crystal structure while in the same phase. A well known example of this phenomenon is carbon. Carbon can be found in a solid state as diamond, graphite and fullerenes. All three of these are a solid made of carbon atoms, but because the atoms are bonded differently, the materials differ in a number of ways.

Pure titanium experiences an allotropic transformation (when the titanium's crystal structure changes) at 882°C (1,4). It changes from a close packed hexagonal α -phase at low temperatures to a body-centred cubic β -phase at high temperatures. Alloying elements used in titanium tends to either stabilise the α -phase or the allotrope β -phase. Elements that are classified as α -phase stabilisers, for example Aluminium (Al), Oxygen (O), Nitrogen (N) and Carbon (C), raise the transformation temperature. For use at ambient and elevated temperatures up to 550°C, aluminium is an extremely effective alloying agent, and its low density is an additional advantage. (4)

When β -stabilisers are used, it results in a decrease in transformation temperature. These alloying elements are divided into β -isomorphous and β -eutectoid. The most important β -isomorphous alloy elements are molybdenum (Mo), vanadium (V) and niobium (Nb). These β -isomorphous elements are mutually soluble with β -titanium, where the β -eutectoids have restricted solubility.(4)

Titanium alloys can be classified in four main categories, α -alloys, near α -alloys, α - β alloys and β -alloys.

The α -alloys contain α -stabilisers resulting in an α -phase microstructure. The only α -alloy still commercially available, except pure titanium, is Ti-5Al-2½Sn. This alloy has excellent tensile properties and creep stability at temperatures up to 300°C. The minimum tensile strength for α -alloys ranges from 170MPa to 480MPa (1). They are primarily used for their corrosion resistance and cryogenic applications. They are not heat treatable and are therefore suitable to be welded.

Near α -alloys have high α -stability and only contain small amounts of β -stabilisers. These alloys are characterised by a microstructure containing mainly α -phase with traces of β -phase. These alloys behave similar to α -alloys and are capable of operating at temperatures of up to 400 - 520°C (1,4).

The β -alloys contain significant quantities of β -stabilisers and are characterised by their ability to be significantly hardened and that they are more easily forged and cold formed (1,4,10). The density of β -alloys are however higher than the other alloys. The strength of these alloys is equivalent to that of α - β alloys at ambient temperatures, although they show inferior properties at elevated temperatures. High strengths can easily be obtained by cold rolling these alloys (1).

The α - β alloys contain both α and β stabilisers and their microstructures consists of both α and β phases. Ti-6Al-4V and IMI 550 (Ti-4Al-2Sn-4Mo-½Si) are the most common alloys that are categorised in this division (4,10). More than 60% of titanium is alloyed to create Ti-6Al-4V and is the most commonly used titanium alloy (1,7,11,12). These alloys have a higher strength than near α -alloys and can be heat treated

to significantly improve their strength. They are mainly used at temperatures between 350 and 400°C and are usually not used when welded joints are required (1,4,5,11).

Although all of the above material properties make Ti-6Al-4V an excellent material to use in manufacturing, titanium is still not as widely used as, for example aluminium. This is due to titanium being difficult to machine (1,4,5,13). Most of the components currently manufactured for the aerospace industry are machined from solid titanium billets. These components will however usually be thin walled. It can therefore be deduced that most of the material will be removed by means of machining. Although Near Net Shape manufacturing is being explored, many difficulties are experienced preventing the process from being accepted for the aerospace industry.

3.2. Challenges of titanium machining

Improvements in titanium machining largely depend on the overcoming of fundamental problems with the machining of titanium. These problems are caused by titanium's superior material properties, namely its high hot strength, low thermal conductivity, low modulus of elasticity and high chemical reactivity.(1,4,5,7,14)

Industry currently machines titanium at cutting speeds in the region of 60m/min (8,14,15). At these cutting speeds, tool wear is reasonable, although productivity is low. When cutting speeds are set above 60m/min the tool wear rate rapidly increases roughly in an exponential proportion to the cutting speed.

When machining titanium, the temperatures in the cutting zone are extremely high and the dominant reason for premature tool failure (2,6,16,17,18). Temperatures in the cutting zone are reported in the region of 1000°C (4,7,14,15). The high temperatures generated in the cutting zone also have a number of negative effects on the finished work piece, for example dimensional deviations, oxidation and corrosion, thermal residual stresses and micro cracks (1,6). These problems can partly be solved by conventional cooling, although a number of environmental, health and disposal issues are associated with the use of conventional coolant (19,20). The generation of heat and its distribution is discussed in section 3.2.1.

The cutting forces measured for the cutting of titanium alloys are reported as being approximately equal to when machining steel. The mechanical stresses experienced by the cutting edge is however much higher due to a small chip-tool contact area. The chip-tool contact area experienced with titanium is significantly smaller than other materials (8µm in titanium compared to 50µm in iron) (4,7). Although

the cutting forces are similar to steel machining, the small chip-tool area results in a much higher tool pressure (15). These tool pressures have a significant effect on the tool life as it results in plastic deformation of the tool at elevated temperatures. The high tool pressures also contribute to catastrophic tool failure of the cutting edge (1). Mechanical stresses are also elevated by titanium's deformation resistance at elevated temperatures. Titanium's resistance to deformation start to significantly reduce at 800°C.

Chatter is a difficulty that is common in the finishing of titanium machining. This is mainly due to the low modulus of elasticity of titanium alloys (110 GPa) (4). Due to the fact that titanium deflects nearly twice as much as common carbon steels, the deflection of the work piece material will result in vibrations, premature flank wear and higher cutting temperatures.

Cutting tools are adversely affected by the drastically increased chemical reactivity of titanium at elevated temperatures when machining titanium above 500°C. This chemical reactivity results in crater wear on the rake face as titanium chips pressure weld to the surface. When the chip that welded onto the tool surface is removed by sheer force of successive machining, tool material is removed from the rake face not only leading to tool material loss, but also degradation of the surface whereby wear is accelerated. The chips welding onto the tool surface is often referred to as a built-up edge.(4,7,14,15)

3.2.1. Heat generation and distribution in cutting operations

Because temperature is the main cause of tool failure modes in machining titanium, it is necessary to understand the causes of heat, as well as how it is distributed when machining titanium. By investigating the underlying reasons behind temperature generation and dissipation, fundamentally sound methods can be devised to target these problems.

Published literature indicates that 80% of the heat generated in the cutting process is transferred to the cutting tool (4). This can be attributed to the low thermal conductivity (7.1 W/mK) and heat capacity (522.5 J.kg/K) of the titanium which makes it reluctant to absorb heat (5,8).

A schematic representation of the heat distribution when machining titanium is shown in Figure 3. As can be seen, the region with the highest temperature is located close to the cutting edge. This is due to the small tool chip contact area. Hong et al (14) created a model to simulate the machining to calculate the heat distribution in the cutting tool. He found that at a cutting speed of 90m/min the temperature in zone 1 will climb to 743°C under conventional cooling. At this temperature the titanium is extremely reactive, and build-up on the tool rake face occurs.

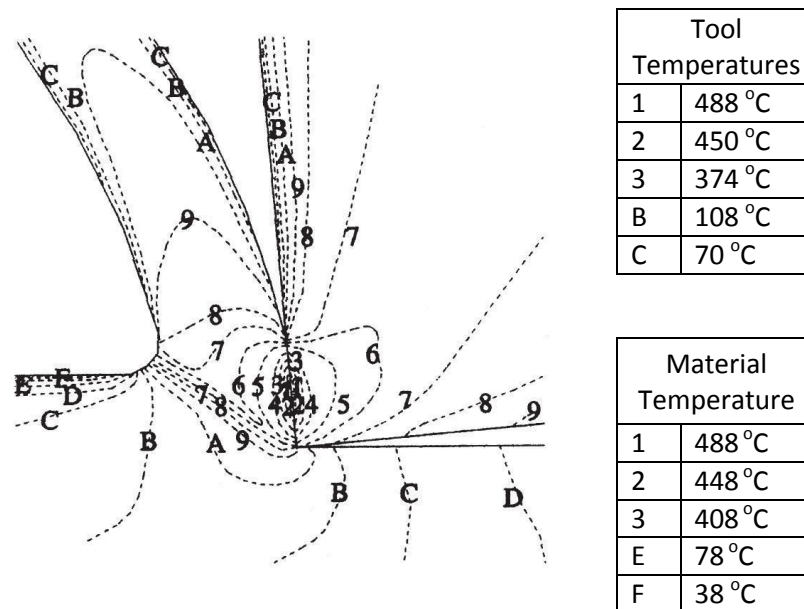


Figure 3: Cutting tool temperature Distribution (14)

As can be seen in Figure 3, the highest temperature is close to the cutting edge where the chip comes into contact with the tool. From this point the temperatures dramatically decrease over a short distance in the titanium, although the temperature around the high heat point on the tool is much higher. This is a result of the lower thermal conductivity of the titanium, as well as its thermal capacity. Because the thermal capacity of the titanium is low, it is reluctant to absorb the heat generated in the cutting zone. Most of the heat is therefore absorbed by the tool. The thermal conductivity of the tool is also higher than that of titanium, resulting in a higher overall tool temperature.

In conclusion, the highest temperatures when machining titanium is close to the cutting zone where in the chip-tool contact zone. Most of the heat generated during the cutting process is transferred to the cutting tool rather than the titanium resulting in a high temperature tool. The highest temperature point is however close to the cutting edge.

3.2.2. Adhesion and diffusion

Adhesion and diffusion wear is the mechanism that creates crater wear on the rake face of the tool. The location of crater wear is shown in Figure 4 (2). During machining, material from the chips will bond with the tool material due to a number of reasons, each of which can be characterised to the work piece and

tool material combination. The continued adhesion of material to the tool rake face will eventually cause a built-up edge to form on the rake face that becomes more prominent. Eventually this built-up edge will bond strongly with the chips, and the deposited material will be ripped off the rake face taking some tool material along. As this process re-iterates, a crater is formed in the rake face. The crater is indicated by 4 in Figure 4. (15)

This type of wear is common when machining titanium, especially with carbide cutting tools. Due to the high chemical reactivity of titanium at elevated temperatures, the titanium creates a strong bond to the tool material. Research has however shown that adhesion and diffusion wear is not common with PCD cutting inserts (5,21).

3.2.3. Flank wear

Flank wear is the most predominant wear present when machining titanium alloys and is shown in Figure 4 (22). Flank wear is caused by the rubbing of the flank face against the work piece. Flank wear is measured as average and maximum flank wear. Average flank wear is defined as the average amount of wear over the whole of the wear scar as indicated by 1 in Figure 4. Maximum flank wear is the single point showing the maximum amount of wear over the wear scar. Maximum flank wear will mostly be defined by chipping or notch wear (number 3 in Figure 4). Flank wear is accelerated by high cutting tool temperatures.

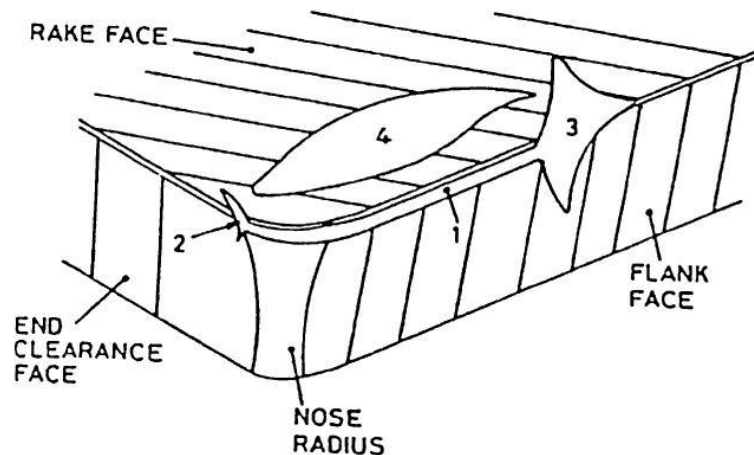


Figure 4: Typical insert Wear (2)

3.3. Tool materials for titanium cutting

The manufacturing industry currently mostly uses coated and uncoated tungsten carbide (WC) tools when machining titanium. Other options for example Poly Crystalline Diamond (PCD) and Cubic Boron Nitride (CBN) are also available although they are not widely used.(1,4,5)

Although many new tools have been developed, none of these tools has proven to significantly improve the machinability of titanium (8). For improvements, Ezugwu et al suggests that the tools need to exhibit the following tool characteristics (1,4):

- High tool hardness to resist high stresses involved
- Good thermal conductivity to minimise thermal gradients and thermal shock
- Good chemical inertness to prevent reaction with titanium
- Toughness and fatigue resistance to withstand chip segmentation process
- High compressive, tensile and shear strength

Research has shown that uncoated tungsten carbide (WC/Co) cutting tools of K20 grade are superior in most cases of machining titanium alloys, although high-speed steel (HSS) tools perform well for interrupted cutting, drilling and reaming (4). Outstanding results have been reported with end milling titanium by using of a tool steel alloy (TiN/Steel compound) with a TiN coating at cutting conditions beyond those of carbide end mills. As a general rule for high speed steel tools, highly alloyed HSS tools yield the best results for milling titanium. Although ceramic carbides have improved, they still haven't replaced tungsten carbide inserts due to their poor thermal conductivity, low fracture toughness and reactivity with titanium. Technology that has proven good performance is cubic boron nitride and polycrystalline diamond, although their high costs limit their application (4,23). In turning coated carbide, CBN and PCBN tools are usually utilised at high cutting speeds, while uncoated carbides are widely used at low cutting speeds (1).

3.3.1. Uncoated carbide tool inserts

Uncoated carbide is the most common insert material used to machine titanium at low cutting speeds (1). These tools exhibit good fracture toughness limiting primary tool failure to flank wear. Uncoated carbides are available in two basic grades, straight and mixed. Straight carbide grades is a mixture of cobalt (Co) and tungsten carbide (WC), while the base composition of mixed grades will also contain titanium carbide (TiC), tantalum carbide(TaC) and other rare-earth elements. Inserts containing

a high weight percentage of Co and coarse grain WC particles enable them to withstand the shocks of interrupted cutting and roughing. (1)

3.3.2. Tool coatings for titanium machining

The use of coatings is a widely used practice in industry to improve the tool life of cutting inserts. The tool manufacturing industry has therefore also investigated using coatings to improve the tool life. Results were however not promising. Tool life improvements were marginal, if any (7). Ceramic coatings are used to increase the hardness of the tool surface, thus reducing its susceptibility to abrasive wear. Ceramic coating also has lubricating properties reducing the friction between the tool and chip. (1,24)

3.3.3. Cubic Boron Nitride (CBN)

The use of CBN tools for the machining of titanium has been investigated by a number of researchers. It has been found that tungsten carbide tools perform superior to CBN tools with regard to tool life when finish machining operations are conducted at high cutting speeds. Excessive notching and chipping was found to be the primary causes of tool failure. (8)

The use of CBN tools in aero-engine alloy machining is negatively influenced by the high cost of the inserts and the material's susceptibility to fracturing and chipping (1). These inserts are used in finishing conditions at cutting speeds up to 350 m/min.

3.3.4. Polycrystalline diamond (PCD)

PCD is a commercially manufactured diamond and is manufactured by sintering fine grained diamond crystals under high pressures and temperatures, using little or no binder materials. Cobalt is typically used as the binder material. Cutting tools have been manufactured using this technology from as early as the 1970's. The motivation behind using diamond as a tool material is based on its hardness (>49GPa) (5), as well as its ability to maintain its hardness at elevated temperatures (Figure 5). PCD material is considerably tougher than single crystal diamond because of the random orientation of the diamond crystals. PCD tools are usually constructed as a substrate, mostly from tungsten carbide, and a PCD layer (Figure 6). The PCD layer is normally approximately 0.5mm thick. These inserts are mostly used in the high speed machining of non-ferrous metals, as well as abrasive non-metals such as fibreglass or wood. (2,8)

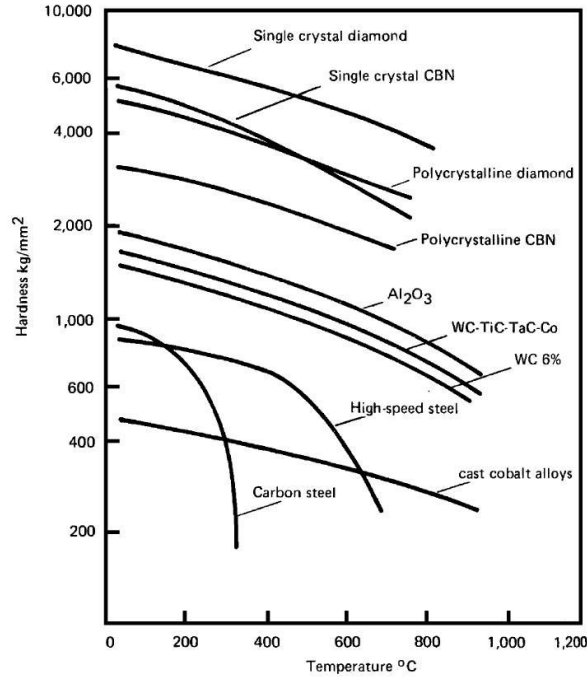


Figure 5: Change in tool hardness of a function of temperature (1,2)

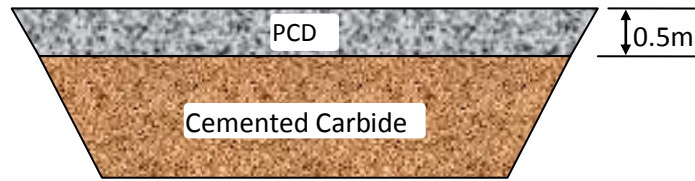


Figure 6: Typical PCD Insert

Table 1: Tool softening temperatures (1,2)

Tool Material	Softening Temperature (°C)
High Speed Steel (HSS)	600
Tungsten Carbide (WC)	1100
Al ₂ O ₃	1400
CBN	1500
Diamond	1500

PCD also has a much higher thermal conductivity (550 W/mK @ 300°C) (4). According to the author, this might create excessive heat build-up in the cutting tool, as the considerably higher thermal conductivity of the PCD tool relative to the titanium work material could facilitate a more than normal amount of

heat flow to the tool, potentially accelerating wear. One could also interpret this attribute to be helpful if utilized in the correct way, seeing as the good thermal conductivity will aid in the cooling of the cutting edge.

An interesting phenomenon that is present with PCD cutting tools regards notch wear. When the notch wear scar on a PCD insert is chemically analysed one will find that graphite is present. Graphite is however not commonly found in the cutting zone. For diamond to undergo a phase change to graphite, either the temperature or the pressure will have to rise significantly (5). In the cutting zone both the pressure and the temperature is high. With these conditions, the PCD will not undergo a phase change. However, at the location of the notch, just outside the cutting zone, the pressure is at atmospheric pressure and because PCD has such a good conductivity, the temperatures are approximately equal to that in the cutting zone. When the phase diagram for diamond (Figure 7) is considered using these conditions, we see that these conditions result in the formation of graphite. It is therefore fair to conclude that this is the reason for the notch wear. Graphite does not have the wear resistance that diamond has, and because of this, the notch wears much faster than the cutting edge.

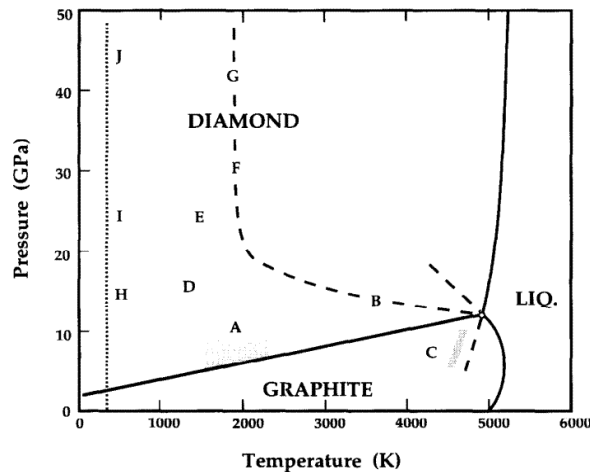


Figure 7: Phase Diagram of Diamond (25)

From research it is clear that the use of PCD cutting tools for titanium machining results in exceptional tool life (8). PCD tools have also been proven to deliver a better surface finish (8).

3.4. Tool failure

The prominent failure modes in titanium machining are notching, crater wear, flank wear, chipping and catastrophic failure which are caused by high temperatures, high pressures, chemical reactivity and the formation of segmented chips (4,13,14). Ezugwu also reports that tungsten carbide and PCD are the best

tool materials to machine titanium (4). This is reportedly due to a stable TiC reaction layer that is formed between the tool and the chip. There is however contradictory results in the form of TiC coatings on commercial tools that are not successful in suppressing wear (4).

Cutting speed has been proven to have the most prominent effect of tool life of all the cutting conditions (4,8). Tool life will exponentially decrease as the cutting speed is increased. For this reason, it is common machining practice to machine titanium at a cutting speed of 60 m/min (7). It has also been reported that the depth of cut influences the tool life negatively. Tool geometry also has a significant influence on the tool life. It has been suggested that a clearance angle of 10° - 15° together with a high negative rake angle (-10° to -15°) can yield significant improvements (26).

When measuring tool wear, there are two main tool wear regions, the rake face and flank face. In each of these regions a number of wear characteristics are measured. A graphic representation of flank wear criteria is shown in Figure 8. With titanium, a crater forms on the rake face due to adhesion and diffusion wear. Two parameters are used to describe the crater formed namely K_m and K_t . K_m defines the distance that the centre of crater is located from the cutting edge, while K_t defines the deepest point within the crater. Flank wear also has a number of parameters that should be measured. Features such as notch wear is also categorised under flank wear. The parameter V_B refers to the abrasive wear that occurs on the flank. V_B does however have sub divisions as shown in Figure 8. Because flank wear is not uniform and has a profile, the parameters V_{BMax} and V_{BAvg} have been defined. V_{BMax} defines chipping or catastrophic failures. V_{BAvg} defines the average wear length of the normal abrasive wear. In titanium machining, flank wear is the predominant tool wear (8,16).

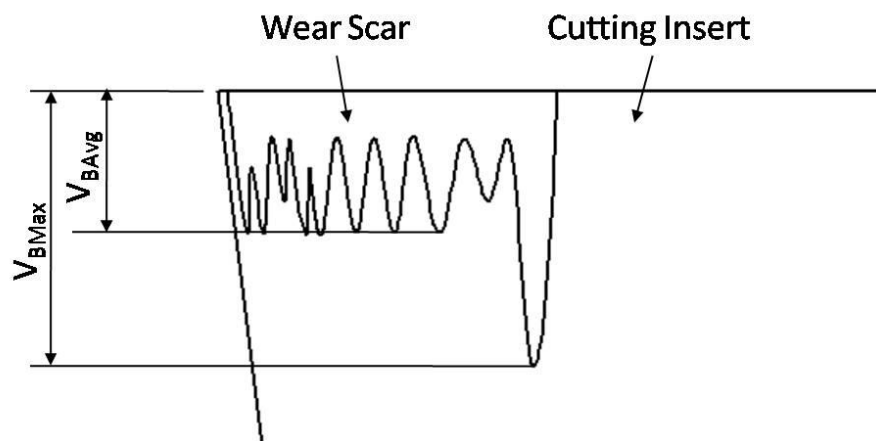


Figure 8: Graphic representation of flank wear factors

3.5. Cooling approaches

The machining of titanium generates a large amount of heat close to the cutting zone. This heat is the primary cause of tool failure, be it directly or indirectly. A number of cooling strategies have therefore been investigated by researchers. The approaches can be divided into flooding, high pressure cooling, gas cooling and cryogenic cooling.

High pressure cooling has shown promising results as the coolant penetrates deep into the chip-tool contact area.

Flood cooling using soluble oil is the most commonly used cooling method in industry. Flood cooling is however insufficient in some cases, one of which is titanium machining. Because titanium has a high cooling demand, the coolant used must be applied effectively, penetrating the tool chip interface as far as possible. Flood cooling is not based on the principle of precise directional application of the coolant stream. Two extreme cases are shown in Figure 9. In the most extreme case, the chip prevents the coolant from being applied to the tool chip interface. The cutting edge therefore experiences a large thermal load resulting in poor tool life.

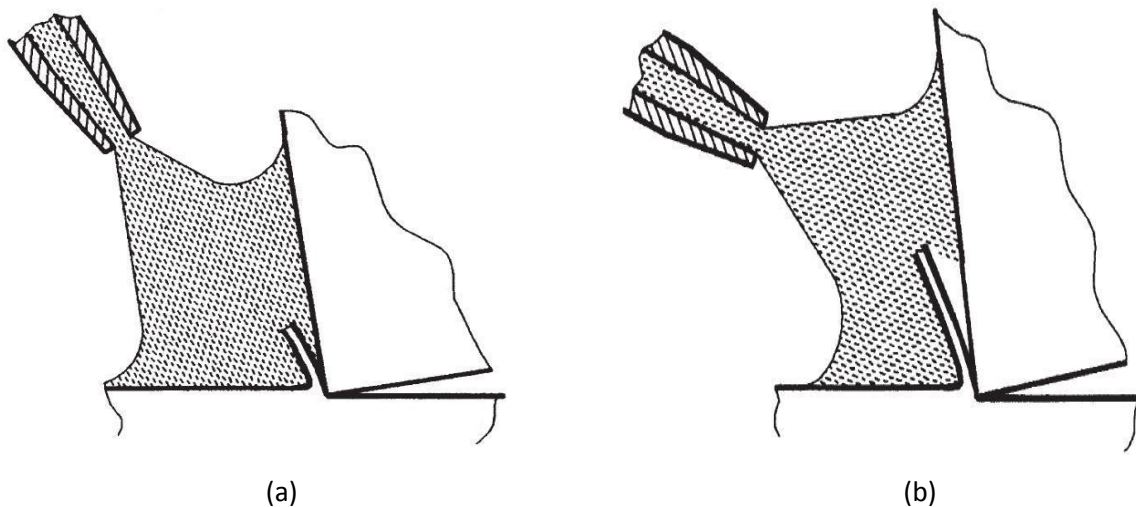


Figure 9: Extreme directional effects of flood cooling (14)

3.6. Cutting fluids

Cutting fluids in general serve two major roles in machining namely cooling and lubrication (4,22). The flow of cutting fluid also aids in the removal of chips, minimise thermal shock in milling operations and keeps chips from igniting. When high pressure cooling methods are used, chips are often small and

discontinuous. A number of coolant variations have been experimentally tested, although most of the methods resulted in a number of problems, be it environmentally related or performance related. (4)

Cutting fluids can be divided into three major categories, namely neat cutting oils, soluble oils and gaseous cooling. Each of these categories has their own characteristic application. Neat cutting oils are mineral oils that may contain additives. They are primarily used when the pressures between the tool and chip are high and when lubrication is a primary concern. Water soluble coolants are suitable when cutting speeds are high and tool pressures are low. It has however been found that cutting fluids do not penetrate the tool-chip interface when cutting speeds are high (22). Here gaseous coolants can be utilised to overcome coolant penetration difficulties. The high cost of gases does however limit their use.

As stated earlier, cooling generally improves tool life. It is however possible to overcool a work piece. When a work piece is overcooled, it will become harder and tougher, resulting in reduced tool life (1). Overcooling can also deteriorate the surface finish and dimensional accuracy of the work piece in severe cases.

Cutting fluids have been reported to cause environmental, health and logistical problems. Typical environmental problems are chemical breakdown of cutting fluid resulting in water and soil contamination. Operators also experience dermatological ailments due to prolonged exposure to cutting fluids. Due to the nature of cutting fluids they also cause logistical problems in terms of the transport of fluids that needs to be disposed of. Furthermore methods of disposing of cutting fluids, storage of the fluids as well as the extra space required in the work place to handle the fluids in terms of filtration, possible cooling and storage before disposal are challenges.

3.6.1. Liquid Nitrogen

Liquid nitrogen (LN₂) as a coolant has been used in a number of studies. It has been conclusively proven that when utilized correctly; it improves tool life, surface finish and dimensional accuracy (14,16).

Effect of temperature on titanium

Temperature has a considerable effect on the strength of titanium. When cooled from room temperature to the cryogenic temperatures of LN₂, titanium's tensile strength changes from 1000MPa to 1700MPa (7), and its ductility and toughness is not significantly reduced like that of carbon steels. Cooling the work piece will harden the titanium, causing it to be more abrasive. It can therefore be concluded that it is completely undesirable to cool the work piece.

As previously stated, cutting temperatures for Ti-6Al-4V can easily reach 1000°C. At this temperature, the cutting tool material will thermally soften which in turn will promote tool failure. When LN₂ is used to cool the cutting edge, the increased tool hardness should improve tool hardness which should improve tool life. The literature states that the impact strength is not weakened under cryogenic temperatures. Although a number of researchers have developed LN₂ cooling systems, none of them are currently economical or practical enough to replace conventional cooling.

Environmental advantages

A number of difficulties exist with the disposal of conventional cutting fluids. Government regulations are very strict with regard to the disposal of these coolants. This results in high costs to companies to transport used coolant to disposal sites (14). Nitrogen on the other hand composes approximately 78% of our earth's atmosphere, and because liquid nitrogen evaporates to nitrogen gas when used, it is considered environmentally friendly (2,14,16). Conventional coolants are also known to cause ailments to operators where none such ailments has been reported with regard to nitrogen.

3.7. Surface integrity

Titanium is usually considered for applications requiring fatigue reliability that implies a well maintained surface integrity. The obstacle however is that titanium's surface is easily damaged during machining and grinding operations. Micro-cracks, built-up edges, plastic deformation, heat affected zones and tensile residual stresses are typical surface damages in titanium (4).

3.8. Effect of tool geometry and cutting strategy on tool life

Tool geometry can have a significant effect on tool life when machining titanium. A positive rake angle will prevent work hardening of the work piece and will therefore reduce the cutting forces of the following cut. The cutting edge should be sharp to prevent the tool from rubbing on the work piece which results in additional heat being generated. However, because the cutting pressure is large in titanium machining, a sharp cutting edge is prone to chipping. For this reason a light hone on the cutting edge is advisable (2). The use of a tool with a large nose radius will reinforce the cutting edge to prevent chipping of the cutting edge. It also engages a longer cutting edge in the material distributing the wear over a larger area which in turn prevents notching.

3.9. Solutions from literature

A number of researchers have conducted research on the improvement of titanium alloy machining. From this research a number of possible solutions have been developed to address what they believe is the factor that needs to be controlled in order to improve the machinability. From this research it is clear that the majority of researchers identify heat as the main factor that impairing satisfactory tool life. (8,22)

3.9.1. Hot machining of work piece

Research has been done on the hot machining of titanium alloys. The concept attempts to utilise the thermal softening of the material to improve the machinability. Pre-heating methods such as furnaces torches, laser and plasma have been experimented with. The research did however result in higher cutting temperatures, poorer tool life and inferior surface finishing (6,13).

3.9.2. Cooling

Cooling is believed to be the method in which a feasible solution is hidden. Research has been done on a number of methods with promising results. The challenge in cooling the titanium machining process is to get close to the cutting edge and to cope with the rate at which heat is generated. The methods investigated include high pressure water jet cooling, liquid nitrogen jets and other concepts. The problem arising with water jets is that they are currently not capable of removing heat at the tempo that the heat is generated. Liquid nitrogen cooling systems have yielded significant improvements, although severe cooling of the work piece influences its ductility. It will therefore be preferred if the work piece is cooled as little as possible (6).

Through insert cooling

Dhananchezian et al (16) modified a standard carbide insert by spark eroding holes from the rake face to the primary and secondary flank face. Photographs of the modifications can be seen in Figure 10.

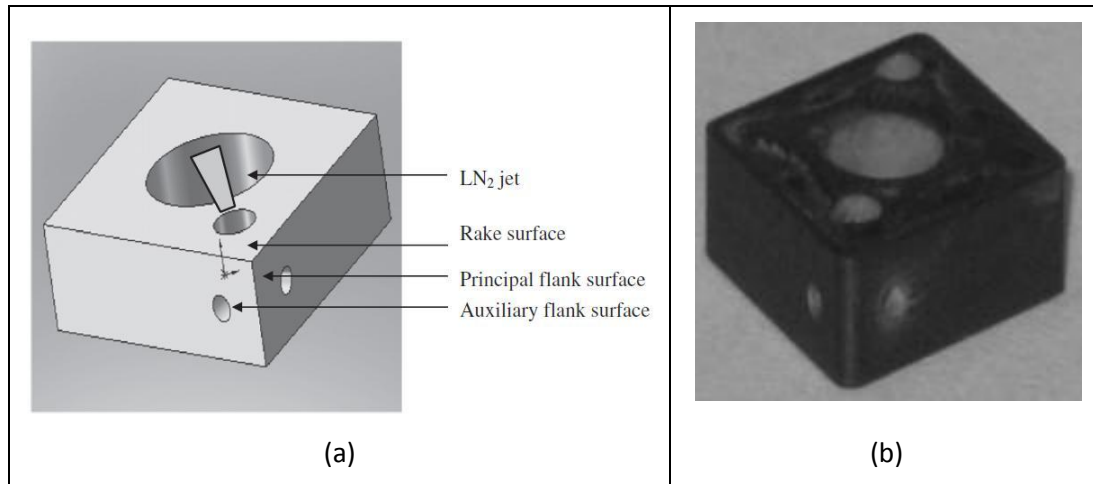


Figure 10: Modified Cutting insert; (a) Cad drawing, (b) Actual insert (16)

The cutting conditions chosen for the experimentation are shown in Table 2. The work piece used is Ti-6Al-4V with an outer diameter of 40mm. The cutting parameters can be classified as rough machining. Conventional coolant and LN₂ is used as coolant mediums in these experiments. A standard insert is used for the experiments with conventional cooling. For cryogenic cooling the LN₂ is applied using a nozzle that is directed at the hole in the rake face. The coolant then passes through both channels to exit to the primary and secondary flank face. During experimentation the author measured the cutting force, feed force and tool (16).

Table 2 : Cutting parameters (16)

Cutting Speeds (v_c)	27, 40, 63, 97 m/min
Feed Rate (f)	0.159 mm/rev
Depth of cut (a_p)	1 mm

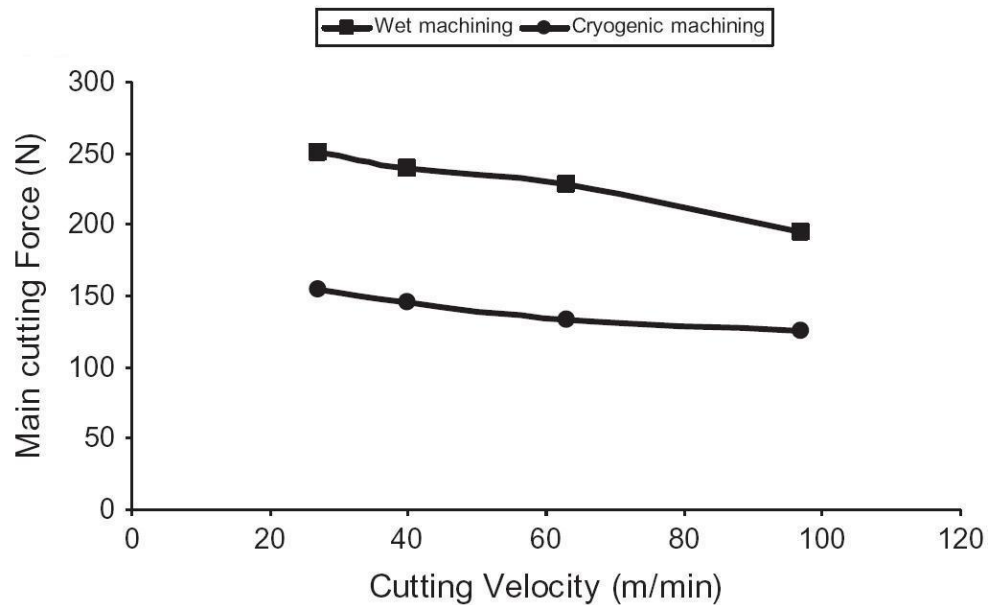


Figure 11: Average cutting forces (16)

The cutting forces measured are shown in Figure 11. When machining with LN₂ cooling, the cutting forces were ranging from 35% to 42% lower than with conventional cooling. Feed forces, as shown in Figure 12, were lowered between 39% and 49% with the use of LN₂ cooling. This is attributed to the reduction in cutting temperature that enable the tool to maintain its hardness and reduces the adhesion of the chip to the tool.

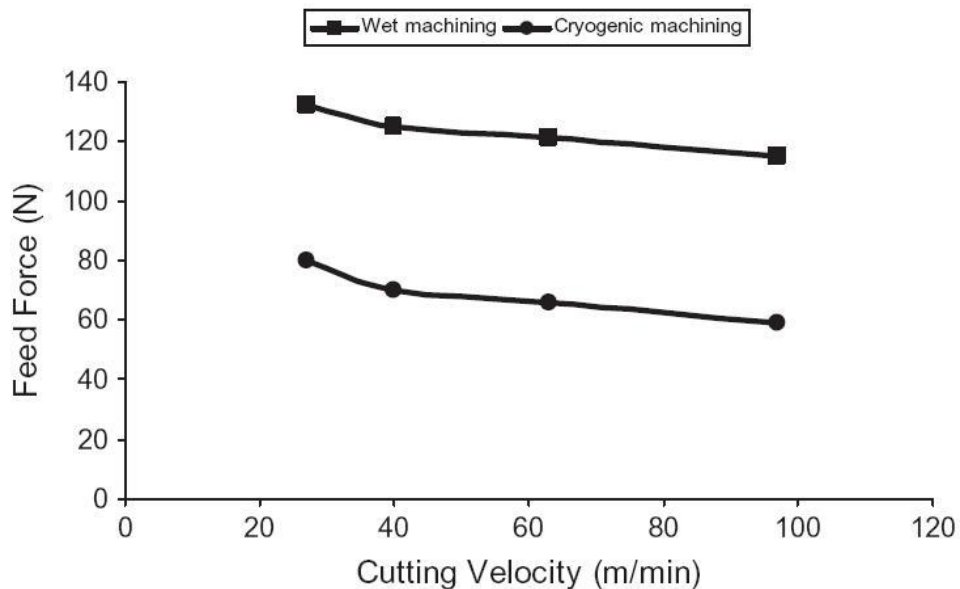


Figure 12: Average feed forces (16)

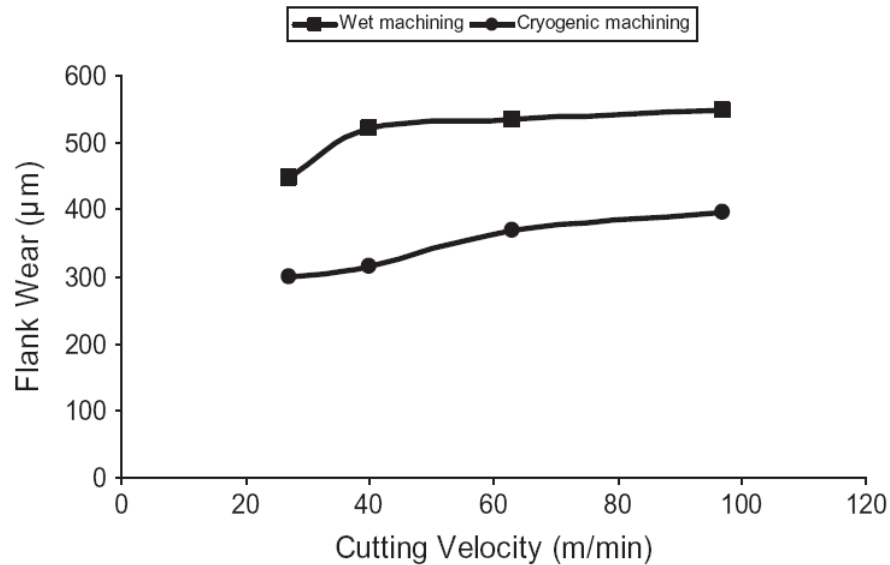


Figure 13: Flank wear (16)

The tool wear growth curve in Figure 13 show the flank wear for cryogenic and conventional cooling. The cryogenic cooling method used also delivered significant improvements in tool life. Flank wear with the use of LN_2 was reduced between 27% and 37% relative to conventional cooling over the cutting speeds investigated. Wear on the rake face was also reported to be reduced. The increase in tool life is attributed to the reduction in cutting temperature. As result of the lower temperatures, the wear resistance of the tool was increased. The lower temperatures also decreased the wear that is attributed to the chemical reactivity between the titanium alloy and the tool. An example of the absence of crater wear under cryogenic conditions is shown Figure 14.

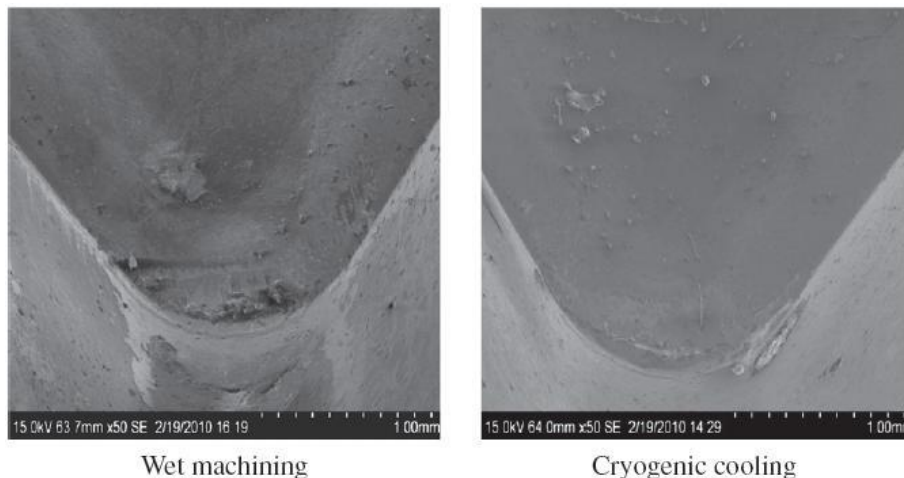


Figure 14: Tool wear after 5 min at 97m/min (16)

Liquid Nitrogen spraying

Venugopal et al (15) investigated the effect on tool life when LN₂ is used to cool the cutting region. The experiments made use of uncoated carbide inserts as tool material when machining Ti-6Al-4V. A nozzle was manufactured to apply the LN₂ and was directed at the rake and flank face of the cutting tool (Figure 15). Cutting was executed on a 150mm diameter bar of Ti-6Al-4V under dry, wet and cryogenic cooling. Cutting speeds of 70, 100 and 117m m/min was tested with a 0.2 mm/rev feed rate and 2 mm depth of cut. The LN₂ application pressure and flow rate was experimentally determined. The goal was to achieve a continuous flow of LN₂ while not overcooling the work piece.

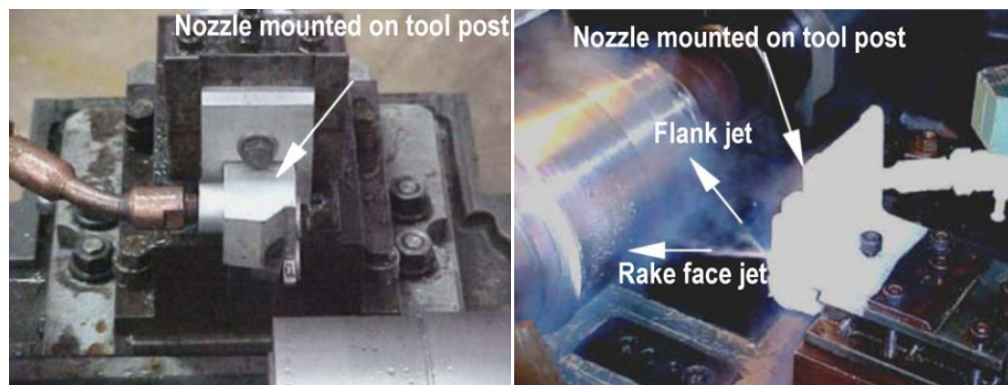


Figure 15: Application Nozzle (15)

Experimentation showed that at a cutting speed of 70 m/min, the use of soluble oil coolant reduced the rate of tool wear in comparison to dry machining while the use of cryogenic cooling reduced the rate of tool wear to an even larger extent. At higher cutting speeds of 100m/min to 117m/min, the advantage of using soluble oil and cryogenic cooling decreased. The reason for this could be that the rate at which heat is generated at the cutting edge exceeded the rate at which the cryogenic cooling could remove heat. It may be that the coolant was not able to reach the chip-tool interface due to the close contact at high cutting speeds. (15)

Tool life at a cutting velocity of 70 m/min was observed to be 7 minutes for dry machining, 14 minutes when soluble oil is used and 24 minutes when cryogenic cooling was implemented. At higher velocities of 100 m/min and 117 m/min, the benefits of using cryogenic cooling decreased. A possible explanation for this is that the liquid nitrogen used did not penetrate the tool-chip interface well enough.(15)

Rake face cooling using liquid nitrogen

Wang et al (13) developed a cooling system that circulates liquid nitrogen on the surface of the cutting insert (Figure 16). The system was constructed using a hollow cap that is fixed to the top of the tool. The

cap is then supplied with liquid nitrogen (LN_2) from a reservoir and the boiled off nitrogen gas is vented through an outlet.

During experimentation the cutting forces as well as temperature of the tool was measured. The temperature was measured using a 0.8mm K-type thermocouple that was mounted approximately 5mm from the cutting edge of the tool. The reasoning behind the large distance from the cutting edge is to prevent the thermocouple from interfering with the machining process. Forces were measured using a Kistler piezoelectric dynamometer. (13)

The objective of this system is to cool the cutting insert without subjecting the work piece material to the LN_2 . When the work piece is subjected to LN_2 a number of undesirable side-effects may occur, such as dimensional reduction and thermal hardening. (13)

Experiments were conducted with cutting conditions as shown in Table 3. The cutting inserts used were supplied by Sandvik and is a H13A square cemented carbide tool. Benchmark experiments were carried out with conventional cooling. (13)

Conventional cooling resulted in 1.1mm, while LN_2 cooling resulted in 0.22mm of flank wear after 46mm of linear machining. This results in a 400% improvement in tool life at these high cutting speeds. The force measurements showed that there is no significant change in cutting forces. It was however noted that when chip entanglement occurred, the cutting forces was extraordinarily high. It can therefore be concluded that the improvement in tool life is due to the tools hardness and toughness being maintained as well as its decreased chemical reactivity due to the lower tool temperature. The lower tool temperatures also resulted in an improved surface finish. One can also argue that the improved surface finish is a result of the cutting edge staying intact for a longer period of time.(13)

Table 3: Cutting Conditions for experiments by Wang et al. (13)

Cutting Speed (v_c)	132 m/min
Feed rate (f)	0.2 mm/rev
Depth of Cut (a_p)	1.0 mm

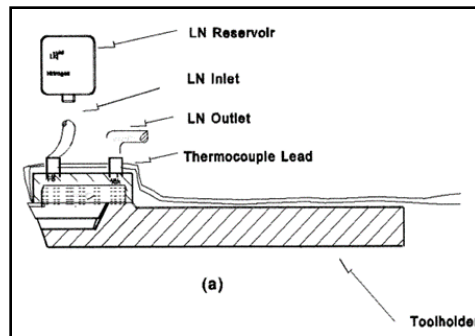


Figure 16: Rake face cooling using liquid Nitrogen (13)

Liquid nitrogen cooling using a modified tool holder

Ahmed et al (6) designed a liquid nitrogen cooling system in which he attempts to cool the cutting insert by modifying the tool holder to cool the cutting insert from the mounting face. The basic principle behind the system is to keep the cutting insert cool in order to maintain its hardness and toughness.

A standard PSBNR 2525 M12 tool holder was used. This tool holder utilises a 12mm square insert with a neutral (0°) rake face. A counter bore was made in the mounting surface of the tool holder with a 10mm diameter and 4mm deep. This pocket contains the LN_2 that is in contact with the cutting insert. A channel was made by EDM through the tool holder that supplies the pocket with LN_2 . Once the insert has been bolted down, it forms a closed pocket with the counter bore. The evaporated gas is discharged through a small hole in the wall of the pocket to the atmosphere. Two different locations have been chosen for the discharge ports. The first is directed at the uncut material right in front of the cutting edge. This design is referred to as design 1. The second was aimed away from the work piece. This design is referred to as design 2. (6)

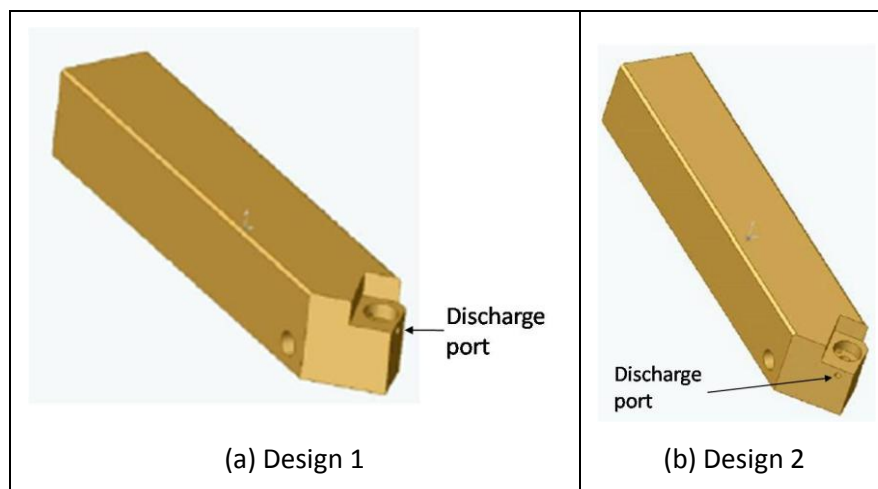


Figure 17: Modified tool holder design (6)

It is clear from the results that the cooling of the insert by means of conduction shows promising results. Another clear result is that cooling of the work piece should be prevented. When the evaporated nitrogen gas is discharged in front of the cutting edge (material still to be removed), the surface finish was drastically worse than dry cutting. This is believed to be due to the hardening of the material when cooled. This is confirmed by another experiment where nitrogen gas is discharged behind the cutting edge, where the tool life was prolonged and surface finish improved. Research using work piece pre-cooling also confirm this result (14).

It is however important to notice that the data reported creates some doubt. The author initially reports flank wear at a cutting speed of 450 m/min, then reports data in terms of constant rpm, although the same numerical values are used. According to the data published, longitudinal cuts has to be performed on a 318mm diameter work piece to obtain the cutting conditions reported. Considering the cost of a test piece of this size, it is possible that inaccuracies may have occurred during data analysis. Another concern is that the wear pattern plots do not correspond to the titles assigned. The way the results are reported also leaves the option for inaccuracy open. (6)

Modified Chip Breaker

This design is based on 3 main principles, to

- Minimize LN₂ waste
- Have the LN₂ flow rate proportional to the heat generation
- To be able to commercially develop the micro-nozzle

The author approached the problem by modifying a chip breaker to form two jets that directs the LN₂ at the cutting edge, as can be seen in Figure 18(7). The chip breaker lifts the titanium chip so that the LN₂ can be forced between the rake face and the chip to penetrate closer to the chip-tool interface. The evaporated LN₂ will also create a vapour cushion to reduce friction and wear(7). To deliver the LN₂ to the cutting zone, channels are etched out on the lower surface of the chip breaker. These channels are directed at the cutting edge where most of the heat is generated. The jets are formed when the chip breaker seals on the cutting insert. An auxiliary jet was added to deliver LN₂ to the flank face. A design of the complete cryogenic cooling system can be seen in Figure 19 and Figure 20. The insert that was used for the tests was a CNMA432-K68 manufactured by Kennametal, a carbide insert recommended for titanium machining. For the experiment, the depth of cut was set to 1.27 mm and the feed at 0.254

mm/rev. The cutting speeds for the tests performed were set at 60, 90, 120 and 150 m/s. Tool life criteria were defined by the values in Table 4. (7)

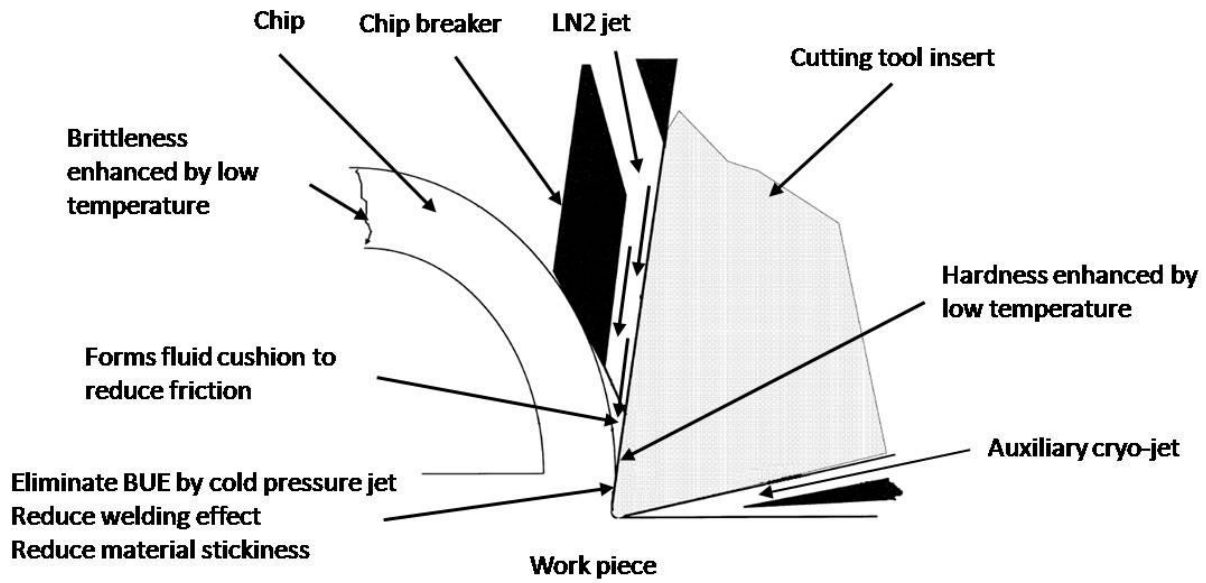


Figure 18 - Schematic drawing of design (7)

Table 4: Tool life criteria (7)

Average flank wear (V_{BAvg})	0.3 mm
Maximum flank wear (V_{BMax})	0.6 mm
Crater depth	$0.06\text{mm} + 0.3 \times \text{Feed}$

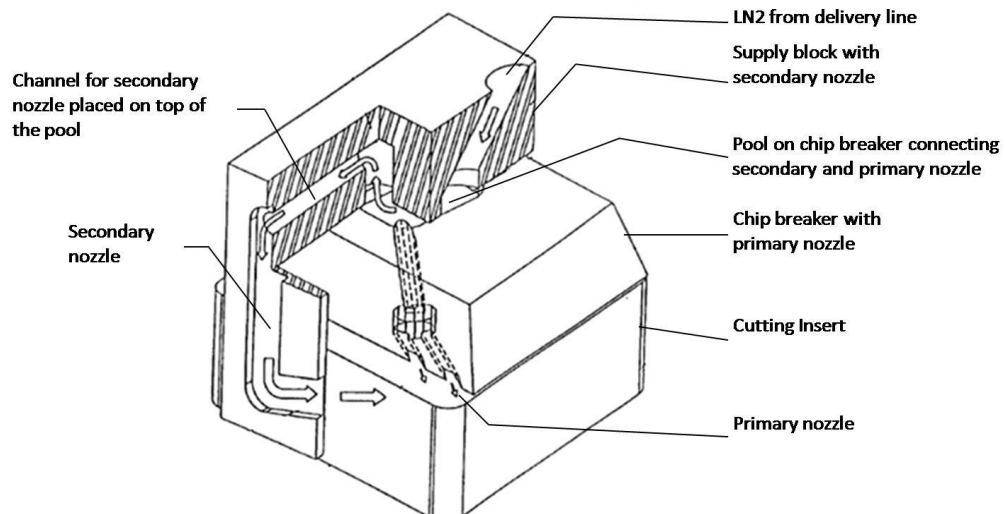


Figure 19 - Design of cryogenic nozzle: Auxiliary nozzle active (7)

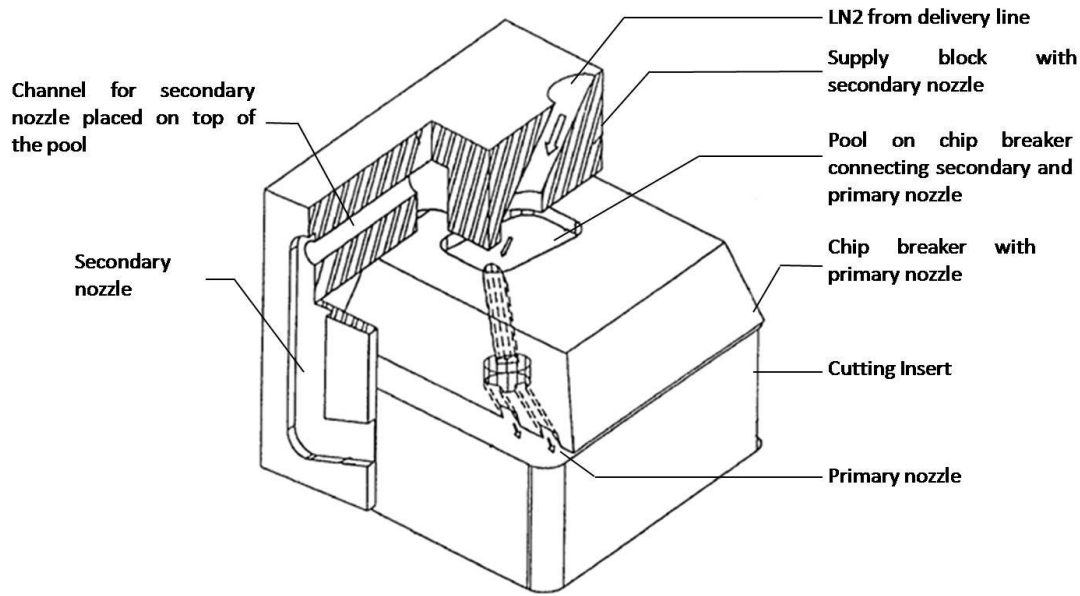


Figure 20 - Design of cryogenic nozzle: Auxiliary nozzle inactive (7)

To establish a baseline, Hong et al. performed their own conventional emulsion cooling test. The emulsion was mixed with water to a ratio of 1:20, and applied at 4.9 l/min. The results they reported represented a longer tool life than other results found in literature. This is believed to be state-of-the-art by machining specialists and can be found in Table 5. (7)

A method of flood cooling with LN₂ was also tested. This method floods the cutting region with LN₂, similar to flood cooling with emulsion coolant. The disadvantage of this method is its high consumption of LN₂ and that it results in poor tool life. The LN₂ was delivered at 1.4 – 2.4 MPa. An improvement in tool life was only noticed after adding a nozzle to the rake face, as well as the flank face, increasing the LN₂ consumption to 3.36 kg/min. This method improved tool life to 8min45sec at a cutting speed of 90m/min compared to the 4 minutes 50 seconds with conventional cooling.

A variety of cooling configurations using the new generation cooling methods were tested. The following configurations were included in the experiments. Configuration 1 consisted of only a rake face nozzle (primary nozzle). Configuration 2 comprised of the flank face nozzle (secondary nozzle) only. Configuration 3 is defined by using both the primary and secondary nozzles. Another two variables that were tested are the angle of the chip breaker relative to the cutting edge (λ) as well as the distance it is placed from the edge (l) Figure 21. These variables influence the effectiveness of the cooling, and it was found that the best configuration was a λ of 15 degrees and an l of 1.25 mm. It was also noted that if the chip breaker was 1.00 mm or closer to the edge, the primary nozzle tended to clog. The tool life using

this method was found to be 8 min 51 sec at a cutting speed of 90 m/min, which is a 79% improvement over their conventional emulsion cooling (7).

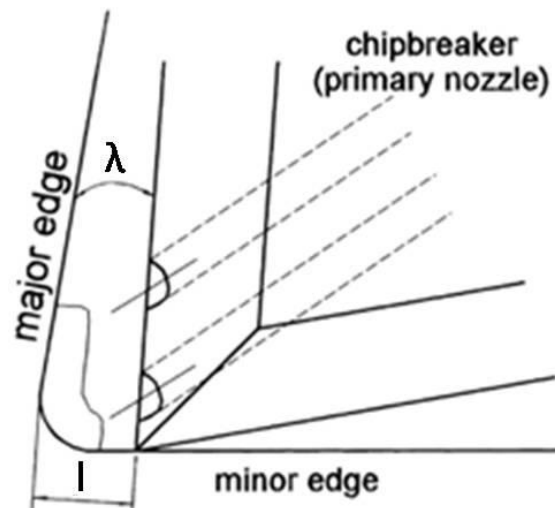


Figure 21 - Chip breaker position (7)

Table 5: Experimental tool life results and comparison (7)

Cooling Method	<u>Cutting Speed [m/min]</u>			
	60	90	120	150
Conventional Emulsion	17min 30sec	4min 50sec	2min 38 sec	56sec
Primary nozzle ONLY	Not tested	547 s	Not tested	Not tested
Primary and secondary nozzle	27min 33sec	15min 48sec	7min 17sec	4min 56 sec
<u>Percentage improvement over conventional emulsion cooling</u>				
Primary nozzle ONLY	Not tested	89%	Not tested	Not tested
Primary and secondary nozzle	57%	227%	177%	429%

Temperatures in cryogenic machining

Hong et al (14) conducted a finite element modelling (FEM) analysis for a number of cryogenic cooling solutions, also described above, to determine their effectiveness in reducing the temperature of the tool. The cutting conditions for the experiments are set at a cutting speed of 90 m/min, a feed rate of 0.254 mm/rev and a depth of cut of 1.27mm. They then conducted experiments to determine the accuracy of the temperatures. The results are shown in Figure 22. From the results we can conclude that the use of the modified tool holder does cool the cutting insert, although the use of conventional emulsion cooling yields lower temperatures. This is due to the thickness of the insert that prohibits the

LN₂ to effectively cool the cutting edge. Of all the singular cooling approaches, the use of rake jets was the most effective. Although the use of work piece pre cooling yields lower tool temperatures than the rake jets, the increased hardness of the material yields poor surface finish and is therefore not a competitor for emulsion cooling.

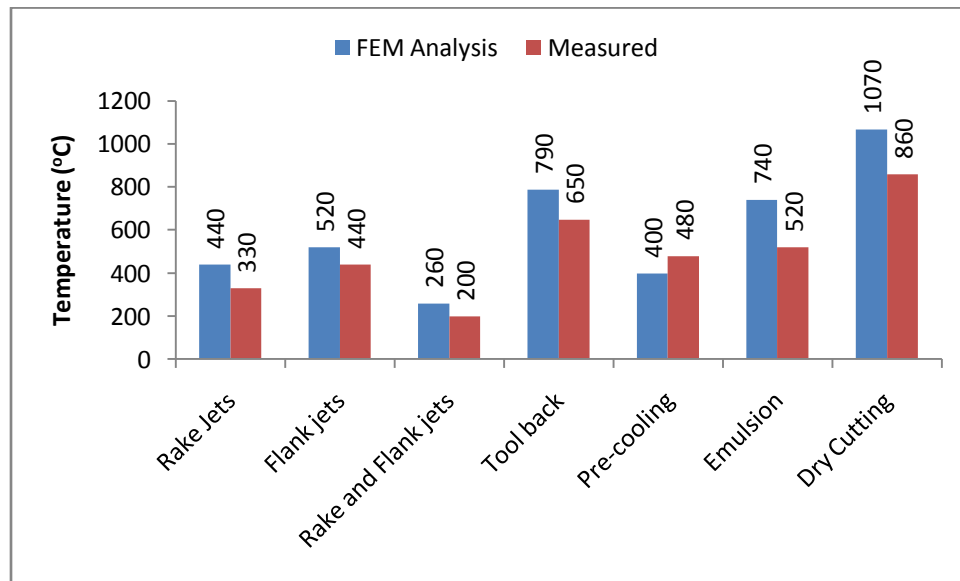


Figure 22: Tool temperatures when machining Ti-6Al-4V (14)

3.10. Design objectives

To be able to investigate the hypothesis, a number of objectives have been identified.

- Cool the insert as much as possible

- Prevent work piece cooling

4. Design Concept

The design aimed to satisfy as many of the objectives as possible. The tool cap approach focuses the LN₂ cooling on the rake face of the cutting insert and prevents it from coming into contact with the work piece. The benchmark tests were performed on RCMW 12 04 M0 H13A inserts, that is an uncoated tungsten carbide (WC) insert. These inserts are held into position by a screw. Research is performed on WC inserts with LN₂ cooling (13) using a similar tool cap type approach. The fundamental principle of this cooling approach is the use of the heat conduction through the insert body to keep the cutting edge cool. PCD has previously been used within the Stellenbosch titanium research group to machine Ti-6Al-4V with considerable success (27). The realisation that PCD has more than 5 times the thermal

conductivity of WC (Table 6) opened the possibility of combining the localised LN₂ cooling with PCD to realise significant improvements. From thermodynamics principles it is known that the amount of heat that is transferred is directly proportional to the contact area between the two media. It would therefore be advantageous to increase the area exposed to the LN₂ to a maximum.

Table 6: Material Conductivity

Material	Conductivity [W(mK) ⁻¹]	Reference
H13A Tungsten Carbide (WC)	100	(13)
CTB010 Polycrystalline Diamond (PCD)	540	(28)

The next topic of discussion is the location of the localised cooling. Two primary approaches are to apply it to the rake face or the back face of the insert. Both approaches have been researched on WC inserts. As described in the literature study, Ahmed et al. (6) investigated the use of localised LN₂ cooling on the tool back. Although the method of discharging the LN₂ influenced the results, improvements were achieved. Wang et al applied localised LN₂ cooling to the rake face with exceptional improvements in tool life. It is therefore possible to conclude that it is better to cool on the rake face, because of the distance between the face being cooled and the cutting edge. With the PCD inserts, the difference in cooling power of cooling the rake face and tool back would be even larger. The PCD layer is deposited on a WC base. If the tool back is cooled, the WC base would diminish the cooling rate because of its lower thermal conductivity. If cooled directly on the rake face, this would not be the case. It was therefore decided that the rake face would be cooled.

In order to maximise the area of the rake face exposed to the LN₂, it was decided not to screw the PCD cutting insert into position, instead the tool cap would be used to clamp down the cutting insert. By not screwing down the insert, the rake face area is increased by 35.5%. However, the tool cap cannot cover the whole insert as 0.6mm of the cutting edge will be exposed and the tool cap will have a wall thickness of 1mm. Taking this into account, eliminating the screw increases the area exposed to LN₂ by 95%.

4.1.1. Tool holder modification

In order to clamp the PCD insert into place, the tool cap had to be securely fastened to the tool holder. To achieve this objective, the tool holder had to be modified. A dowel and an M6 threaded hole were drilled in the shaft of the holder. The dowel hole has the purpose of fixing the position of the tool cap, as well as to keep it horizontal when clamping down the insert. An M6 Allen cap bolt is used to bolt down

the tool cap and exert the required pressure on the insert. Figure 23 show both the original and modified tool holder.

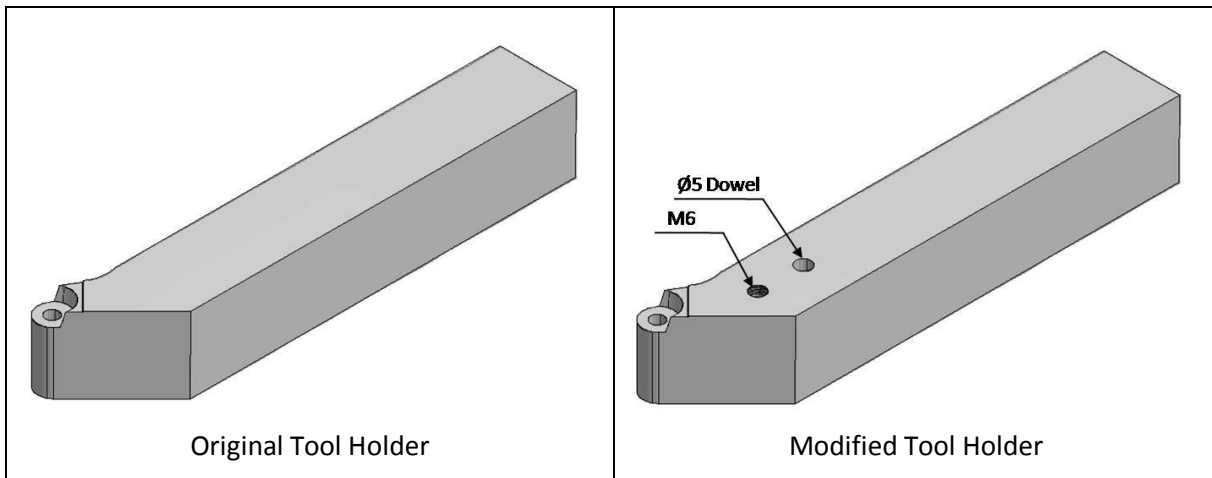


Figure 23: Tool Holder: SRSCl 12 04 M0

4.1.2. Tool Cap

The initial tool cap design is attached as Appendix 1, and a 3D Model is shown in Figure 24. In this design the LN_2 enters the tool cap from the side of the tool cap. The LN_2 then drops down to the tool rake surface. Here the LN_2 boils off to nitrogen gas, expanding approximately 700 times in volume, while absorbing latent heat from the insert during the phase change from liquid to gas. The resulting nitrogen gas contains no water vapour. This gas purges the air out the system through the venting port on top of the tool cap (Figure 24). This is important because the air contains water vapour that could form an ice plug in the system. When the tool cap is bolted down, it presses down on the insert to clamp it into position. The tool cap was manufactured from EN36B steel. This is the same steel grade as the tool is manufactured from.

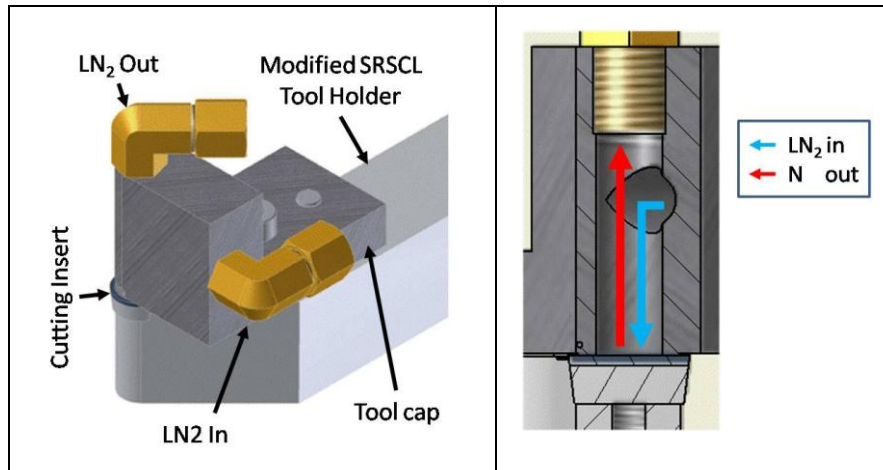


Figure 24: Tool Cap design 1

Initial testing was done with the tool cap and a WC insert with conventional soluble oil cooling. The cutting insert failed catastrophically within 10mm of cutting. The reason for this occurrence was chip flow obstruction. The tool cap is designed with the chip breaker having a 90° angle with the rake face. This configuration prevented the chips from clearing away from the cutting region. This resulted in the chips being accumulated between the tool cap and the work piece, preventing the coolant from reaching the cutting region. The result was that the cutting edge temperatures increased drastically, softening the cutting insert. With the insert in a softened state, the cutting edge could not withstand the cutting forces, and the suffered catastrophic chipping. It is therefore concluded that chip flow and removal might have a large influence on the tool life of a cutting insert.

A new tool cap and experimental plan was then designed in order to aid in chip removal. The new tool cap design is added in Appendix 1, and a 3D model is shown in Figure 25. This tool is designed to do longitudinal cuts instead of facing cuts. With longitudinal cuts the tool is cutting for longer intervals. This may demonstrate the effect that cutting cycle time has on the tool life of the cutting insert. The new design uses the same fixing points, while the LN_2 enter and exit the tool cap at the top of the tool cap. The aim of this supply configuration is too simultaneously test tool life improvements and whether it is possible to supply the LN_2 by a gravity feed system. The weight of the LN_2 on the surface should counter the coolant jet impingement effect (29) on the surface of the tool. The LN_2 will boil off and the nitrogen gas will return up the supply pipe and escape from the supply reservoir to the atmosphere.

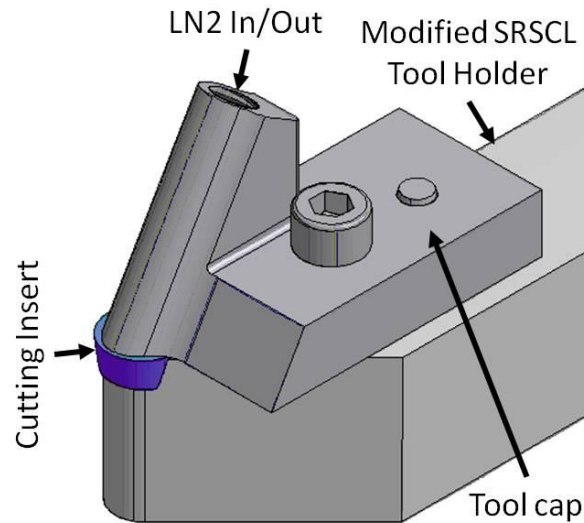


Figure 25: Tool cap design 2

The new tool cap design did however have a number of sharp edges that is exposed to the chip flow. Considering that the wall thickness around the LN₂ feed tube is thin (1mm) and the cap is responsible for holding down the PCD inserts in place, it was decided that the original EN36B material will not be sufficient for the new application. Although the EN36B steel has a high wear resistance, its high carbon content makes it brittle at cryogenic temperatures. As the new tool cap requires a tougher material under cryogenic conditions, 316 stainless steel was used.

In the new tool design, the feed tube is situated at a 60° angle relative to the tool rake face. This creates the chip breaker clearance angle as well as aids in cooling the insert. The 60° angle was adopted from a CSKNL tool holder that utilises a shoe to press down to hold the insert in place. As the tool cap will also perform this purpose with the PCD inserts, it was decided to utilise the same angle. The angled feed tube creates an oval area on the insert surface that increases the surface that is exposed to the LN₂. This in turn is expected to result in better cooling of the insert.

5. Methodology

A research plan was drawn up to ensure that the research done will supply the data required to support the conclusions of the research. The research design also aids to determine the work piece material required, material preparations, cutting tools and quantity required. It also allows the researcher to devise a plan of action to obtain the required data.

5.1. Research design

The research design defines the experimental procedure that needs to be followed in order to address the research objectives that were set. For this experimentation, operations are focused on turning as this eliminates the complex task of supplying a moving tool with liquid nitrogen.

To simplify data capturing during the experimental procedure, facing cuts are to be done on titanium. Facing cuts allow the amount of material removed per cut to stay constant for the entire experiment, thus keeping the cutting time per cut constant. This simplifies the calculations and minimizes the data that needs to be collected during experimentation.

Facing cuts do however require the rotational speed to change during the cut in order to keep the cutting speed constant. To achieve this, the G96 code of the lathe is utilised. This function keeps the cutting speed constant by changing the rotational speed to correspond with the immediate diameter. The rotational speeds were confirmed during pilot testing by photographing the digital readout and comparing the rotational speed with the co-ordinates. During the pilot testing it was noted that the lathe is not able to maintain the correct cutting speed over the complete length of the cut when cutting from the outside diameter (OD) to the inside diameter (ID) (Figure 26(b)). To correct this, either the cutting parameters can be changed or the tool path can be changed. The influence of the parameters was calculated and is shown in Figure 27. By trial and error, it was determined that the acceleration of the lathe is limited to approximately 500rev/s^2 . This was done by taking a video of the digital readout and then analysing it frame by frame. The X-axis dimension, corresponding to the diameter of the work piece, was compared with the graph in Figure 27 to determine the limit of the machine.

When the tool cuts from the OD to the ID, the lathe has to increase its spindle speed according to the graph from the right to the left. Toward the end of the cut, the rotational speed acceleration required for speeds greater than 120 m/min and feeds greater than 0.10 mm/rev becomes too large for the machine to achieve. The decision was therefore made to change the tool path. To eliminate the rapid acceleration of the lathe as the tool moves to the centre, the tool path was changed to execute a facing cut from the ID to the OD (Figure 26(a)). This cutting path utilises the forces of the cutting operation to aid the lathe in deceleration. This makes it possible to change any of the parameters without the risks of the rotational speed not being achieved. The ID of the work piece was also increased to 22.5mm to allow enough time between cuts for the spindle to accelerate.

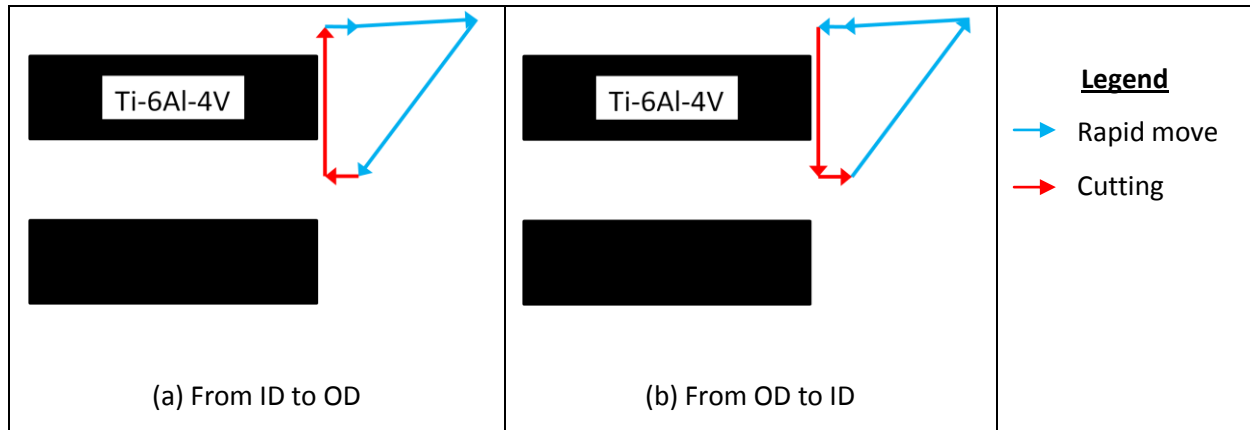


Figure 26: Tool Movements

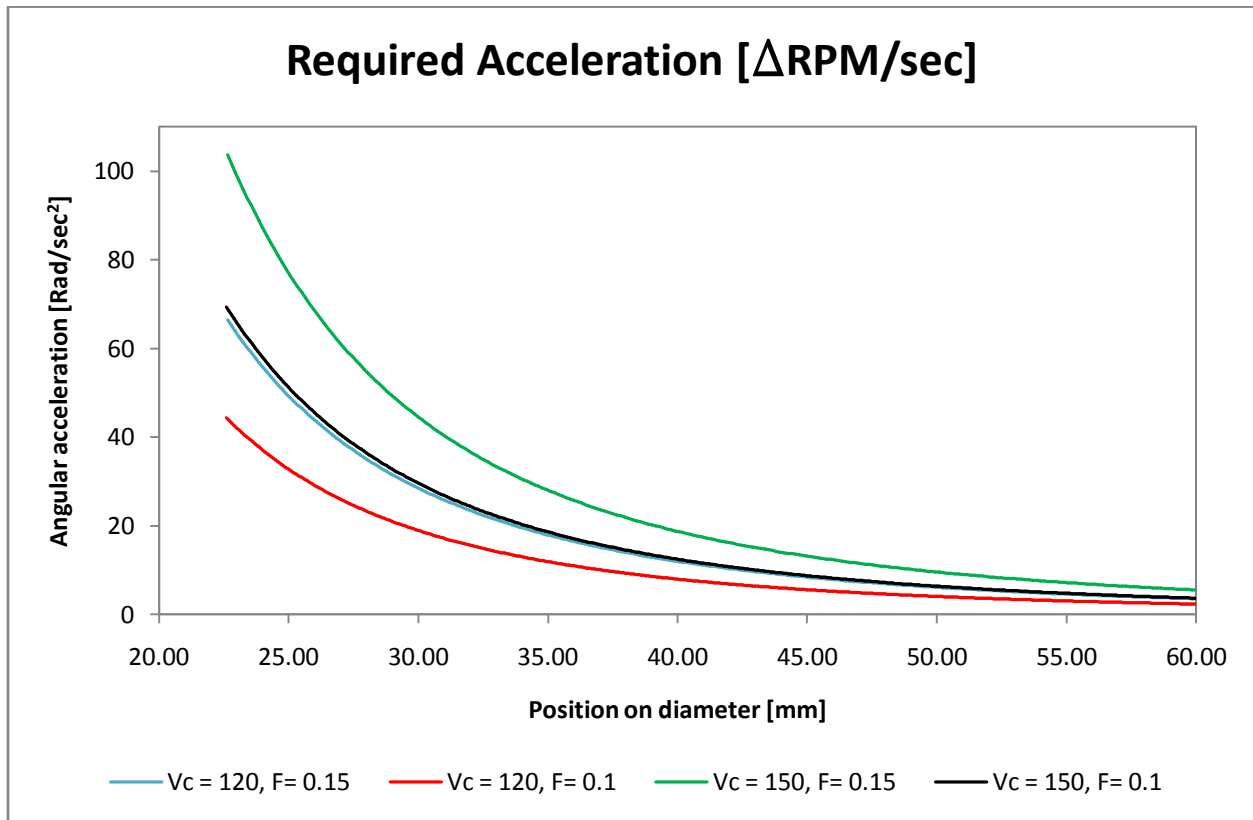


Figure 27: Rotational acceleration requirements

The CNC program for the lathe is shown in Figure 28. As stated earlier, the G96 code has been used to keep the cutting speed constant. Together with this, the G71 code is used to program the facing cuts. In order to allow the spindle to achieve the required rotational speed, the cut was programmed to start at a diameter of 10mm instead of 22.5mm.

WC PILOT TESTS	Vc	150	DOC: 0.25	Feed: 0.15	OD: 55	ID: 22.5	# CUTS: 1
O0189							
N01	G96	S 150.0	T0707	M 04	M 08		
N02	G50	S 2200.0					
N03	G00	X 10.0	Z 0.0				
N04	G72	W 0.25	R 0.2				
N05	G72	P 06	Q 07	U 0.0	W 0.0	F 0.15	
N06	G01	Z -0.25					
N07	G01	X 60.0					
N08	G00	X 150.0	Z 150.0				
N09	M05	M 09					
N10	M30						

Figure 28: CNC facing cycle code

The work piece material used was a Ti-6Al-4V annealed only round bar with an OD of 57.15mm (2¼"). To accurately calculate the material removed and remove any irregularities on the surface, the OD was turned down to 55.0mm. The centre was drilled to a diameter of 22.5mm to ensure accurate calculation of the material removed by the tool.

To aid data capturing during experimentation, a spreadsheet was compiled on which the data can be filled in. The templates for facing cuts are added in Appendix 2.

After initial pilot testing the research design was changed. The costs of drilling the centre of the titanium to a 22.5mm diameter proved to be a very costly and time consuming exercise. The solution is to change to longitudinal cuts. Longitudinal cuts require more calculations and meticulous record keeping of the experimental parameters and conditions. Because the total length of the material cannot be machined in one operation, the fillet effect described in section 7.2 had to be counteracted. This was done by conducting clearance cuts with a square type insert to produce a small fillet radius of 0.8mm.

The CNC code for the machining had to be continuously adapted to control the number of cuts made. The CNC code is shown in Figure 29. The parameter noted 1 in the figure defines the work piece diameter before machining and the parameter noted 2 the work piece diameter after machining. These two parameters are constantly adapted during experimentation.

WC PILOT TESTS	Vc	150	DOC: 0.25	Feed: 0.15	OD: 55	LOC: 100	# CUTS: 1
O0195							
N01	G96	S 150.0	T0707	M 04	M 08		
N02	G50	S 2200.0					
N03	G00	X 55.0 ¹	Z 1.0				
N04	G71	U 0.25	R 0.2				
N05	G71	P 06	Q 07	U 0.0	W 0.0	F 0.15	
N06	G01	X 54.5 ²					
N07	G01	Z -50.0					
N08	G00	X 150.0	Z 150.0				
N09	M05	M 09					
N10	M30						

Figure 29: CNC code for longitudinal cutting

The data capturing sheet created for the experiments is added in Appendix 2.

5.2. Instrumentation

The instrumentation and equipment required to conduct the experimentation is described in the following sections.

5.2.1. Cutting tools

To ensure significance of the experimentation, the tool grade for benchmark experimentation has to be representative of a common industrial tool material. The uncoated carbide grade H13A from Sandvik was therefore chosen as the benchmark tool grade. H13A is the carbide grade recommended by Sandvik for Ti-6Al-4V machining. Industry does however use inserts with coatings. The coatings tend to differ from one manufacturer to the next. To eliminate the effects of the different coatings, uncoated inserts are used. The merit of coatings for titanium machining is currently a controversy, with several literature sources reporting economic benefit to be unproven, supporting the decision to use uncoated carbide as tool material. (1)

A round insert was chosen to avoid unnecessary complications when manufacturing the liquid nitrogen (LN₂) tool cap. As the tool cap is required to seal on the rake face of the insert, the insert needs to have a smooth rake face. The rake angle was also decided to be neutral to avoid unnecessary manufacturing complications. With all these specifications in mind the RCMW 12 04 M0 H13A insert from Sandvik was chosen. This insert has a 7° flank clearance angle and a total thickness of 4.76mm.

From these specifications, specialized PCD inserts was supplied by Element 6. The inserts has the same diameter (12mm) and flank clearance angle (7°) as the carbide inserts. The rake face of the insert is flat with no geometric features and no hole for fixing it to the tool holder. This exposes the maximum amount of surface area. These inserts will therefore be held in position by the force exerted by the tool cap. The inserts has a carbide base with a PCD layer on top of approximately 0.5mm. The total thickness of the inserts is 3.2mm. Because this differs from the standard insert, a customised spacer had to be manufactured to lift the PCD insert to the correct level. The drawing for the spacer is attached as Appendix 3.

Table 7: RCMW Insert geometry

Insert Diameter (id)	12 mm
Clearance angle	7°
Rake face (γ)	Neutral (0°)

5.2.2. Experimental set-up

The experimental set-up is shown in Figure 30. The LN_2 was decanted from the Dewar into the reservoir. The initialisation of the system is a rather time consuming process. When the system is set up, all the components are at the temperature of the CNC room (approximately 22°C). At this temperature, the LN_2 evaporates at a rapid rate. It is therefore necessary to allow the system to settle to the lower temperatures before starting experimentation. At the same time the system is essentially purged from atmospheric air, containing water vapour. The atmospheric air contains water vapour that will freeze at LN_2 temperatures. This could cause a frozen plug in the LN_2 supply system preventing the LN_2 from reaching the tool rake face. After the LN_2 has reached the tool cap, the reservoir is refilled. At this time, the system has acclimatised and the evaporation rate has dramatically declined. The system is then ready for experimentation.

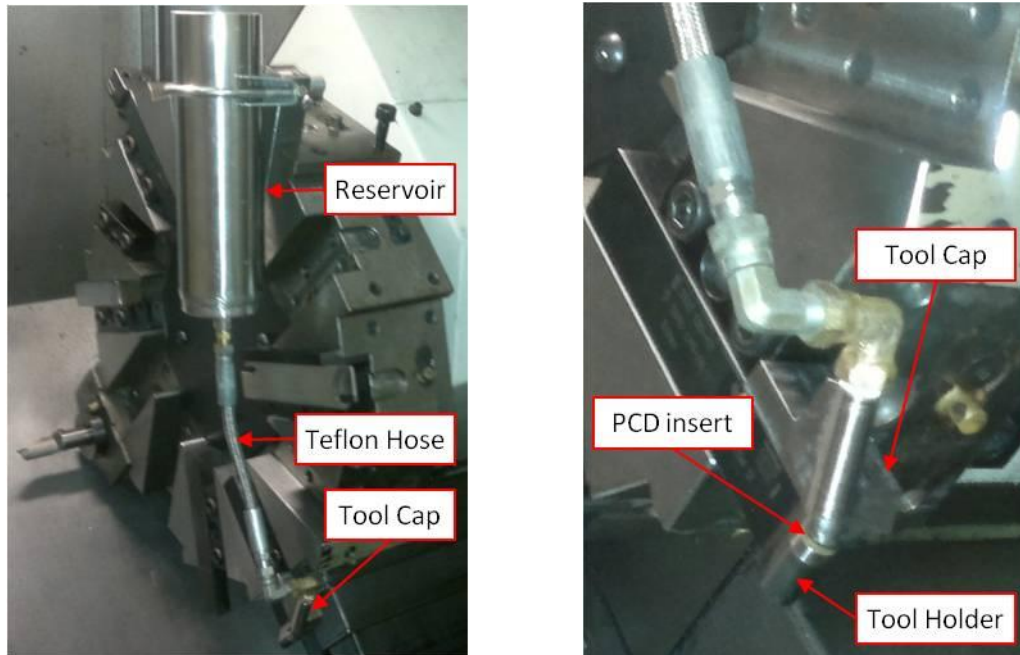


Figure 30: Experimental setup

5.2.3. LN₂ supply

If not used correctly liquid nitrogen can have serious repercussions. When liquid nitrogen changes from the liquid phase to gaseous phase, its volume increases 700 times. This results in a dramatic increase in pressure in an enclosed vessel. It is therefore critical that pressure relief valves be installed between any two points in a system that can be closed off, for example between two valves. Equipment such as ball valves cannot be used with LN₂ due to the hole through the ball creating a pressure vessel when in a closed position. The extreme sub-zero temperatures also limit the materials that can be used. Most materials become brittle at cryogenic temperatures. Consultation with the engineers at the LN₂ suppliers approved brass, stainless steel (S/S) and Teflon (PTFE) to be used for parts made for cryogenic use.

Taking these factors into account, it was decided that the LN₂ will be supplied by gravity feed. Although this would not be a commercially viable solution due to evaporation, it is sufficient for experimental purposes. The design consists out of a reservoir, a fixing adapter and the connection pipe. The complete design is attached as Appendix 4.

The reservoir consists out of a S/S pipe with a 60mm OD and a manufactured pipe end. The pipe end was originally manufactured from Teflon and was then press fitted into the stainless steel pipe. Due to the large difference in expansion coefficient of S/S (16×10^{-6} m/m-K) and Teflon (110×10^{-6} m/m-K), as

well as a vapour layer, the Teflon shrunk at a much higher rate than the S/S. This resulted in a clearance fit causing the LN₂ to leak out through the fit within the first minute. A vapour layer also developed between the S/S pipe wall and the LN₂ (Figure 31) limiting the contact of the LN₂ with the reservoir wall. This layer develops as the LN₂ boils when it comes into contact with the S/S pipe wall. This is however not the case with the Teflon base. Because of the weight of the LN₂, it is always in contact with the base. The temperature of the PTFE base is therefore cooled much more rapidly than the S/S pipe and as a result the base shrinks more rapidly. These effects causes the interference fit to become a clearance fit causing the reservoir to rapidly leak. The reservoir was therefore redesigned using a S/S base. The base was welded onto the S/S pipe to prevent it from leaking.

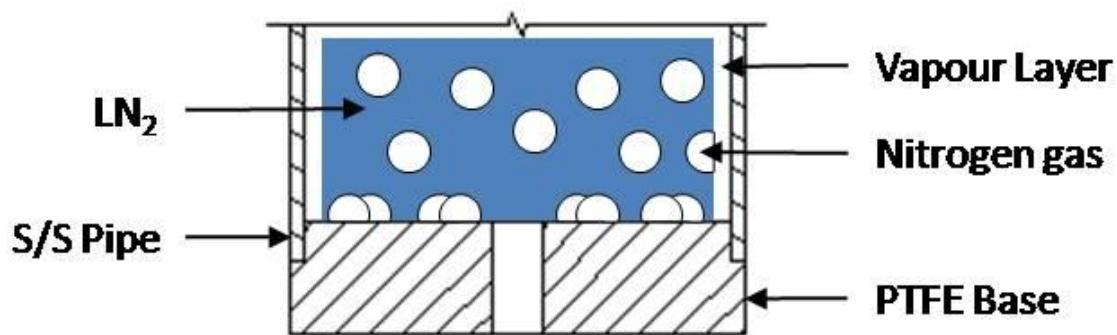


Figure 31: Reservoir with PTFE Base

The reservoir is fixed to the tool turret of the lathe. This eliminates the tool cap from moving relative to the reservoir. The result is that the pipe connecting the tool cap with the reservoir will not be required to move once the system is set up. Although vacuum jacketed piping is most suitable for LN₂, it is expensive. Teflon braided stainless steel hose is considerably lower in cost and delivers adequate insulation for the experimental requirements. The pipe is fitted with two female couplings on both sides, one of which is a swivel fitting.

5.2.4. Connecting the Reservoir with the tool cap

The reservoir is connected to the tool cap by means of a stainless steel braided Teflon hose with adaptor fittings. With the tool cap design 1 (Figure 24) the Teflon hose was connected to the tool cap using a straight M8 x 1/8 BSP fitting. LN₂ was then deposited into the reservoir. The system is then left to cool down, minimising the boil-off due to the temperature of the system. When the system starts to settle, the edge of the cutting insert develops an ice layer (Figure 32). This indicates that the LN₂ has reached the tool cap and the cutting insert. It is critical that the LN₂ rapidly reach the cutting insert. Pure nitrogen gas is denser than air and when the LN₂ boils off from the insert rake face, the nitrogen gas displaces the

air that contains moisture, towards the open end of the system. This is known as purging the system. Once this has been achieved we are certain that all the water vapour has been forced from the system and the risk of a plug forming has been eliminated.

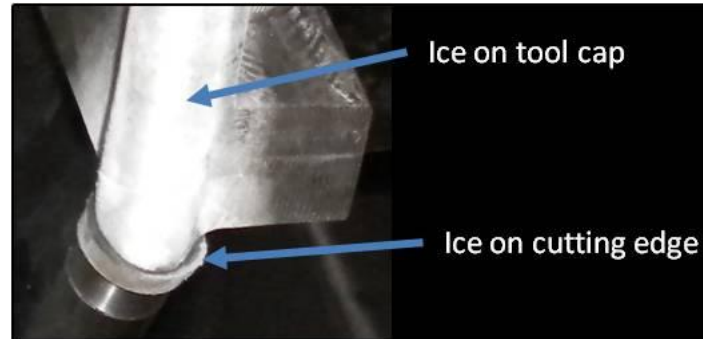


Figure 32: Ice developing on cutting edge

The situation with the second tool cap design is however different. The design of the tool turret renders the connection method used with tool cap design 1 infeasible. Initially two 90° connections were used to connect the reservoir (Figure 33).

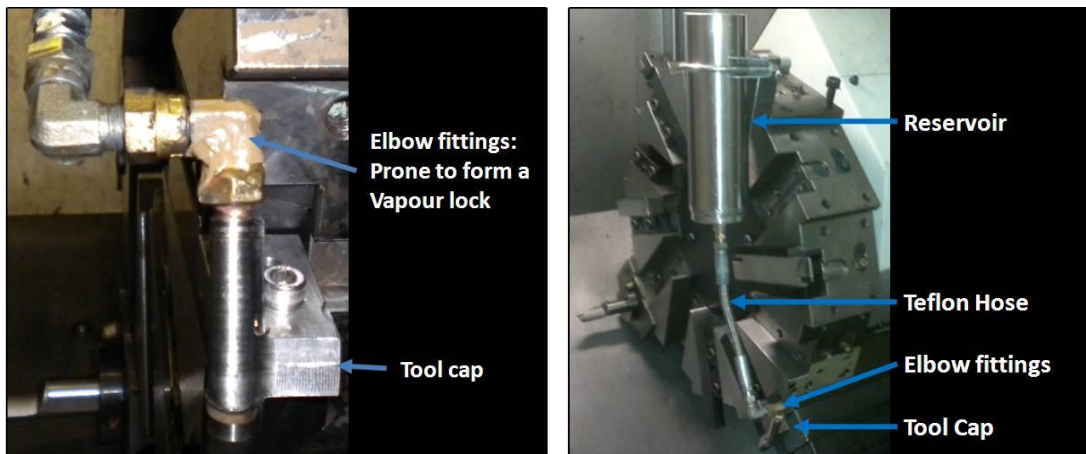


Figure 33: LN₂ supply setup – Prone to forming ice plugs

This setup was however prone to cause an ice plug in the pipe. Because the inner diameter of the piping is of relative small diameter (4mm), the sharp turns in the 90° elbows restricted the flow of LN₂ as a result of turbulence as well as improved heat transfer. The LN₂ then boiled off in the elbows instead of the tool cap which considerably slowed down the purging process. This allows the water vapour to freeze to the walls of the Teflon hose, resulting in an ice plug (Figure 34).

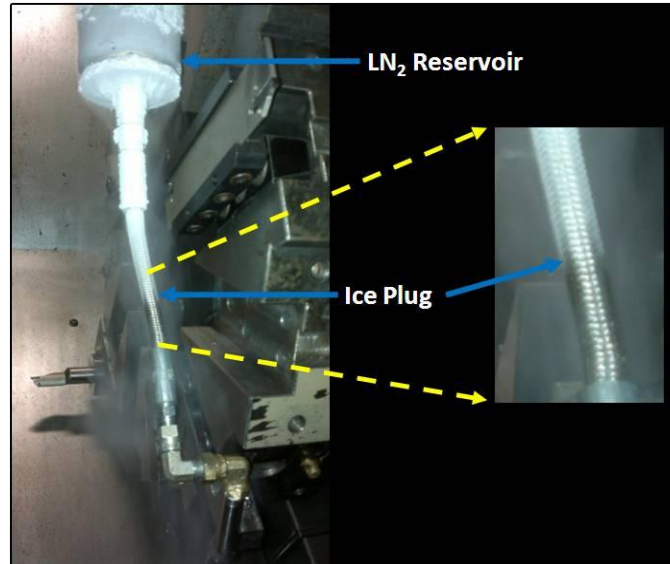


Figure 34: Forming of an ice plug

The solution to the situation was a custom made copper pipe. To allow the LN₂ to descend to the insert rake face as rapidly as possible, the connection should be as straight as possible. The custom connection pipe was therefore made with a gradual bend (Figure 35). Because the clearance between the tool cap and tool turret is only 30mm, there is no space for off the shelf fittings. A banjo bolt was therefore modified and brazed onto the bottom end of the copper pipe. The other end was fitted with a 1/8 NPT female fitting using a ferrule type of fitting.



Figure 35: Custom copper pipe

5.2.5. Confirmation of material properties

To ensure that the experiments are comparable to literature, the material properties are to be confirmed. This is done by conducting a hardness test. The hardness of a material has a direct correlation with the tensile strength of the material. The hardness of the material was therefore tested using a Vickers type indentation hardness tester. A conical diamond tip was used with a 150kg load, resulting in a Rockwell C reading. Some material specifications of the titanium supplied is shown in Table 8. Five pieces of Ti-6Al-4V with dimensions $\varnothing 57.15 \times 250$ mm was supplied by Titanium a2z. The material was supplied from two different batches. A sample from each batch was therefore chosen for to confirm the hardness. The hardness test results for both samples are shown in Table 9. The hardness of the material was tested on the circumference and on the face of the material at different radial positions. This confirmed that the material conforms to the standard right to its core.

Table 8: Ti-6Al-4V annealed only material specifications (30)

Ultimate Tensile strength	950 MPa
Yield Tensile Strength	880 MPa
Hardness	36 HRC

Table 9: Measured hardness of Ti-6Al-4V samples

Position	Sample: Batch 1	Sample: Batch 2
On OD	37 HRC	40 HRC
$\varnothing 49$	37 HRC	36 HRC
$\varnothing 41$	36 HRC	37 HRC
$\varnothing 33$	37 HRC	35 HRC

As can be seen from the results, the material supplied conforms to the ASM material specifications (30). This allows the experimental data obtained to be compared to those reported by other researchers.

5.3. Safety with LN₂

Although nitrogen is an abundant gas in our atmosphere, it could also be a dangerous gas. Nitrogen gas displaces oxygen in the air, and for this reason it could cause suffocation if present in an enclosed space in a large proportion (31,32). The situation is further complicated by the lack of reaction from the human body. Unlike gases such as carbon dioxide, nitrogen will not cause a human to feel suffocated

when low amounts of oxygen are present. The operator could therefore suddenly lose consciousness without any warning from his body. For this reason, it is critical that the space where the nitrogen is used is well ventilated (31,32,33). An oxygen sensor is also a necessity. The best solution is a personal oxygen sensor. These sensors are widely used in mining and other industries to monitor the volume of oxygen in the air, normally reported as volumetric percentage. The sensor is calibrated once a year by the manufacturer. The sensor also has an audible and visual alarm for when the oxygen level drop below 19.5%vol.

It is important to note that LN₂ expands approximately 700 times its volume when it evaporates (31,34). For this reason, a pressure relieve valve that is suitable for cryogenic applications has to be included in the system in certain situations. The valves need to be installed between any two closed off points in the system, for example two taps (Figure 36) (33). When the LN₂ is closed off between two points and it evaporates, the pressure increases dramatically. The piping systems are usually not designed to handle these high pressures, and could burst. Because the pipes used usually contain some type of metal, the busting pipe could cause shrapnel that can cause serious injury or even death.

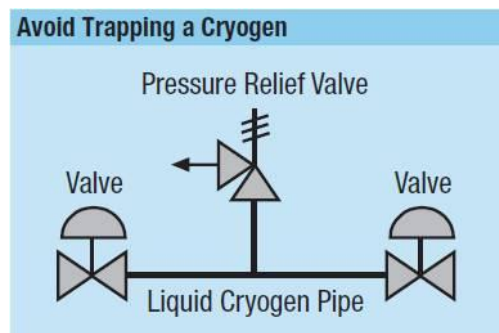


Figure 36: Use op pressure relief valve (34)

Due to the extreme low temperature of LN₂ (-196°C), it is absolutely necessary to wear safety clothing when handling LN₂. Because the eyes are sensitive to the cold temperatures of the liquid and gas, it is required that the user wear safety spectacles with a full face shield. The hands should be protected by loose fitting leather gloves. The loose fitting gloves minimises the risk of the gloves freezing to the operator's skin and aids in the quick removal in the event of a spill. The operator should also wear a long sleeved shirt and trousers without any cuffs. Cuffs have the risk of trapping the fluid that could aggravate the situation. Safety shoes are also recommended for handling the dewars (31,32).

The dewars used for the transportation of LN₂ is similar in construction to a vacuum insulated flask (Figure 37). The main difference is the cap. Due to the LN₂ constantly evaporating, the dewar cannot be sealed. Dewars are therefore fitted with a loose fitting cap that allows the evaporated gas to escape and prevent moisture from freezing around the outlet.

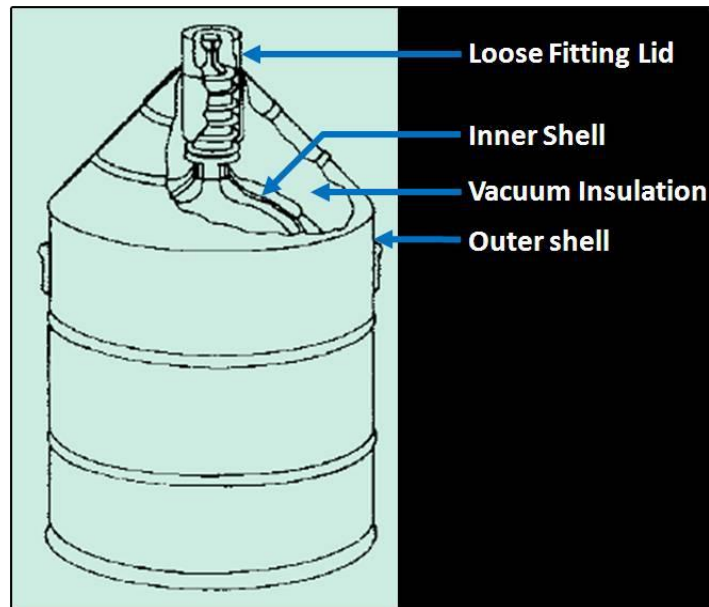


Figure 37: Typical dewar construction (adapted from (31))

5.4. Analysis

The performance of the new cooling method is analysed by measuring the flank wear of the inserts. The flank wear was measured with an inverted optical microscope.

5.4.1. Analysis of wear

The wear analysis was performed on an Olympus GX51 inverted optical microscope (Figure 38). Software that has been calibrated to the specific microscope was used to measure the amount of wear. The accuracy of the microscope is however limited. The visualization of the wear on an optical microscope is based on the interpretation of the operator. This particular microscope does not combine the image of the wear scar at different focal lengths and therefore the complete wear scar is not visible in a single photograph. In cases where the wear on the tool is minimal, it is not always possible to clearly distinguish between wear and build-up. The analysis thus requires some experience to complete. The accuracy with this specific microscope is accepted as $\pm 10\mu\text{m}$. This is determined experimentally by repeatedly measuring the same dimension from the same captured image. This was done for four different images, and the average range was used to determine the accuracy range.

Due to the non-locating geometry of round cutting inserts, the inserts could not be removed from the tool holder for inspection. The insert was therefore inspected by removing the tool holder from the lathe. For the inspection of wear on facing cuts, the tool was placed horizontally on the microscope bed. For longitudinal cuts, an inspection plate was designed to position the tool in an angled vertical position (Figure 39).

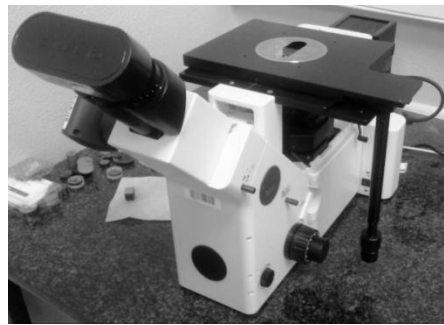


Figure 38: Olympus GX51 Microscope

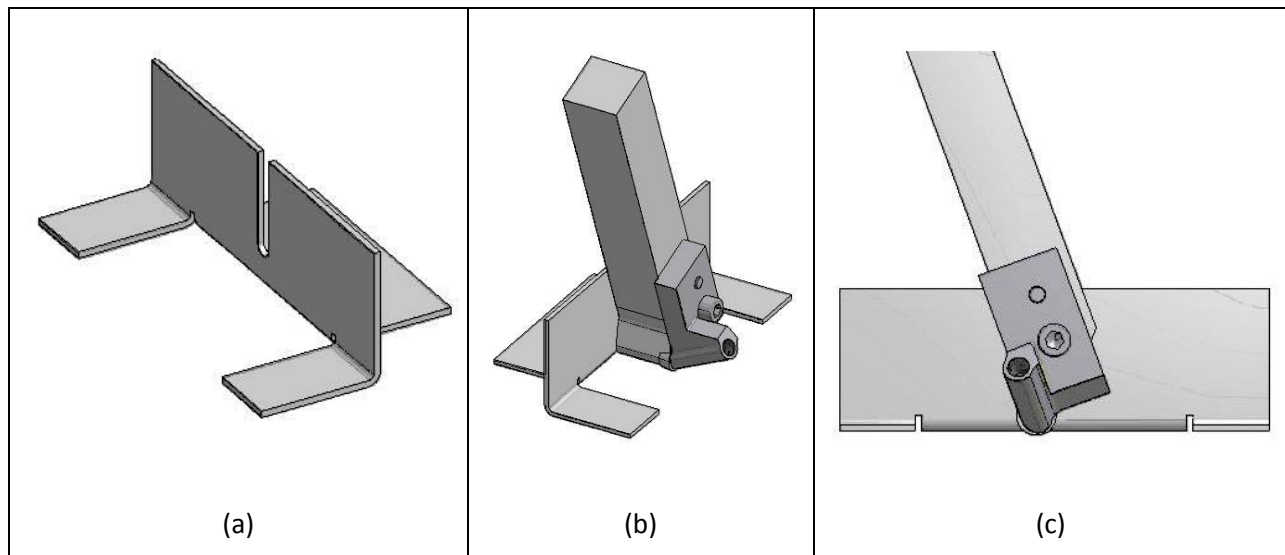


Figure 39: Inspection Plate

Tool life criteria for the wear are specified by the ISO 3685 standard for tool life testing and are shown in Table 10.

Table 10: Tool life criteria (7)

Average flank wear (V_{BAvg})	0.3 mm
Maximum flank wear (V_{BMax})	0.6 mm
Crater depth (K_t)	0.06mm + 0.3 x feed

5.4.2. Calculation formulas

In order to analyse the wear measured relative to each other, several factors have to be calculated. To calculate the machining time of facing cuts, we use the material removal rate and the amount of material removed.

Equation 1: Material Removal Rate for turning operations [cm^3/min]

$$MRR = v_c f a_p$$

With v_c = Cutting Speed [m/min]
 f = Feed rate [mm/rev]
 a_p = Radial depth of cut [mm]

Equation 2: Material removed in a single cut [cm^3]

$$MR = \pi(r_o^2 - r_i^2)a_p$$

With r_o = Outer radius [mm]
 r_i = Inner radius [mm]

We can now use Equation 1 and Equation 2 to calculate the machining time for a single facing cut.

Equation 3: Machining time for a single facing cut [min]

$$T_m = \frac{MR}{MRR} = \frac{\pi(r_o^2 - r_i^2)}{v_c f}$$

The equation for the time to conduct a longitudinal cut needs to take the length of cut into account. To calculate this, we utilise Equation 4.

Equation 4: Machining time for a single longitudinal cut [min]

$$T_m = \frac{\pi D_o L}{v_c f}$$

with D_o = Outer Diameter [mm]
 L = Axial length of cut [mm]

6. Results

6.1. Pilot testing

To ensure that all the aspects of the experimentation function correctly, pilot testing was conducted. The first aspect to be tested was the programming code. Considering that Ti-6Al-4V is a high cost material, code testing was conducted on steel rods with similar dimensions. Minor changes to the program were made to eliminate the forming of burrs and ensure that all chips are cleared between cuts. Initial difficulties with the capabilities of the machine to rapidly accelerate the spindle speed were experienced. The feed rate was therefore lowered to enable the machine to achieve required constant cutting speed. After initial experimentation, the wear results showed that a low wear rate was achieved at a cutting speed of 120 m/min and a feed rate 0.1mm/rev. These cutting parameters were however the highest material removal rate (MRR) that the machine could achieve given the cutting path. The path was therefore changed as described in Section 5.1.

6.2. Tungsten Carbide with Conventional Cooling

Initial experimentation was conducted to determine a benchmark for the LN₂ experimentation. As the graph shows in Figure 40, tool wear can be divided into three major regions. The first is the break in period during which the tool wears rapidly. This is followed by the steady state wear period. This period is responsible for the majority of the tool life and the tool wear slowly progress in a linear fashion. At the end of this period the wear starts to rapidly accelerate. This is due to higher temperatures being generated due to the increased wear on the tool. This effect escalates and causes the tool to fail. When wear is analysed, the experimental tool life results are depicted in this manner. There could however be restrictions when experiments are conducted. These are typically the costs of experimentation or the amount of raw material available. In such cases the general tool life curve can aid in the interpretation of the tool life data available.

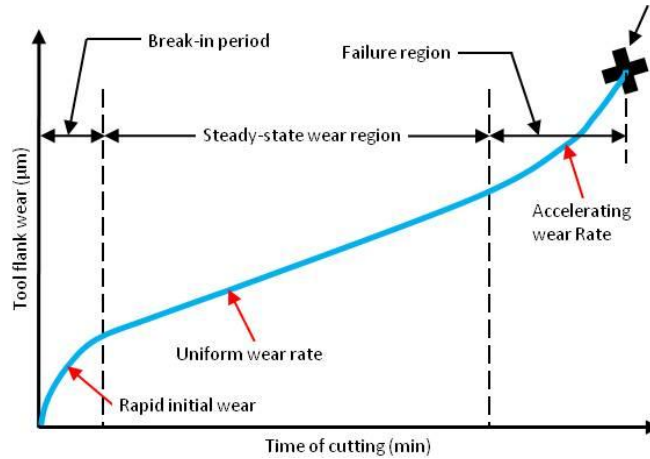


Figure 40: Typical tool wear curve (23)

The expected tool life of square cutting inserts at 60 m/min is given in literature as 15-20 minutes. Literature has also proven that cutting speed is the most dominant parameter to influence the tool life in titanium machining. The Sandvik catalogue and cutting experts at their office in Jet Park, Johannesburg, were also consulted for cutting parameters. The cutting parameters suggested by Sandvik are based on a tool life of 15 minutes. The Sandvik catalogue also suggests a cutting speed (v_c) of 60 m/min and a feed rate of 0.15 mm/rev.

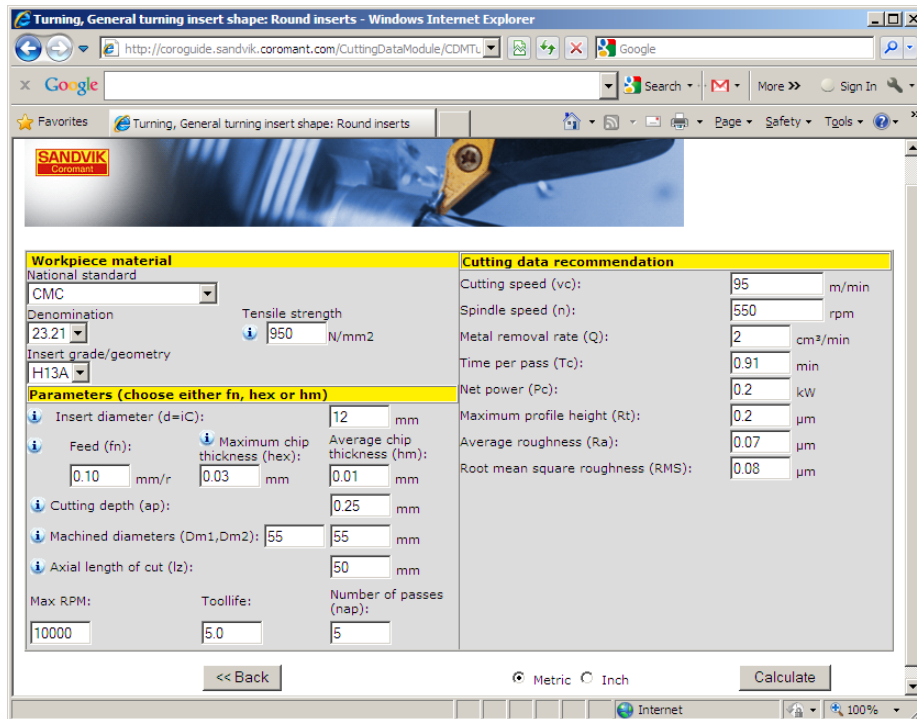


Figure 41: Tool life prediction for RCMW 12 04 M0 H13A (35)

The first experiments were conducted with parameter set 1 given in Table 11. Considering that the experimentation was conducted at twice the cutting speed of the literature, the expected tool life was much less. The online tool life calculator of Sandvik was also consulted for a tool life estimate. Their calculator states that for a cutting speed of 95 m/min and a 0.1mm/rev feed rate, a tool life of 5 minutes can be expected (Figure 41). The expected tool life at 120 m/min is therefore less than 5 minutes. However, as seen in Figure 42, the maximum flank wear measured during experimentation at 19.78 minutes was 74 μm , while the average wear on the flank measured 47 μm . Figure 43 shows the maximum and average tool wear at a 50x magnification. This is approximately 10% of the tool wear required to meet the failure criteria. By analysing the wear results the end of the break in period can be identified at approximately 2 minutes of machining. After this time, the wear increases at a marginal rate. The wear has thus entered the uniform wear region. Due to cost implications, the wear test could not be completed to the point where the tool fails. The extremely low wear did however arouse the author's interest. The decision was therefore made to terminate experimentation at 16 minutes.

Table 11: Round insert experimental conditions

	Parameter Set 1	Parameter Set 2	Parameter Set 3
Cutting Speed (v_c)	120 m/min	150 m/min	150 m/min
Feed (f)	0.1 mm/rev	0.1 mm/rev	0.15 mm/rev
Depth of cut (a_p)	0.25 mm	0.25 mm	0.25 mm

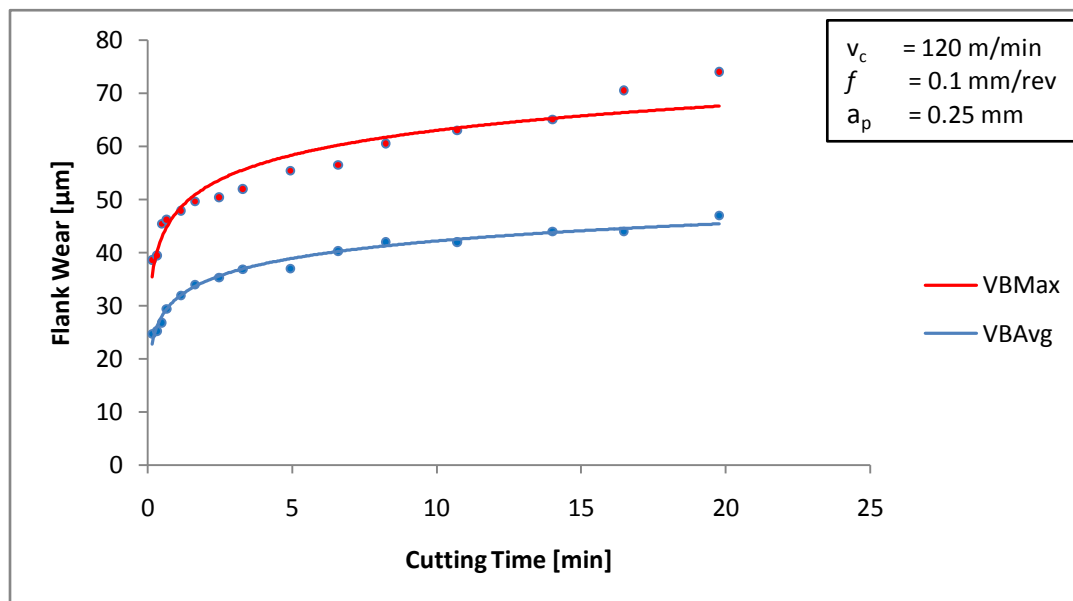


Figure 42: Flank wear relative to cutting time

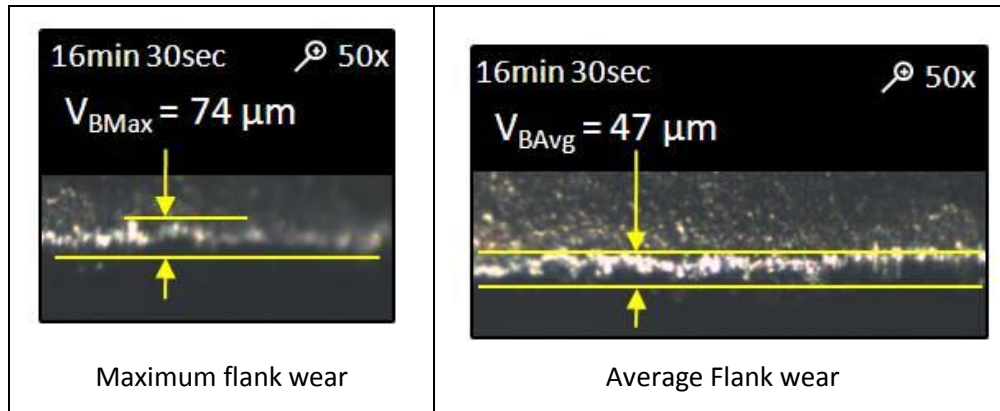


Figure 43: Flank wear at 16.49 min on WC, $v_c = 120 \text{ m/min}$, $f = 0.1 \text{ mm/rev}$, $a_p = 0.25 \text{ mm}$ (50x)

In an attempt to increase the wear rate of the tool, the cutting speed was increased to 150 m/min while the feed rate and depth of cut was kept constant (parameter set 2 in Table 11). This did however not increase the wear rate significantly. After 13.19 minutes of machining the wear scar peak was measured as $62 \mu\text{m}$ (Figure 44a), while the average wear measured $45 \mu\text{m}$ (Figure 44b). As this is a minor increase in wear, the experimentation with these cutting conditions was terminated. By analysing Figure 45 we can also conclude that the tool is already in the uniform wear region.

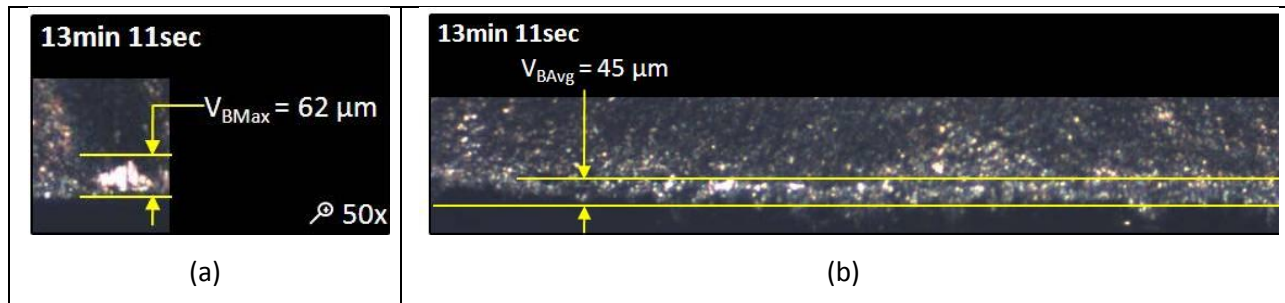


Figure 44: Flank wear at 13.19 min on WC, $v_c = 150 \text{ m/min}$, $f = 0.1 \text{ mm/rev}$, $a_p = 0.25 \text{ mm}$ (50x)

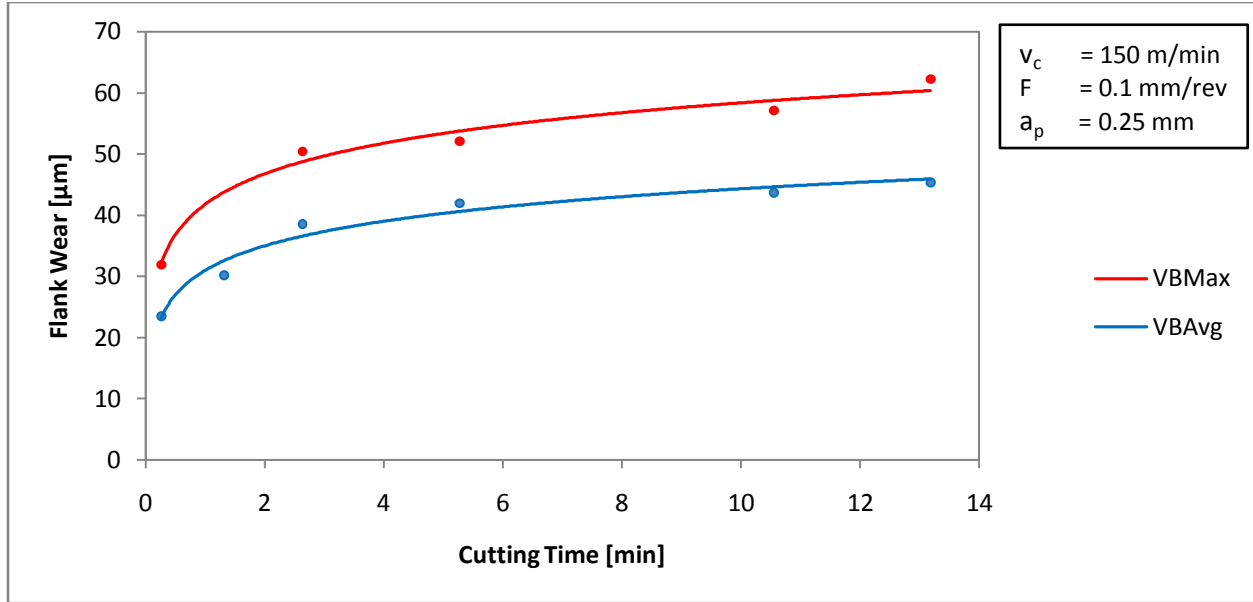


Figure 45: Flank wear at $v_c = 150$ m/min, $f = 0.1$ mm/rev, $a_p = 0.25$ mm

The experimental conditions were then changed to parameter set 3 in Table 11. These are rigorous conditions for Ti-6Al-4V machining according to all sources. Tool life was therefore expected to be in the region of 8 minutes (4,7,13,16) although tool life as low as 2 minutes has also been reported (15). The cutting insert did however perform exceptionally well. At 19.34 minutes of machining, the maximum flank wear measured $70 \mu\text{m}$ while the average flank wear measured $50 \mu\text{m}$ (Figure 46). The start of the uniform wear period was yet again at approximately two minutes. It is also clear that the tool was still in the uniform wear stage when the experimentation was terminated at 29.89 minutes. At this time the average flank wear measured $55 \mu\text{m}$, while the maximum flank wear measured at $74 \mu\text{m}$. The microscope photos of the tool wear is shown in Figure 47.

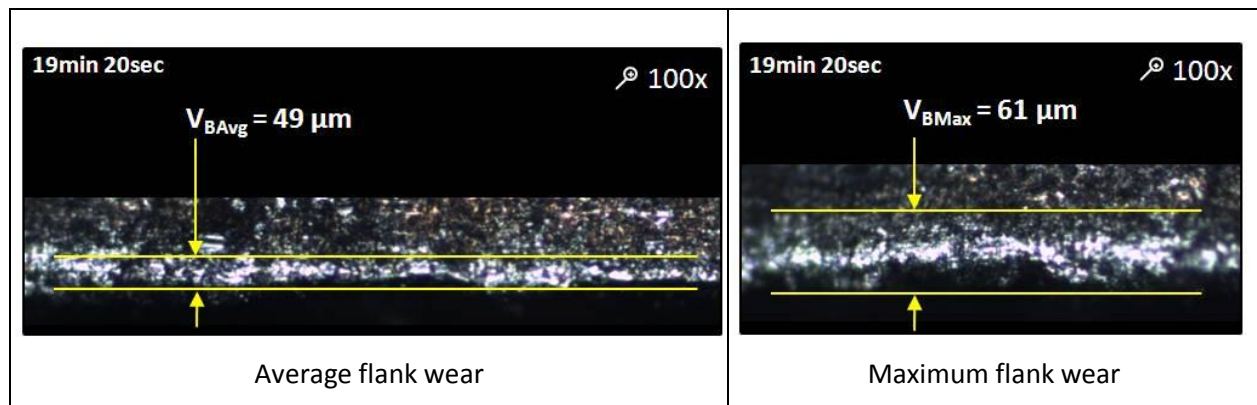


Figure 46: Flank wear after 19.34 minutes, $v_c = 150$ m/min, $f = 0.15$ mm/rev, $a_p = 0.25$ mm

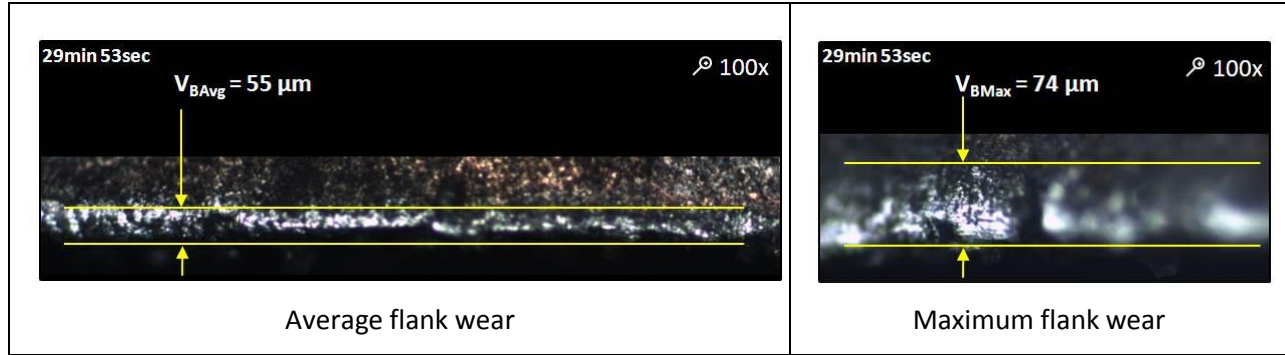


Figure 47: Flank wear after 29.89 minutes, $v_c = 150$ m/min, $f = 0.15$ mm/rev, $a_p = 0.25$ mm

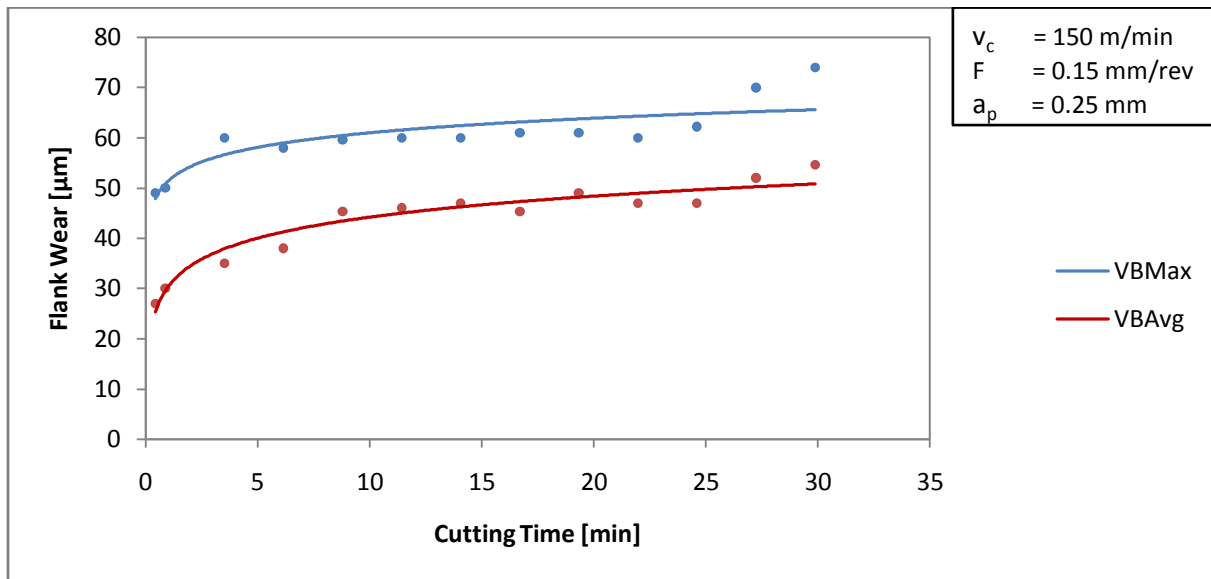


Figure 48: Flank wear at $v_c = 150$ m/min, $f = 0.15$ mm/rev, $a_p = 0.25$ mm

6.3. PCD inserts with conventional cooling

Experimentation with a square type PCD insert (Table 12) was also conducted on grade 5 Ti-6Al-4V material with the cutting parameters shown in Table 13. The experimentation did however result in catastrophic failure of the cutting insert after only 5mm of travel.

Table 12: Insert geometry

Nose radius (r_ϵ)	0.8 mm
Clearance angle	6°
Rake face (γ)	Neutral (0°)
Entering Angle (K_r)	90°

Table 13: Experimental cutting conditions

Cutting speed (v_c)	160 m/min
Feed (f)	0.2mm/rev
Depth of cut (a_p)	2.0 mm
Cooling	Dry

With the baseline experiments completed, the PCD experimentation was conducted. When working with PCD inserts it is important to ensure that the inserts are properly clamped down. Although PCD is excellent in coping with the high temperatures generated in titanium machining because of its high hot hardness, it is brittle. The first step in securely fastening the insert is the back face. Due to the difference in thickness between the WC and PCD inserts, a new shim had to be manufactured to ensure that the insert is located at the correct height (Figure 49). It is vital that the top and bottom faces of the shim are parallel and flat. If this is not the case, the possibility exists that the insert will be bent to the contour of the top face of the shim. This could cause the brittle PCD layer to fracture. The shim is screwed into place using the same mechanism as the original tool holder.

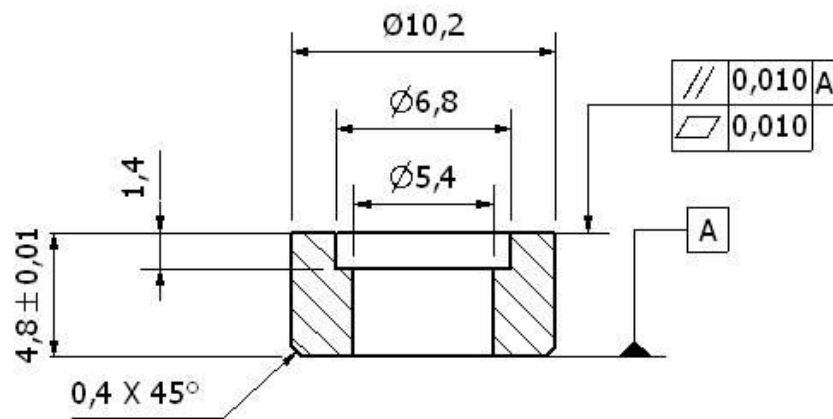


Figure 49: PCD Shim

Once the basis for the insert is correct, the insert needs to be securely clamped down on the insert. All the inserts have a width tolerance, and the tool cap has to be adaptable for this. The tool cap is therefore lifted off the tool shank by brass shims in order to properly clamp the insert. A visual inspection is done to ensure that the insert presses firmly all around the shim. Except for the risk of breaking the insert, improper seating on the shim can result in insert movement that will cause severe chatter.

Experimentation with the PCD insert was executed with parameter set 3 in Table 13. Given the exceptional tool life that has been achieved by earlier work (27), the tool life of the PCD inserts were expected to be far superior to the WC inserts. Figure 50 shows a new PCD insert cutting edge at 50x magnification. The figure shows that the PCD cutting insert has a sharp cutting edge.

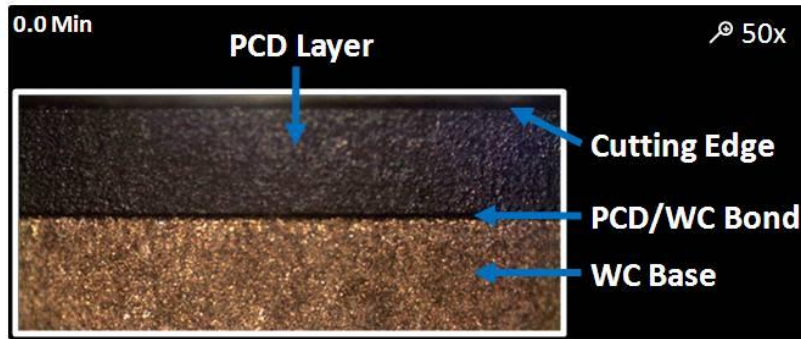


Figure 50: New PCD Insert edge

The first tests were conducted with the PCD insert, the tool cap and soluble cooling. This experimentation creates the baseline for experimentation with the LN₂. Clamping down the PCD insert proved to be a much more complicated task than initially expected. Initial clamping caused excessive chatter. After only 45 seconds of machining, the tool suffered a maximum of 339 μm of wear due to chipping (Figure 51). The chatter was an unacceptable machining condition and the sole causal factor responsible for the premature failure.

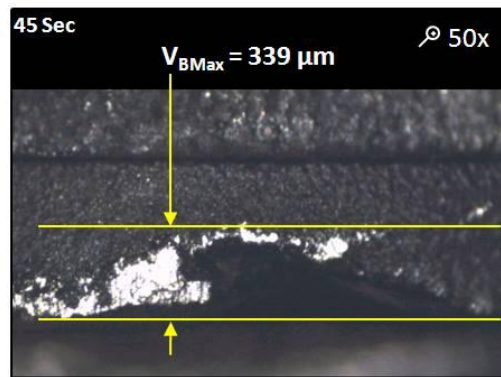


Figure 51: Flank wear after 45 seconds with excessive chatter

Figure 52 shows the chipping damage that the chattering of the tool caused on the rake face. It is clear that a major part of the rake face has fractured. Although the wear is however still within the 600 μm limit and therefore the tool was not considered to have failed. The surface finish of the work piece is however poor and considered defective.



Figure 52: Chipping on rake face due to chatter

After 1.5 minutes of machining, the situation has however changed considerably. The cutting edge has sustained a second major fracture, and the average flank wear has now progressed to $306\ \mu\text{m}$ (Figure 53). This tool has therefore reached the end of its tool life and did not deliver a surface finish that is that is at all useable.

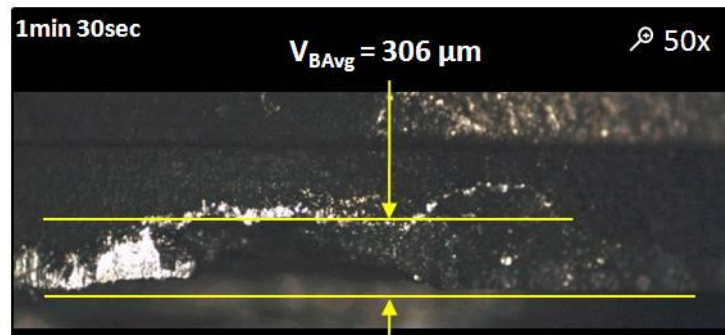


Figure 53: Flank wear of PCD insert under flood cooling after 1 minute 30 seconds (Excessive chatter)

This experimentation is however not valid for comparison purposes. Because chatter has a major influence on tool life and is considered an unacceptable machining condition, experimentation conducted while chatter is present does not have any value in terms of tool life determination. The shims that are used to level the tool cap were therefore changed to experimentally determine the required thickness to properly clamp the insert and prevent chatter. The width of each cutting insert is however different. This requires this process to be repeated for each new insert.

The experimentation concerning the PCD insert with soluble oil flood cooling was therefore repeated when a chatter free solution was determined. The wear measured is shown in Figure 55. The initial wear on the PCD was very low, with the average flank wear (V_{BAvg}) measuring $14\ \mu\text{m}$ while the maximum flank

wear (V_{BMax}) measured $39 \mu\text{m}$ after 45 seconds of machining (Figure 54). This low trend of machining continued with V_{BAvg} measuring $18 \mu\text{m}$ and V_{BMax} measuring $50 \mu\text{m}$ at 1.5 minutes.

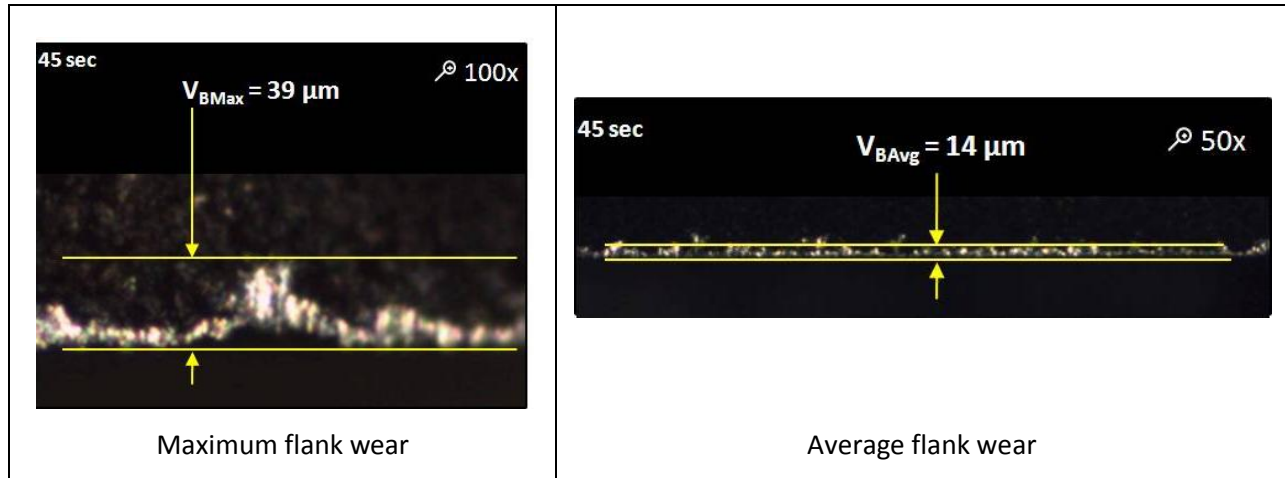


Figure 54: Flank wear of PCD insert under flood cooling after 45 seconds

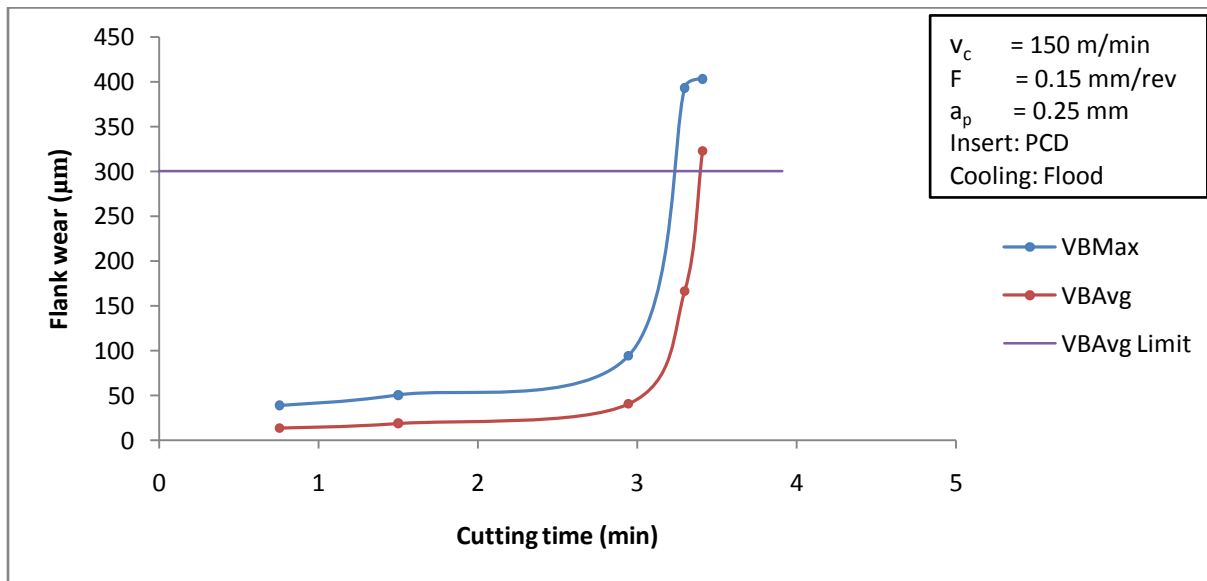


Figure 55: Flank wear growth trend of PCD insert under Soluble cooling

After 2.6 minutes of machining, the tool developed a slight chatter during the cut. The tool was removed at 2 minutes and 57 seconds to inspect the wear scar. The tool wear, shown in Figure 56, measured $94 \mu\text{m}$ for V_{BMax} , while V_{BAvg} measured $40 \mu\text{m}$.

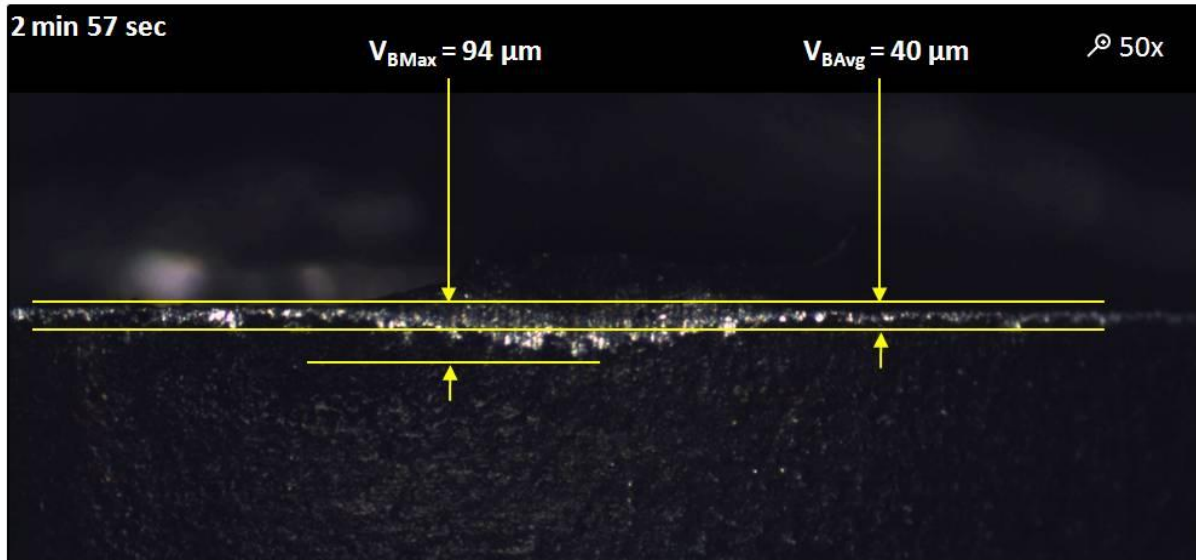


Figure 56: Flank wear of PCD insert under flood cooling after 2min 57 sec

From this point the wear accelerated at an alarming rate. By this time the tool had now started to chatter excessively and after another 21 seconds of machining the wear was inspected. The total machining time had now accumulated to 3 minutes and 18 seconds and the wear had now significantly changed with V_{BMax} and V_{BAvg} measuring 393 μm and 166 μm respectively (Figure 57).

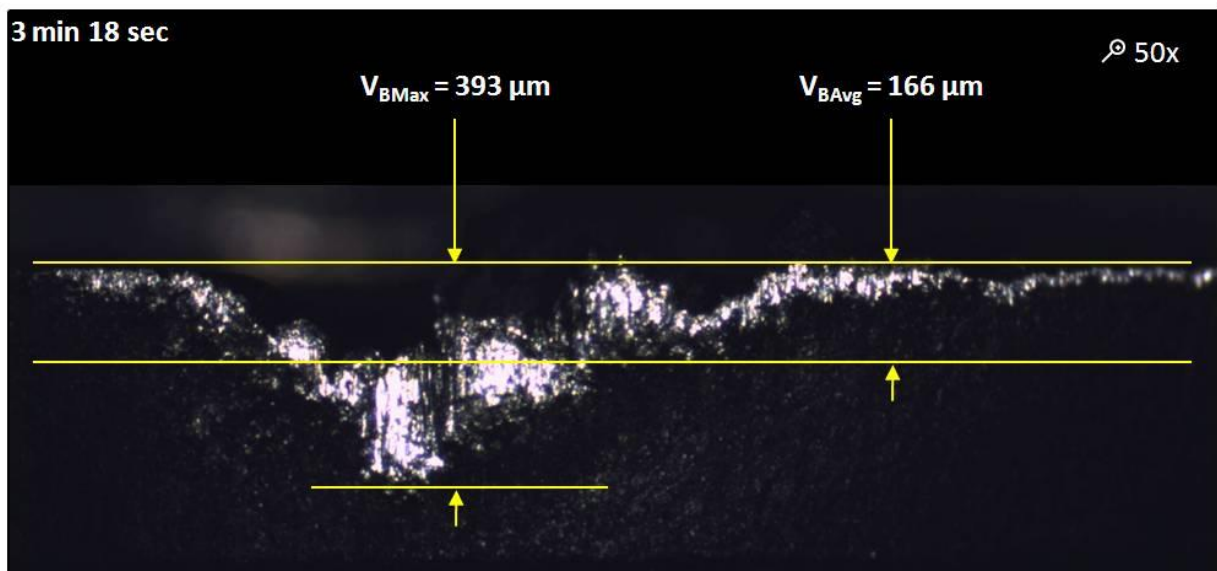


Figure 57: Flank wear of PCD insert under flood cooling after 3min 18 sec

The next cut resulted in excessive chatter that led to the experimentation being terminated after 7 seconds due to fear of damaging the experimental setup. With the total machining time for this PCD

cutting edge at 3 minutes 25 seconds, the wear progressed to $403 \mu\text{m}$ for $V_{B\text{Max}}$ while $V_{B\text{Avg}}$ exceeding its allowable limit to $322 \mu\text{m}$. Experimentation was therefore terminated.

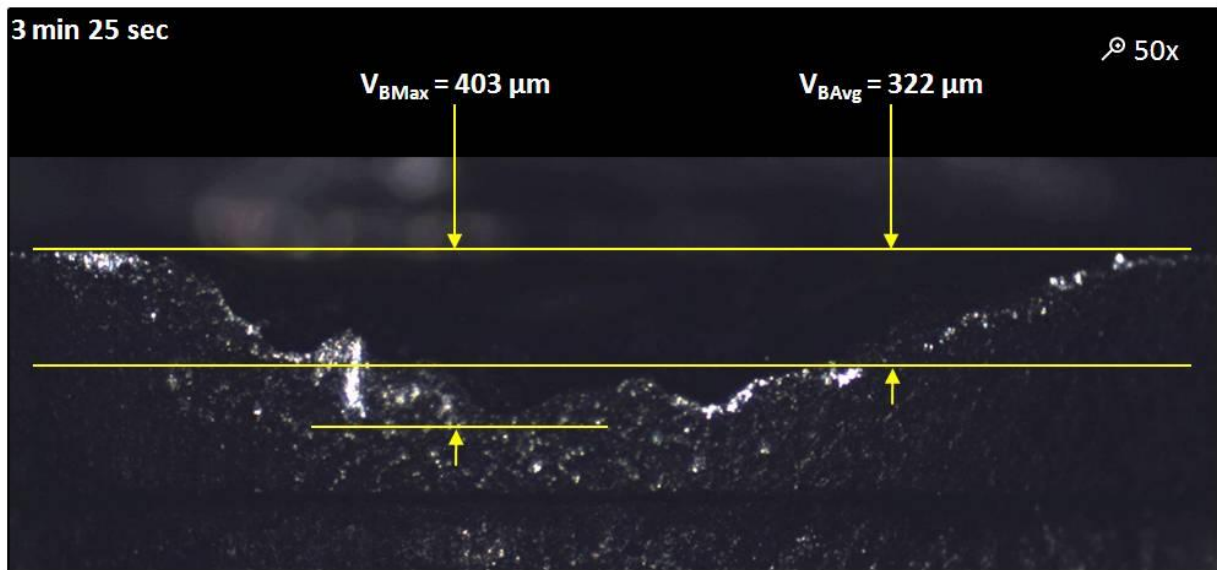


Figure 58: Flank wear of PCD insert under flood cooling after 3min 25 sec

6.4. PCD insert with liquid nitrogen (LN_2) cooling

The next step in determining the feasibility of the LN_2 cooling system is to test PCD inserts with LN_2 cooling. The same setup procedure as for the PCD under conventional cooling was followed for the LN_2 tests. Before each experimental run, the procedure for preparing the system, as described in section 5.2.2, was followed to prevent moist containing air from forming an ice plug. No chatter was observed during experimentation. Light sparks were however noted on top of the chips while machining.

Figure 59 shows the wear after 46 seconds of machining. The initial average flank wear ($V_{B\text{Avg}}$) is measured at $50 \mu\text{m}$, while the maximum flank wear ($V_{B\text{Max}}$) measures $299 \mu\text{m}$. The $V_{B\text{Max}}$ in Figure 59, which is significantly larger than the rest of the wear, is located in section 5 of the insert (Figure 60).

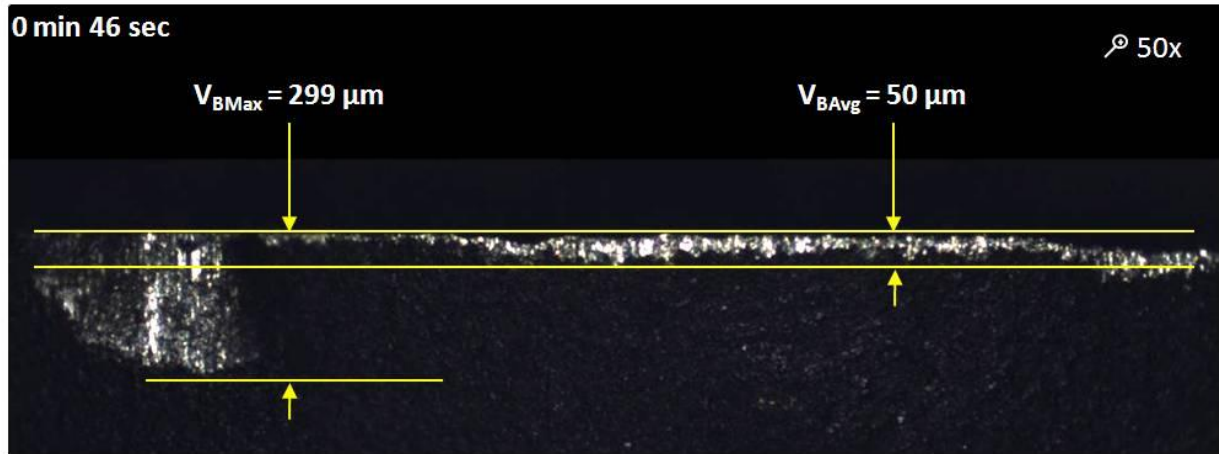


Figure 59: Flank wear of PCD insert under LN₂ cooling after 46 sec

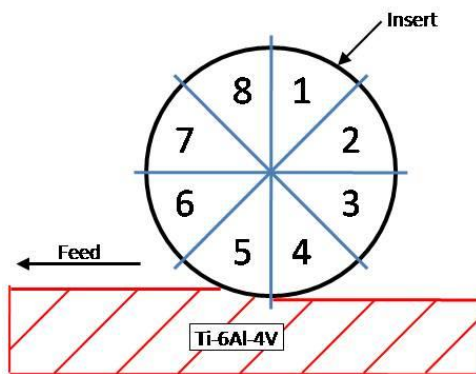


Figure 60: Insert cutting edge identification

As shown in Figure 61, the wear growth increased steadily up to final cut that resulted in a total machining time of 3 minutes and 41 seconds, where the chips adhered to the tool cap. The chip was however easily removed. The tool was inspected and it was found that V_{BAvg} measured $75 \mu\text{m}$ (Figure 62), which is little more than the $70 \mu\text{m}$ measured at 1 minute 31 seconds. However, V_{BMax} measured $620 \mu\text{m}$ at 3 minutes 41 seconds (Figure 62), which is a large difference from the $319 \mu\text{m}$ measured at 1 minute 31 seconds. It is important to note that the chip adhering only took place on the last cutting cycle of 21 seconds before the tool was inspected.

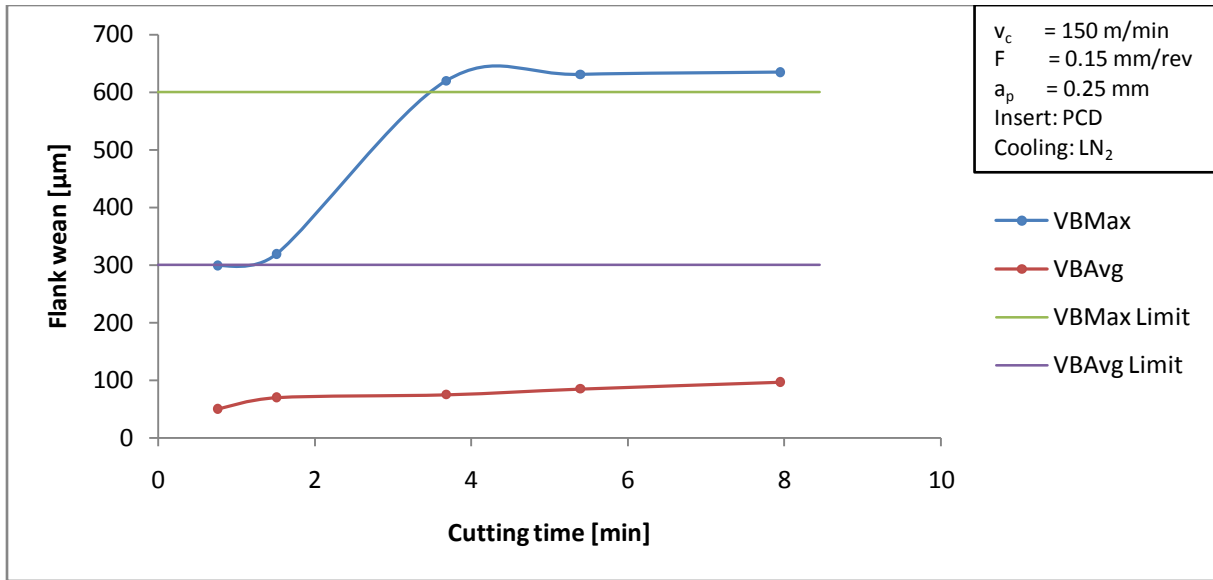


Figure 61: Flank wear growth trend of PCD insert under liquid nitrogen (LN_2) cooling

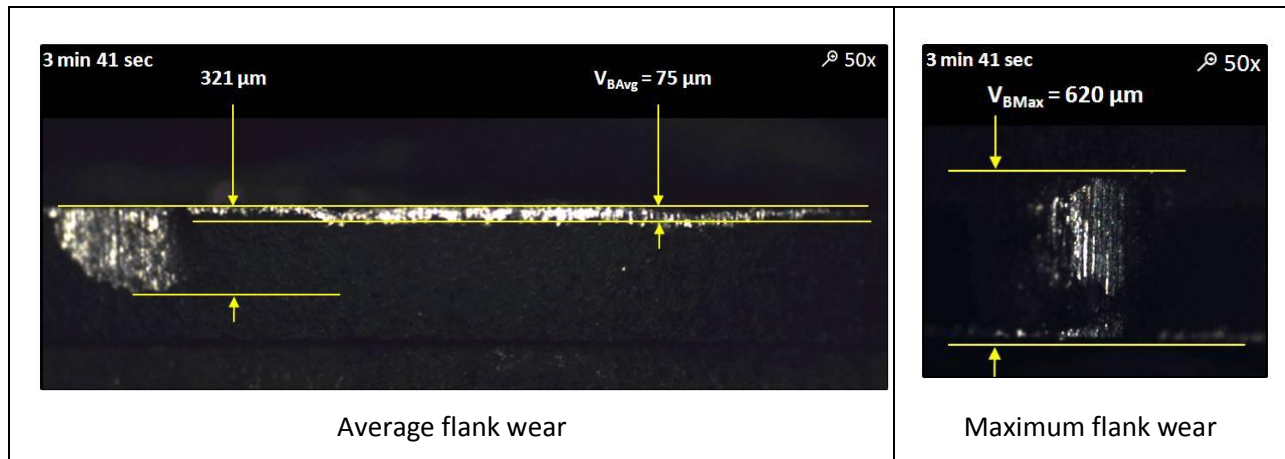


Figure 62: Flank wear of PCD insert under LN_2 cooling after 3 min 41 sec

With continued experimentation no chips adhered to the tool cap or insert up to 5 minutes 24 seconds, when the tool was inspected. Tool wear has now progressed to 631 μm for V_{BMax} and 85 μm for V_{BAvg} (Figure 63).

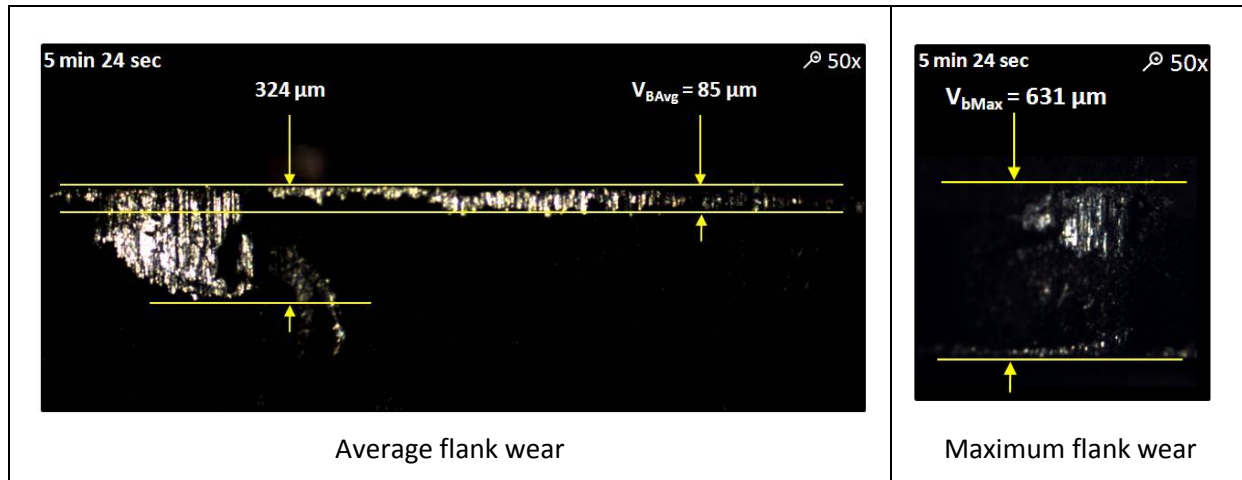


Figure 63: Flank wear of PCD insert under LN₂ cooling after 5 min 24 sec

Experimentation was continued to 5 minutes 57 seconds when the chip yet again adhered to the chip tool cap interface. The chip could however not be easily removed this time. It was also noted that during the last cut the chip became red hot, after which the experimentation was terminated for inspection. Inspection showed that the chip did not adhere to the rake face of the PCD insert (Figure 64). The conclusion to be later investigated was that the chip adhered to the tool cap. With the inspection of the wear, V_{BAvg} was measured at 97 μm (Figure 65) while V_{BMax} peaked at 635 μm (Figure 66). A crater was noted at the point where the OD meets the insert (sector 5, Figure 60). At 7 minutes 57 seconds, the crater measured 165 μm (Figure 66).

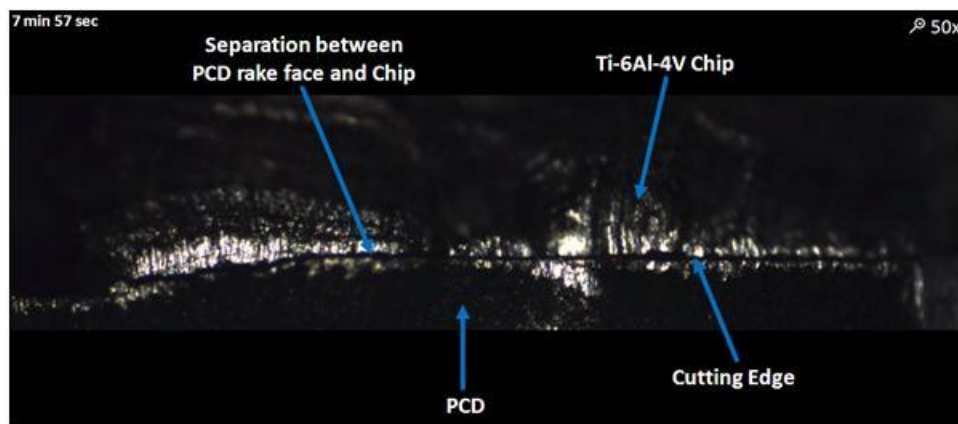


Figure 64: Separation between the rake face of the PCD and the Ti-6Al-4V chip

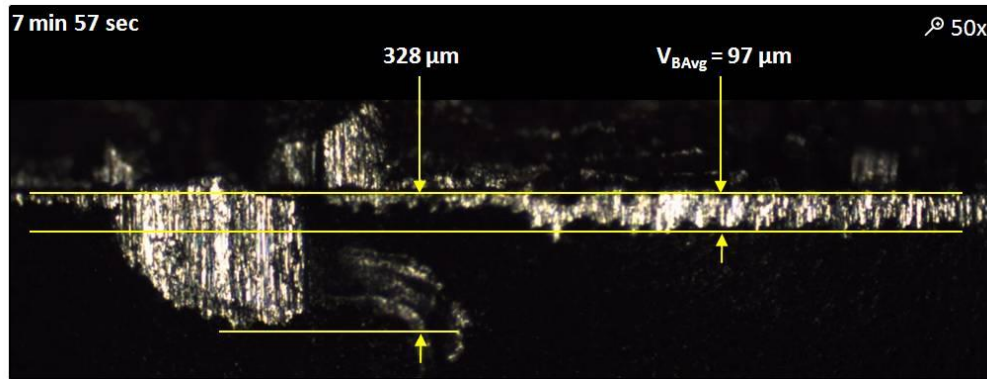


Figure 65: Flank wear of PCD insert under LN₂ cooling after 7 min 57 sec

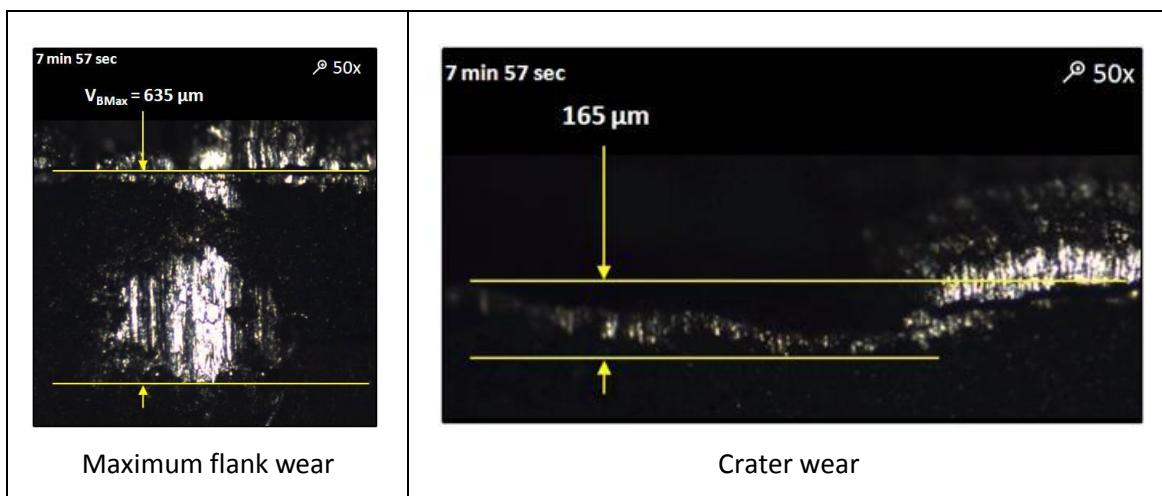


Figure 66: Flank wear of PCD insert under LN₂ cooling after 7 min 57 sec

7. Discussion of results

7.1. Tool life reporting and productivity

Tool life is mostly reported in terms of cutting time or length of cut. This method of reporting makes it difficult to compare the tool life results. Ideally the objective of improving tool life is to decrease the cost and/or time required for the operation. Researchers also rarely use the exact same experimental conditions, and experience has proved that not all experimental conditions are always supplied. In order to compare experimental results on a level playing field, it is necessary to report tool life relative to a common scale. Material removed per cutting edge is therefore the best option for comparing the productivity of the tool.

The use of the material removed per cutting edge combines the cutting speed (v_c) and depth of cut (a_p), compared to cutting time which incorporates cutting speed and feed rate when roughing or material removal is the objective. When plotting the tool life against cutting time, it is not possible to get an accurate representation of the productivity of the tools when two different sets of cutting conditions are tested. Consider the hypothetical situation shown in the graphs in Figure 67. The interpretation of the plot of tool life against cutting time would be that Parameter Set 1 (PS1) performs superior to Parameter Set 2 (PS2) because the tool life of PS2 is half that of PS1. This is however not the case. When we plot the tool life against the total material removed per edge (TMR), we see that PS2 removed more than three times the material that PS1 removed before reaching failure criteria. PS2 also results in a much higher productivity, which is seen when the material removal rate (MRR) is calculated. A plot of tool life against cutting time will however be sufficient if tools are all tested under the same parameters.

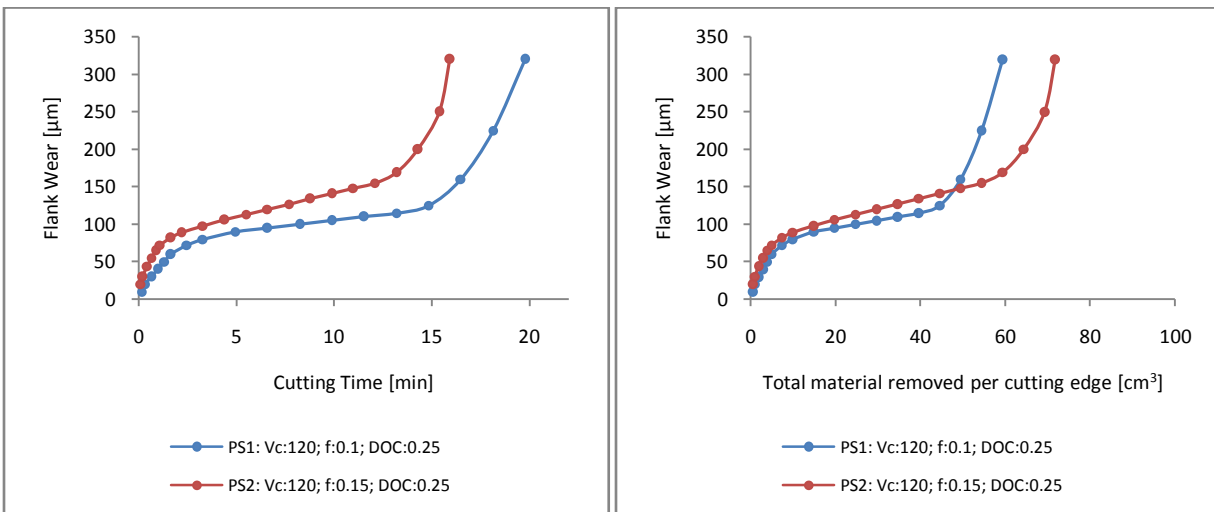


Figure 67: Tool life representations

When comparing different machining strategies for productivity, be it change in cutting parameters, cutting strategies or cooling strategies, a plot of the material removed per tool against the material removal rate best aids the decision making process (Figure 68). This plot incorporates v_c , f and a_p to represent the production capabilities of a tool. When comparing machining strategies in this manner, the better strategy will be located towards the top right hand corner of the graph. This will then also result in the most productive solution of the available options.

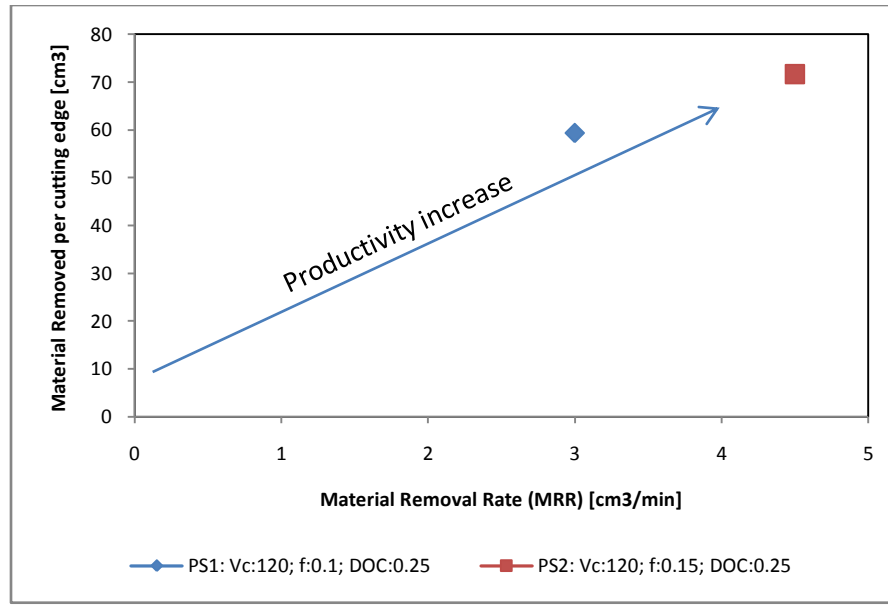


Figure 68: Tool Life measured as material removed

7.2. Insert geometry and tungsten carbide tool discussion

Research has proven that insert geometry does play a role in tool life (27). Round inserts are known to perform better in machining than square or C-shape inserts (Figure 69). This is attributed to the reinforcement of the cutting edge and the distribution of thermal load. Because round inserts don't have sharp corners such as square inserts, the cutting edge is better reinforced. Radii are however applied to inserts with sharp corners to counteract chipping fractures. With titanium machining most manufacturers utilise a 0.8mm nose radius. The round insert also has a longer cutting edge in the cut than square inserts which distributes the thermal and mechanical loads over a larger length of cutting edge. Round inserts also have the advantage of a continuous cutting edge. Where positive C-shape inserts have only two cutting edges, and positive square inserts four, the positive round insert can have much more, depending on the depth of cut taken. With all these reasons in mind, round inserts should generally have a longer tool life.

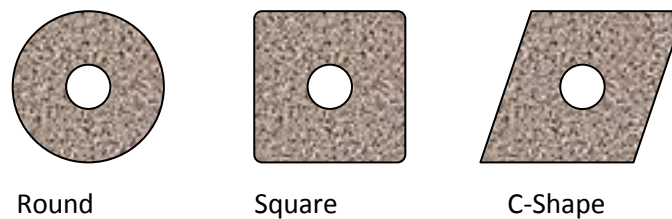


Figure 69: Some insert geometries

Round cutting tools also have the advantage of a generally superior surface finish of the work piece relative to square type inserts. This is a result of the chip thinning effect prominently present with round inserts effectively resulting in the final diameter being re-machined a number of times. An $\varnothing 12$ round insert will have 0.78mm of its cutting edge in the last 50 μm of the cut, whereas a 12mm wide square insert with a 0.8mm nose radius will have 0.28mm in the cut. Measured axially, this translates into 0.77mm for the round insert and only 0.28mm for the square type insert. Considering that the feed is normally less than 0.2 mm/rev, the result is that a point along the axis will be in cut for 3.85 revolutions with the round insert, while it will only be in cut for 1.4 revolutions with the square insert. The result is much lower peaks between cuts resulting in a better surface finish. Calculations show that the ideal surface roughness for the square insert is approximately 9 times higher than that of round inserts.

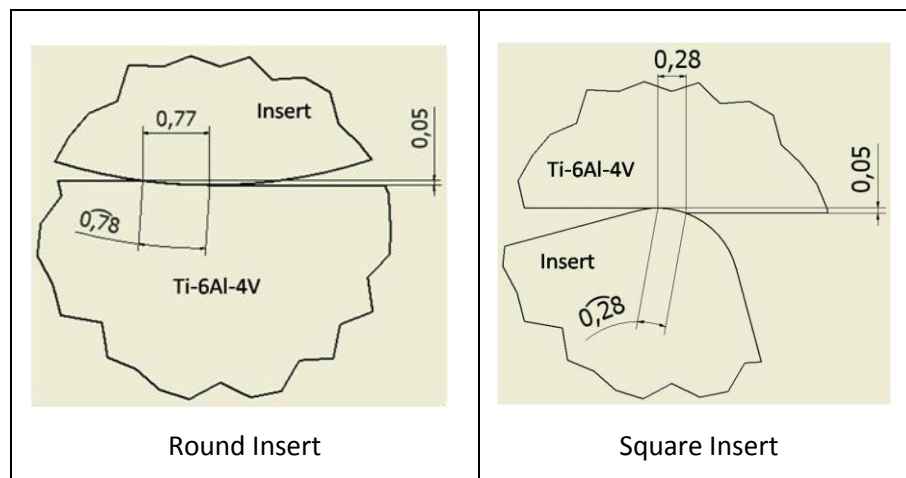


Figure 70: Insert – work piece interface

The experimentation conducted with positive round tungsten carbide inserts, reported in section 6.2, proved this theory, but to a considerably larger extent than expected. As stated earlier, tool manufacturers suggest cutting conditions for the tools they supply. These cutting parameters are calculated to result in approximately 15 minutes of tool life. The recommendations for cutting parameters for the Sandvik RCMW 12 04 M0 H13A inserts are shown in Figure 71.

<p>Cutting recommendations for SCMT square insert(36)</p>	<p>Cutting recommendations for RCMT round insert (37)</p>

Figure 71: Sandvik cutting recommendations

The experimental results show that these parameters can be largely increased and still deliver a tool life longer than 15 minutes. The experimental conditions with the applicable MRR are given in Table 14. The MRR gives a good indication of the increase in productivity from parameter set 1 through to parameter set 3.

Table 14: Round insert experimental conditions

	Parameter Set 1	Parameter Set 2	Parameter Set 3
Cutting Speed (v_c)	120 m/min	150 m/min	150 m/min
Feed (f)	0.1 mm/rev	0.1 mm/rev	0.15 mm/rev
Depth of cut (a_p)	0.25 mm	0.25 mm	0.25 mm
Material Removal Rate (MRR)	3.00 cm ³ /min	3.75 cm ³ /min	5.63 cm ³ /min

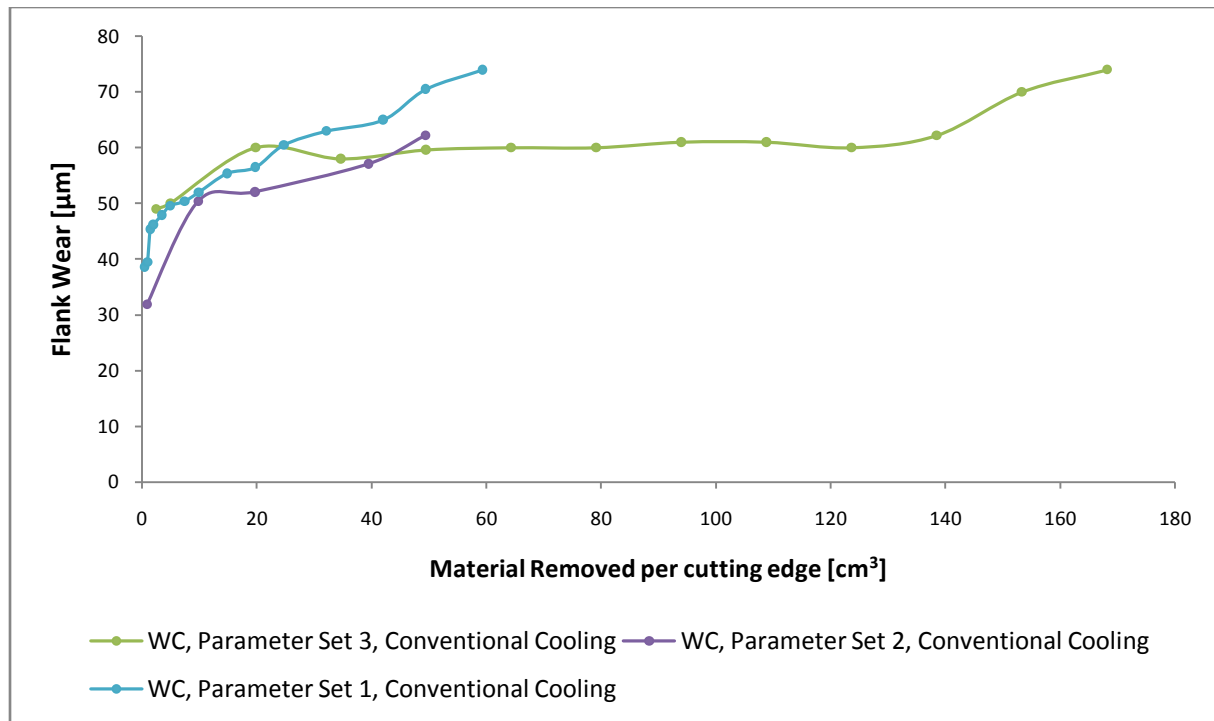


Figure 72: Average flank wear on WC inserts with conventional cooling

Figure 72 shows the flank wear results of the WC experimentation in terms of the material removed per tool. The parameter sets referred to in the graph is listed in Table 14. It is clear from the results that the increase in feed rate influenced the amount of material that is removed before the tool enters the uniform wear region. The wear increases slowly from this point. The results show that the maximum flank wear after 168 cm³ of material has been removed at 150 m/min and 0.15mm/rev feed, is approximately the same as to remove 60 cm³ of material at 120 m/min and a 0.1mm/rev feed. More importantly, we see that the wear is exceptionally low at 74 μm. What is more surprising is that this exceptionally low wear is achieved at 150 m/min, which is more than twice the recommended cutting speed (60m/min) for titanium. By increasing the cutting speed, the material removal rate is increased from 2.25 cm³ to 5.63 cm³ resulting in a much higher productivity rate, especially as the wear rate does not increase significantly.

These results in are attributed to the insert geometry. The use of a round insert reinforces the cutting edge of the tool, and thereby counteracts chipping that is commonly seen in titanium machining. The large nose radius of the tool creates a chip thinning effect over the complete length of the cutting edge, an effect not as significant with square inserts. This effect is visually presented in Figure 73 which shows the cutting process for machining with a round and square insert. During the cutting process the tool

displaces by the feed amount (shown as *feed* in Figure 73) in the direction of feed (also indicated in Figure 73) for every revolution. The chip thickness is however not measured in the direction of feed, but measured perpendicular to the cutting edge, as indicated in Figure 73.

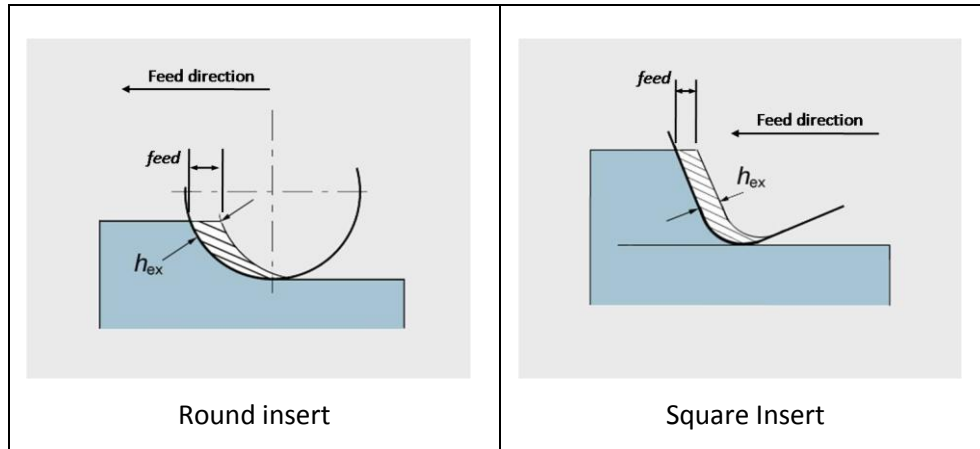


Figure 73: Chip thickness and chip thinning

The maximum chip thickness (h_{ex}) is marked in Figure 73 for both round and square inserts. For square inserts the chip thickness is constant over the complete length of the straight edge. Chip thinning only starts at the tangent point between the straight edge and the nose radius and approaches zero at the machined diameter. Chip thinning is therefore only experienced over a small percentage of the cutting edge length. With round inserts, the chip thinning effect is experienced for the whole length of the cutting edge for a maximum depth of cut of half the insert diameter. This spreads the thermal load and cutting forces over a larger length of cutting edge, resulting in a longer tool life.

It is therefore clear that round cutting inserts have a large potential in titanium machining, a potential that is not being utilised in South African industries. As stated earlier, titanium is known for its low machining productivity. With the round inserts, the productivity can be increased significantly without compromising tool life or surface finish. Constraints in costs limited the amount of experimentation that could be conducted, and the round WC inserts could not be tested up to failure point. The complete tool life is therefore not known, although it is known that the tool has exceptionally low wear ($V_{BAVG} = 55 \mu\text{m}$) after 30 minutes of machining (Figure 48). It is believed that further experimentation will prove that the material removal rate can be significantly improved further with round inserts before tool life will fall to 15 – 20 minutes.

Table 15: Recommended cutting data

	Square Insert	Round Insert
Cutting Speed (v_c)	60 m/min	150 m/min
Feed (f_n)	0.15 mm/rev	0.15 mm/rev
Depth of Cut (a_p)	0.25 mm/rev	0.25 mm/rev
Material Removal Rate (MRR)	2.25 cm ³ /min	5.63 cm ³ /min

Comparing the material removal rate of a square insert under finishing conditions to the parameters achieved with the round inserts (Table 15) results in a 250% improvement in material removal rate. This improvement does however not come at the cost of tool life, but with an improvement of tool life.

These round inserts do however have some technical difficulties. Most components that are turned have sharp corners to seat bearings and several other small radius features. Because these tools effectively have a large nose radius (6 mm) their finishing uses are limited. It is however also known that titanium aircraft components are normally light weight components that are manufactured from a solid billet. It therefore requires a large percentage of the material to be removed, resulting in a large amount of roughing. Experimental runs were conducted where the depth of cut has been increased up to 1.0 mm where no chatter or noticeable change in cutting conditions was noticed. These conditions could however not be extensively tested due to material restrictions. Literature does however confirm that depth of cut does not extensively influence tool life and considering that no chatter is experienced, there is no doubt that tool life will not be adversely affected. These round inserts can therefore be used to conduct roughing operations in titanium machining to significantly improve the productivity.

Some caution will however need to be taken at the end of repetitive cuts that do not reduce the diameter over the complete length of the stock (Figure 74). The nose radius on inserts results in an automatic depth of cut increase at the fillet at the end of the cut. On inserts with a nose radius of 0.8 mm, this effect is minor and not applicable when the depth of cut is larger than the nose radius. With round inserts this effect is unavoidable as the depth of cut will steadily increase at the end of the cut to a maximum of the cutter radius. Depending on the rigidity of the machine, this could cause chatter. The solution to this problem is to lower the feed rate for the last 6 mm (equal to the insert radius) of the cut when the diameter will be significantly reduced.

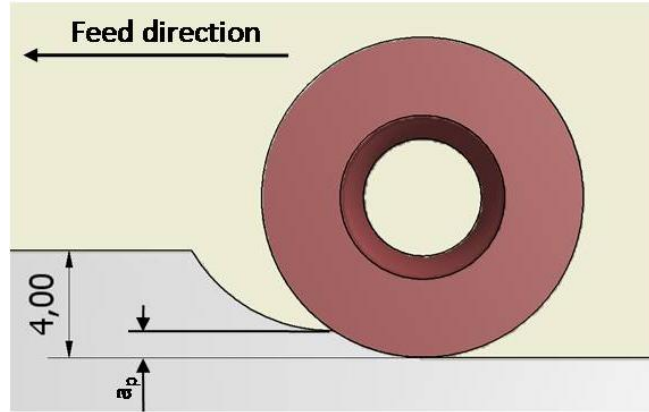


Figure 74: Effect of large nose radius on end of cut

7.3. Polycrystalline diamond (PCD) insert performance

7.3.1. PCD with soluble oil cooling

Experimentation with round 12mm diameter polycrystalline diamond (PCD) inserts was conducted as the follow-up experimentation on the WC inserts. The WC inserts was evaluated as a benchmark for the PCD experimentation as the current technology.

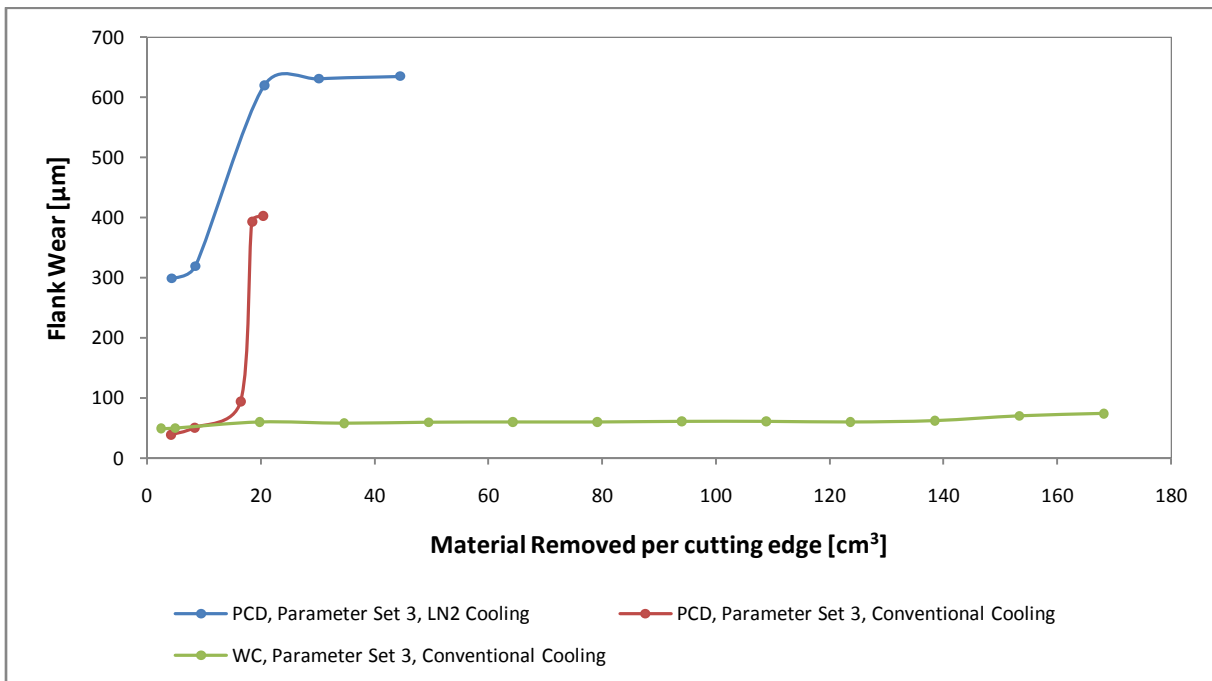


Figure 75: Maximum flank wear with regard to material removed

To be able to determine the factor resulting in tool life change, only one factor is changed at a time. For this reason WC inserts and PCD inserts were tested under conventional flood cooling conditions. This

would provide the results to compare the two cutting materials. Figure 75 shows the results of the maximum flank wear for the PCD inserts. Yet again, the parameter sets referred to is listed in Table 14. Due to the geometry of the PCD inserts, the inserts had to be clamped down by the tool cap that is used for the LN₂ cooling.



Figure 76: Build up on rake face of PCD insert

The reporting of the amount of wear relative to the amount of material removed shows that the PCD inserts are not performing as expected. This is believed to be due to the chatter that was experienced after 2minutes 35 seconds of experimentation. At 2 minutes and 57 seconds, after the chatter occurred, the tool was analysed for wear. Analysis showed that a build up has developed on the rake face of the PCD insert (Figure 76). Wear on the tool was however still minimal.

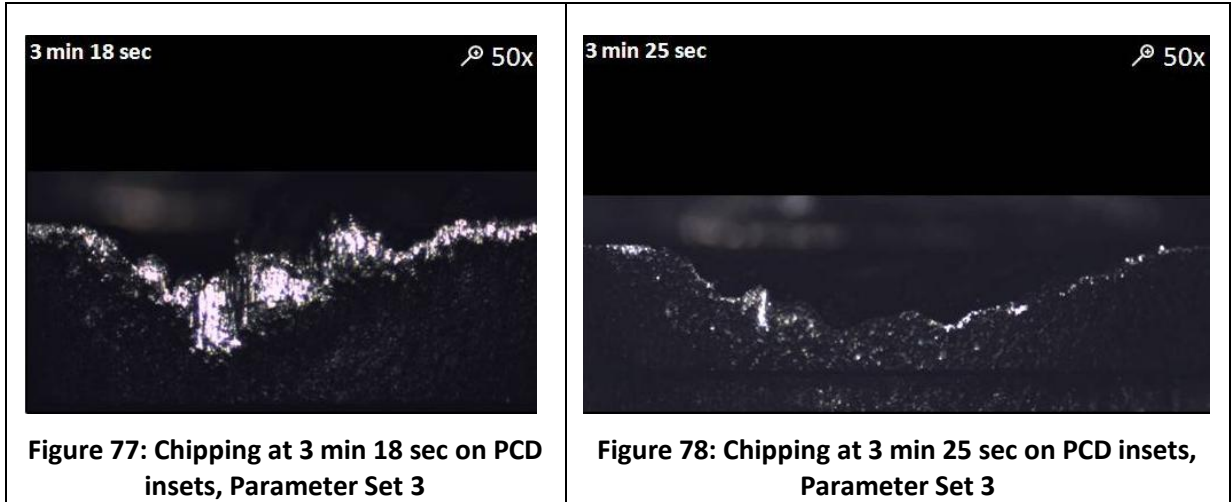


Figure 77: Chipping at 3 min 18 sec on PCD insets, Parameter Set 3

Figure 78: Chipping at 3 min 25 sec on PCD insets, Parameter Set 3

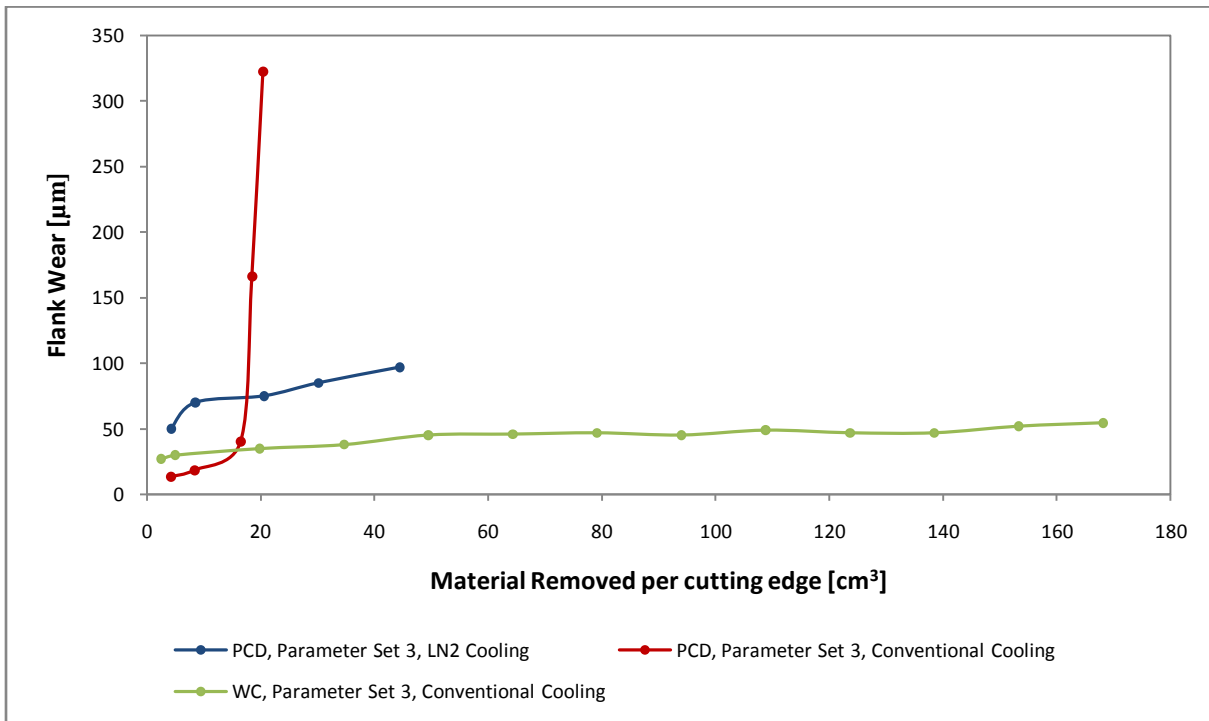


Figure 79: Average flank wear relative to material removed

Excessive wear was however experienced in the following cut. The tool was analysed to find that the cutting edge had fractured. The PCD inserts are hard and tough against wear and handle the high heat load well, but the trade-off is that the material is brittle. The inserts are sensitive to impact shocks that causes chipping of the sharp cutting edge. As shown in Figure 75 and Figure 79, the situation changed rapidly and drastically during the next cut. The next cut experienced excessive chatter during the cut. This was caused by the build-up to tear off the rake face, leaving the cutting edge weakened. The cutting

edge fractured causing the chipping seen in Figure 77. In the next cut the excessive chatter caused the chipping to progress, causing most of the cutting region to fracture. This resulted in the average wear exceeding the 300 μm limit, and the tool being classified as failed.

The wear pattern present in this experimentation is however not typical for PCD inserts. Chatter was considered the cause of the poor tool life during this experiment. The question to be asked is what caused the chatter. The chatter is not attributed to the combination of cutting parameters and machine stiffness, but rather in the clamping of the insert.

As stated earlier, the clamping of inserts is important to prevent chatter. This is even more important with PCD inserts, as they have increased hardness, but are also brittle and will not withstand the abuse of chatter. Chatter can occur under two circumstances, either the tool or the work piece moves. It is highly unlikely that chatter will develop during machining, unless the material stiffness is compromised, for example on thin walled components. The tool could cause chatter if it is not stiff enough to withstand the cutting forces and therefore bends elastically to such an extent that chatter occurs. The stiffness of the machine could cause chatter if the tool turret moves during cutting. The last reason for chatter due to the tool is if the insert is improperly clamped, and the insert moves within the tool holder.

To identify the cause of chatter, these possibilities have to be considered. As we had no chatter with WC machining, the PCD experimentation will be compared to the WC machining to identify the cause. The work piece diameter when chatter occurred was 51 mm. At this diameter the bar is still stiff and will not cause the chatter experienced. The tool holder and machine stiffness has also been proven not to induce chatter by the WC experimentation. The only option left is the clamping of the insert. This is also confirmed by the difficulty experienced initially with chatter where the clamping of the insert caused chatter from the first cut.

It can therefore be deduced that the design used in the experimentation is not sufficient to adequately clamp the insert. It is therefore recommended that the tool cap be redesigned for future experimentation. Suggestions for modifications are made in a later section of the document (section 7.3.3).

7.3.2. PCD inserts with Liquid nitrogen (LN₂) cap cooling

Research has shown that LN₂ cooling yields a longer tool life when machining Ti-6Al-4V (6,7,13,15,16). Research has also been completed on a similar cryogenic cooling system as developed. The major differences in designs are the method of supplying the LN₂ and the cutting inserts used. It was envisaged to simultaneously test whether the LN₂ could be supplied to the tool cap by means of a single pipe gravity supply system and if improved wear results could be obtained by using PCD inserts instead of WC inserts.

The same setup was used as in the PCD with soluble oil cooling to clamp the PCD insert in the holder. Insert clamping was successful on the first attempt and no chatter was experienced during the experimentation. Some difficulties were initially experienced in purging the LN₂ system but were overcome without difficulty.

During experimentation light sparks were noted on the top of the chips as it was cut. This is due to the reactivity of the Ti-6Al-4V chips with the oxygen at high temperatures. The liquid nitrogen does not come into contact with the chips that are formed. The chips are thus not cooled at all, resulting in high temperatures. These high temperatures result in the small stays of titanium burning in the atmospheric air. It has to be noted that the chips did not catch fire and there is thus no need for concern. Overall no visual signs were noticed that any difficulties were experienced during machining.

This is also shown in the experimental results shown in Figure 75 and Figure 79. The average wear rate over the complete experimental period proved to be exceptionally low reaching a maximum of 97 µm after 44.48 cm³ of material was removed (7min 57 sec). Maximum flank wear measured 319 µm after 8.48 cm³ of material has been removed (1 min 31 sec), although the flank wear growth at this point was slow. The adhering of the chip after 3 minutes 41 seconds did however have a large effect on the maximum flank wear. During this cut, the chip became red hot towards the end of the cut. The high temperature that the chip reached allowed the Ti-6Al-4V to weld to the tool cap. The chip was removed, the tool inspected and experimentation continued. Maximum flank wear did however increase to beyond the allowable limit, although the extreme wear was measured where the uncut material OD meets the tool at the end of the cut. It was decided to continue machining as this was not within the normal wear region. The maximum flank wear for the cutting edge region in cut during a 0.25mm a_p is added to the graph shown in Figure 80.

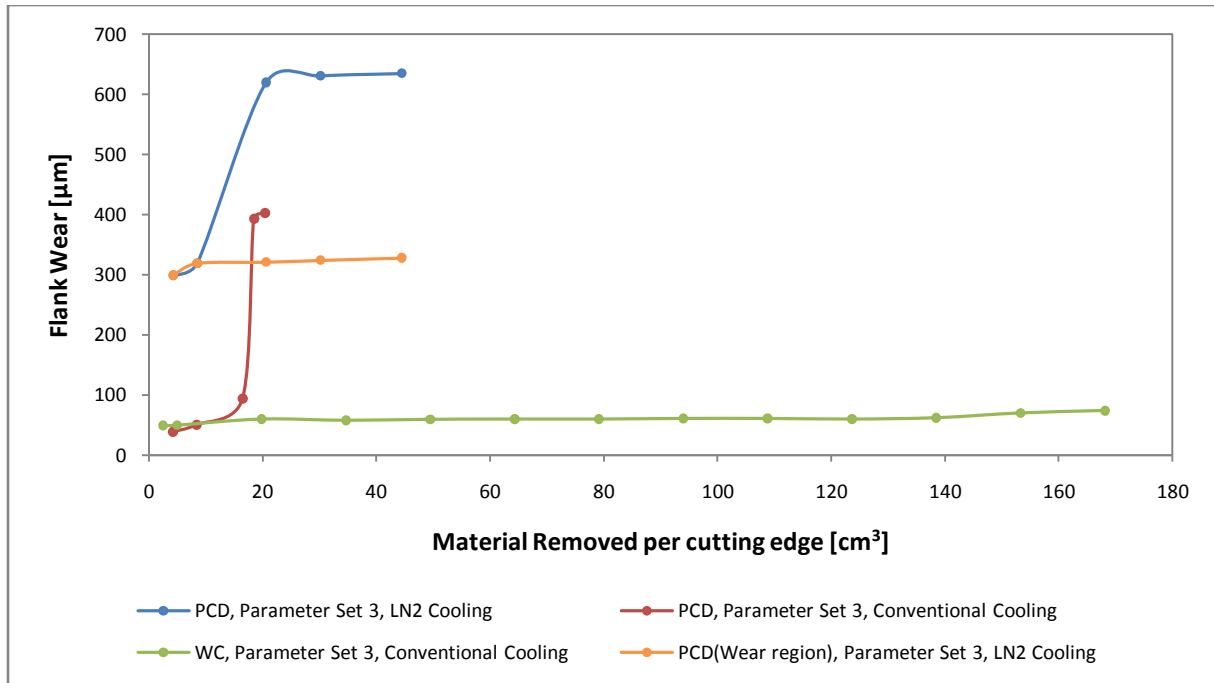


Figure 80: Maximum flank wear at parameter set 3

The tool was again inspected after another 1 min 43 sec of machining during which time no chip adherence occurred and wear on the tool increased marginally. After a total of 44.48 cm³ of material was removed, the equivalent of 7 minutes and 57 seconds of machining at these conditions, the chip again adhered to the tool cap. With the last cut before termination, the chip became red hot early in the cut. After this cut the chip could not be easily removed from the tool cap. The tool was inspected for wear. Tool wear inspection also showed that the chip did not adhere to the rake face of the insert at all, seeing as a clear separation between the rake face and the chip was visible (Figure 64). This was confirmed by inspection of the tool cap that showed no separation between the tool cap and the welded chip (Figure 81).

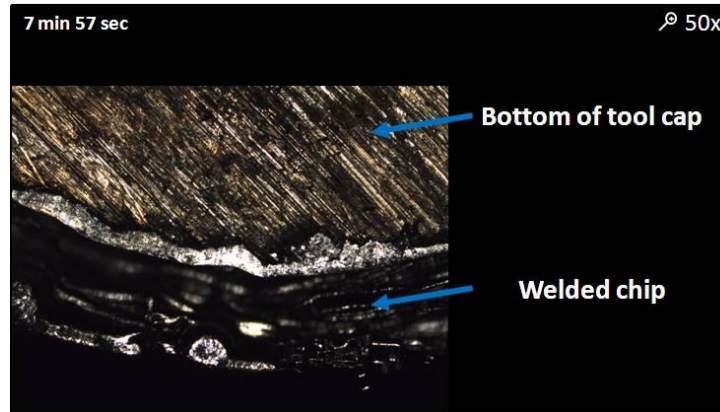


Figure 81: Chip welded to tool cap

To be able to remove the chip from the tool cap, the tool cap had to be removed. Due to the geometry of the insert, it is not possible to clamp the insert with the exact same position once the insert has been removed. As the tool cap held the insert in place, experimentation would have to be terminated once the cap was removed. After the cap was removed the chip had to be removed with force, leaving welded Ti-6Al-4V deposit on the bottom edge of the tool. This had to be removed by sanding. This shows that the chip temperature was higher for longer than with the previous adhesion. The temperature difference between the tool cap and chip was therefore less, and a better fusion could be established between the two materials.

It is believed that if the chips had not adhered to the tool cap, machining would have continued and resulted in good wear results. This is based on the wear results measured within the region of the 0.25mm a_p wear scar which was well below the limit. As stated in section 7.2 the a_p increases dramatically at the end of the cut. To be able to keep the cutting conditions constant, precautions for this effect could not be taken in experimentation. This resulted in the increased wear at the OD mark on the insert. Seeing as no chatter occurred while machining with PCD inserts with LN₂ cooling, it is possible to compare the results of these experiments to that of WC inserts. The specific cause of the change in wear results can however not be determined, as two factors have been changed between the experimentation. A judgement can however be made on the success of PCD inserts with liquid nitrogen cooling relative to conventional cooling before chatter occurred.

PCD inserts with LN₂ cooling show promising results when compared to conventional cooling. The average wear pattern available shows a slow wear growth rate, indicating that the LN₂ is sufficiently cooling the cutting insert to prevent excessive wear. Initial wear is however higher than that of PCD

inserts with conventional cooling. This is attributed to the sharp cutting edge of the PCD that is vulnerable to micro chipping when cooled to cryogenic temperatures. This same mechanism is responsible for the large wear scar at the engagement mark of the insert.

It is therefore concluded that round PCD inserts with closed LN₂ cooling system are sufficient to provide good wear results, although it does not yield improved tool life compared to WC inserts with conventional cooling. Initial wear of the PCD inserts with LN₂ is greater than that of PCD with conventional cooling. Chatter caused by the clamping method did however result in rapid failing of the PCD tool with conventional cooling, and it is therefore not possible to come to a conclusion in this regard. Further experimentation with an improved clamping method will have to be conducted to result in a fair conclusion. The suggestion is therefore that titanium machining with round inserts is conducted with WC inserts and conventional cooling. The costs of WC inserts are also inexpensive compared to PCD, which strengthens the case for the use of WC inserts.

7.3.3. Tool cap performance analysis

It has been noted that chip adhesion occurred when more than 5 consecutive cuts were made (equivalent of 1 minute 49 seconds of machining). This indicates that during multiple consecutive cuts, the cooling is not able to keep the cutting temperatures under control. It is believed that the reason for this is in the supply system of the LN₂.

As stated earlier, part of the experimentation was to test whether the LN₂ could be delivered by a single pipe gravity feed system. The reason for this is the simplicity of the system. If the system operates successfully the need for flow control valves, pressure relieve valves and many other required control and safety equipment required with complex systems is eliminated.

The challenge with LN₂ is however that it reacts quite differently than substances that are fluid at room temperature. It was noted during experimentation that the frost that initially accumulate around the tool cap before machining starts, melts away rapidly. Although experimental results show that the LN₂ does cool the cap significantly during the first 5 cuts of machining, the same cannot be said after 5 cuts. The only reason for this would be that the LN₂ cannot keep the tip and tool cap cool enough to prevent welding. It is believed that the LN₂ is not present on the rake face of the tool after 5 cuts. The answer for this lies in the operation of the system, as there was always LN₂ left over in the reservoir after machining was completed, even after the chip had welded to the tool cap.

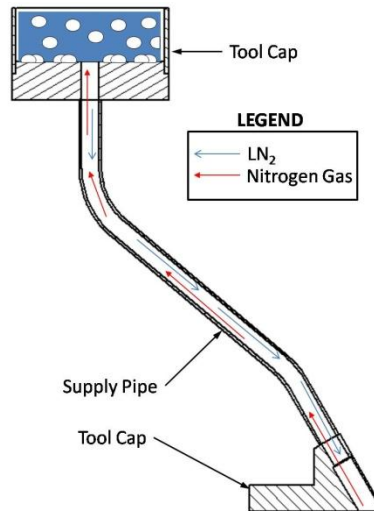


Figure 82: LN₂ Supply System

Figure 82 shows the LN₂ supply system for the tool cap. The LN₂ flows down the supply pipe to the tool cap where it flows down to the tool cap. At the same time, the evaporated nitrogen gas moves up the supply pipe to the reservoir where it escapes to the atmosphere. In theory the system seems simple enough to work, although the dynamics of what happen is quite different. When the LN₂ evaporates, it expands approximately 700 times in volume, and this causes problems in the single pipe system under steady state machining conditions. The piping used for this system has a 4mm internal diameter. When the LN₂ evaporates during system initialisation, the system cools down and settles to a large extent. The evaporation rate at this point is manageable for the system. The situation changes when machining commences. During machining a large amount of heat is transferred to the insert and tool cap from the chips. This accelerates the evaporation rate drastically, causing a large volume of gas at the lowest point of the system to form. The result is that the flow of gas upward in the tube displaces the LN₂ and prevents an even flow. Due to the small diameter of the tube, this becomes a major problem, as the amount of gas is so large that it prevents the LN₂ from entering the tool cap. The situation changes when the pressure of the evaporated gas in the tool cap falls below the gravity feed pressure from the LN₂ in the reservoir. For this to happen, all the LN₂ has to be evaporated in the tool cap. The amount of LN₂ that is delivered to the rake face of the tool is therefore much less than intended. This reduces the effect of the LN₂ to a large extent as the flow of LN₂ to the tool cap is not constant but periodical.

It is therefore reasonable to conclude that the supply system used in this design is not successful. The diameter of the pipe is too small to accommodate the LN₂ and the evaporated gas. One solution could be to increase the diameter of the supply pipe, although the principle of the supply system on the first

tool cap design is a better option. This will allow the evaporated gas to escape unrestricted and will allow the LN₂ to reach the tool cap unhindered. This in turn will improve the cooling capacity of the LN₂ system.

There is also the cumbersome issue of tool cap's ability to clamp the insert, which is the most important issue at hand. As described earlier the tool cap could not clamp the PCD insert effectively enough to prevent chatter. This is due to the system through which the system clamps the insert. Two options exist to rectify this problem. Either the insert should be clamped down independently of the tool cap, for example with a screw, like the WC inserts, or the tool cap must be redesigned to exert a more distributed level force on the insert. The current tool cap is rigidly designed, machined from a single billet, and self alignment does not occur as expected. The inserts manufactured are not all of same height, which requires the tool cap to adjust for height issues. The new tool cap will also have to ensure that the force exerted on the insert will be automatically aligned to be perpendicular to the insert rake face. Although this was the aim of the current tool cap, this did not realize. This can be accomplished using a two piece tool cap design. The part that will be located on top of insert will be free to rotate in order to firmly seat its bottom face on the rake face of the insert. A finger type clamp will then be used to exert the force onto the tool cap in order to clamp the tool. This method will however also require number of design repetitions to perfect. The safest and most secure method will however still be to screw the insert into place.

In conclusion, the tool cap designed is not sufficient to perform the task at hand. This is however seen as very important ground work for further research into this method of cooling. It is believed that there is a large potential in this method of cooling and further research is advised.

8. Additional work

The following articles were published during the period of the study:

A review of novel cooling methods in titanium machining – SAIIE 2009 (attached as Appendix 5)

Investigating novel cooling methods for titanium machining – COMA 2010 (attachment as Appendix 6)

9. Conclusion

Although it is common knowledge that round inserts have a better tool life than angular type inserts, the extent to tool life improvement in titanium machining with tungsten carbide round inserts were beyond expectation. Machining at 150 m/min resulted in exceptionally low maximum flank wear of 74 μm . The round inserts will result in a significant improvement in productivity during roughing conditions without compromising the surface finish of the work piece. Although the inserts have some technical considerations, the use of the inserts will significantly reduce machining time. This is achieved by an improvement of 250% in material removal rate compared to the current roughing parameters for square inserts, with no compromise in tool life. The author is of opinion that further research with larger depth of cuts and higher feed rates will yield even better improvements in material removal rate before the tool life will drop to the norm of 15 to 20 minutes.

The results obtained with the round tungsten carbide experimentation show a significant improvement compared to the 5 minutes of tool life reported on round tools used by Kishawy et al.(38). It is a significant improvement over that on square type tungsten carbide inserts as well, of which the expected tool life is in the approximately of 1 minute at 150 m/min (7,13).

Research into the use of PCD inserts with localised liquid nitrogen cooling show promising results. Due to early design iteration imperfections in the design of the tool cap used, chips welded to the tool cap and prevented the inserts from being tested to the failure point. The tool wear progression pattern is however flat and it is believed that the tool will last well beyond the norm of 15 minutes of tool life. The maximum flank wear for PCD with LN_2 measured 328 μm within the wear region of the tool, which is classified as notch wear at the depth of cut mark. The maximum average flank wear was measured at 97 μm after 7 minutes and 57 seconds of machining. A longer tool life was achieved with the PCD with LN_2 cooling than with PCD and soluble oil cooling under the same conditions. The short tool life of the PCD insert with soluble oil cooling is attributed to the chatter that developed after 3 minutes of machining.

The primary part of this study was testing the designed tool cap. After two tool cap design iterations the tool cap performance was still not satisfactory. The primary problem experienced was the lack of clamping capability when machining with soluble oil cooling. This problem was however not experienced with LN_2 cooling experimentation. However, after critical assessment of the tool cap, the method that the tool cap presses down on the insert was identified as a feature with room for improvement. The

suggestion for eliminating the difficulties experienced with clamping is to screw the inserts into position. This will result in more design freedom for the tool cap as it will no longer be required to be structurally rigid to keep the inserts in position.

Experimentation also showed that the method of LN₂ supply to the tool cap was not sufficient. The combination of pipe diameter and the rate at which the LN₂ evaporates prevent a constant flow of LN₂ to the tool cap. This reduces the cooling power of the tool cap and PCD insert combination, resulting in inferior cooling to that of which the system is capable. The author is of opinion that a redesigned supply and venting system will eliminate this problem.

The tool cap does however eliminate the cooling of the work piece as no cooling is applied to the cutting region. The effect of the cutting operation is therefore similar to that of dry cutting conditions.

Bibliography

1. Ezugwu EO, Bonney J, Yamane Y. An overview of the machinability of aeroengine alloys. *Journal of materials processing technology*. 2003; 134: p. 233-253.
2. Ezugwu EO. Key improvements in the machining of difficult-to-cut aerospace superalloys. *International Journal of Machine Tools & Manufacture*. 2005; 45: p. 1353 - 1367.
3. Lütjering G, Williams JC. *Titanium*. 2nd ed. Verlag Berlin Heidelberg: Springer; 2007.
4. Ezugwu EO, Wang ZM. Titanium alloys and their machinability - a review. *Journal of Materials Processing Technology*. 1997; 68: p. 262 - 274.
5. Corduan N, Himbert T, Poulachon G, Dessoly M, Lambertin M, Vigneau J, et al. Wear Mechanisms of New Tool Materials for Ti-6Al-4V High Performance Machining. *Cirp Annals-Manufacturing Technology*. 2003; 52(1): p. 73 - 76.
6. Ahmed IM, Ismail AF, Abakr YA, Nurul Amin AKM. Effectiveness of cryogenic machining with modified tool holder. *Journal of Materials Processing Technology*. 2007; 185: p. 91-96.
7. Hong SY, Markus I, Jeong Wc. New cooling approach and tool life improvements in cryogenic machining of titanium alloy Ti-6Al-4V. *International Journal of Machine Tools & Manufacture*. 2001; 41: p. 2245-2260.
8. Rahman M, Wang ZG, Wong YS. A review on high-speed machining of titanium alloys. *JSME International Journal*. 2006; 49: p. 11-20.
9. Ezugwu EO. High Speed Machining of Aero-Engine Alloys. *Journal of the Brazilian Society of Mechanical Sciences and Engineering*. 2004; 26(1): p. 1-11.
10. Machado AR, Wallbank J. Machining of titanium and its alloys. A review. *Proceedings of the Institution of Mechanical Engineers. Part B. Management and engineering manufacture*. 1990; 204: p. 53-60.
11. Arrazola PJ, Garay A, Iriarte LM, Armendia M, Marya S, Le Maitre F. Machinability of titanium alloys

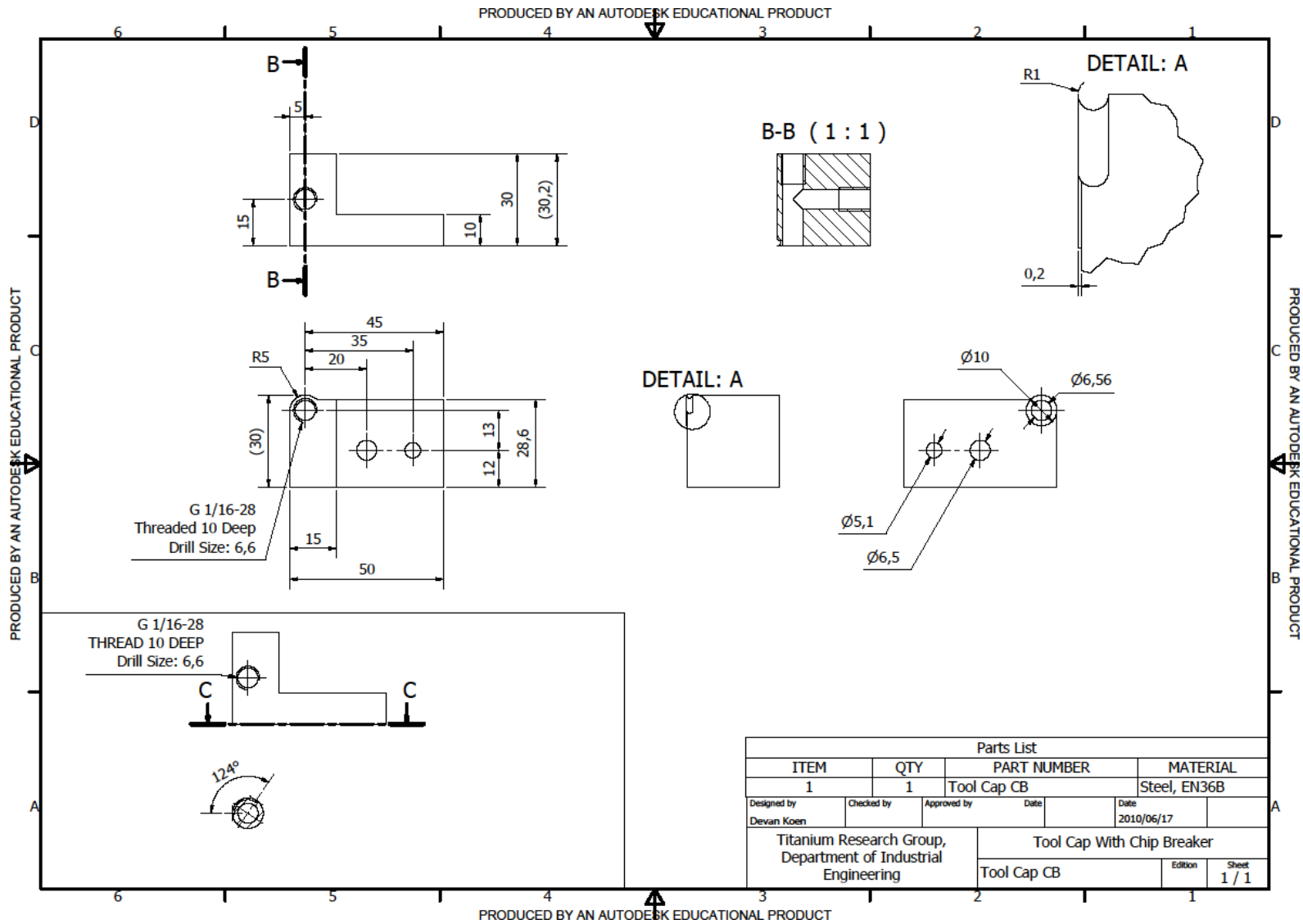
-
- (Ti6Al4V and Ti555.3). *Journal of materials processing technology*. 2009; 209: p. 2223-2230.
12. Campbell FC. *Manufacturing Technology for Aerospace Structural Materials* Great Britain: Elsevier Ltd.; 2006.
 13. Wang ZY, Rajurkar KP. Cryogenic machining of hard-to-cut materials. *Wear*. 2000; 239: p. 168-175.
 14. Hong SY, Ding Y. Cooling approaches and cutting temperatures in cryogenic machining of Ti-6Al-4V. *International Journal of Machine Tools & Manufacture*. 2001; 41: p. 1417-1437.
 15. Venugopal KA, Paul S, Chattopadhyay AB. Growth of tool wear in turning of Ti-6Al-4V alloy under cryogenic cooling. *Wear*. 2007; 262: p. 1071-1078.
 16. Dhananchezian M, Pradeep Kumar M. Cryogenic turning of the Ti-6Al-4V alloy with modified cutting tool inserts. *Cryogenics*. 2011; 51: p. 34-40.
 17. Khan AA, Ahmed MI. Improving tool life using cryogenic cooling. *Journal of Materials Processing Technology*. 2008; 196: p. 149-154.
 18. Hong SY, Ding YH, Jeong W. Friction and cutting forces in cryogenic machining of Ti-6Al-4V. *International Journal of Machine Tools & Manufacture*. 2001; 41(15): p. 2271-2285.
 19. Hong SY. Lubrication mechanisms of LN2 in ecological cryogenic machining. *Machining Science and Technology*. 2006; 10: p. 133-155.
 20. Hong SY. Economical and ecological cryogenic machining. *Journal of Manufacturing Science and Engineering, Transactions of the ASME*. 2001; 123(2): p. 331-338.
 21. Nabhani F. Machining of aerospace titanium alloys. *Robotics and Computer-Integrated Manufacturing*. 2001; 17(1-2): p. 99-106.
 22. Yildiz Y, Nalbant M. A review of cryogenic cooling in machining processes. *International Journal of Machine Tools & Manufacture*. 2008; 48: p. 947 - 964.
 23. Groover MP. *Fundamentals of modern manufacturing* Hoboken: John Wiley & Sons, Inc.; 2002.

-
24. Abdel-Aal HA, Nouari M, El Mansori M. Influence of thermal conductivity on wear when machining titanium alloys. *Tribology International*. 2009; 42(2): p. 359-372.
 25. Bundy FP, Bassett WA, Weathers MS, Hemley RJ, Mao HK, Goncharov AF. The pressure-temperature phase and transformation diagram for carbon; updated through 1994. *Carbon*. 1996; 34(2): p. 141 - 153.
 26. Komanduri R, Reed WR. Evaluation of carbide grades and a new cutting geometry for machining titanium alloys. *Wear*. 1983; 92: p. 113 - 123.
 27. Oosthuizen G. Innovative cutting materials for finish shoulder milling of Ti-6Al-4V aero-engine alloy. Thesis. Stellenbosch University; 2009.
 28. Ezugwu EO, Bonney J, Da Silva RB, Cakir O. Surface integrity of finished turned Ti-6Al-4V alloy with PCD tools using conventional and high pressure coolant supplies. *International Journal of Machine Tools & Manufacture*. 2007; 47: p. 884 - 891.
 29. Barnett-Ritcey DD, Elbestawi MA. Tool performance in high speed finish milling of Ti6Al4V. In *Proceedings of IMECE'02*; 2002. p. 1-9.
 30. ASM Material Data Sheet. [Online]. [cited 2011 July 03. Available from: <http://asm.matweb.com/search/SpecificMaterial.asp?bassnum=MTP641>.
 31. Safetygram 7. [Online].; 2006 [cited 2011 August 05. Available from: <http://www.airproducts.com/safetygrams>.
 32. MS006-Liquid Nitrogen. [Online].; 2009 [cited 2011 August 05. Available from: http://www.afrox.com/downloads/./Material_safety_datasheet/Liquid_Nitrogen.pdf.
 33. Safetygram 47. [Online].; 2010 [cited 2011 August 05. Available from: <http://www.airproducts.com/safetygrams>.
 34. Safetygram 27. [Online].; 2000 [cited 2011 August 05. Available from: <http://www.airproducts.com/safetygrams>.

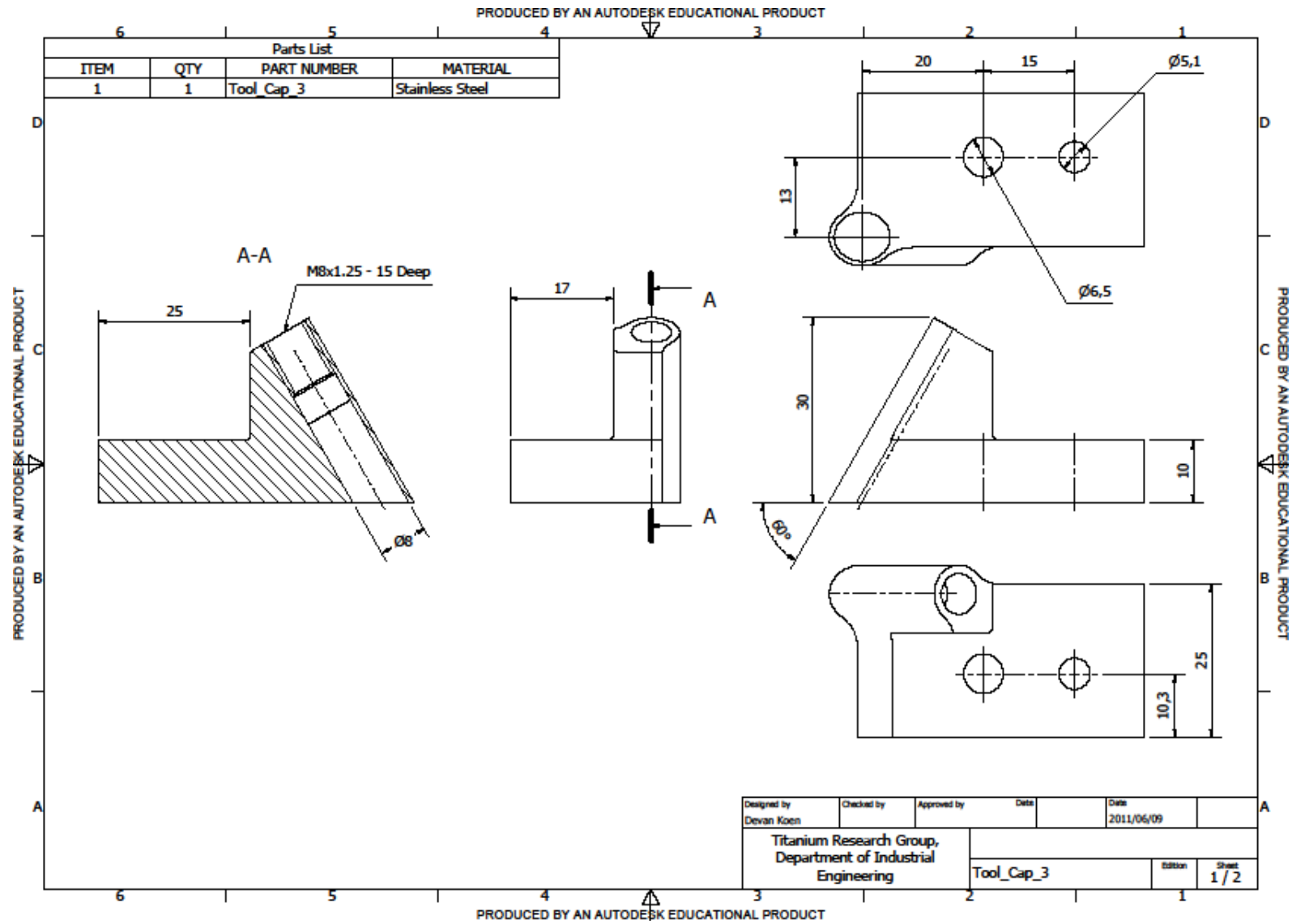
-
35. Turning, General turning insert shape: Round inserts. [Online]. [cited 2011 07 24. Available from: <http://coroguide.sandvik.coromant.com/CuttingDataModule/CDMTurning.asp>.
 36. SCMT 12 04 08-KM H13A Cutting data recommendations. [Online]. [cited 2011 08 19. Available from: <http://coroguide.sandvik.coromant.com/infotype/>.
 37. RCMT 12 04 08-KM H13A Cutting data recommendations. [Online]. [cited 2011 08 19. Available from: <http://coroguide.sandvik.coromant.com/infotype/>.
 38. Kishawy HA, Becze CE, McIntosh DG. Tool performance and attainable surface quality during the machining of aerospace alloys using self-propelled rotary tools. *Journal of materials processing technology*. 2004; 152: p. 266-271.

Appendix 1:

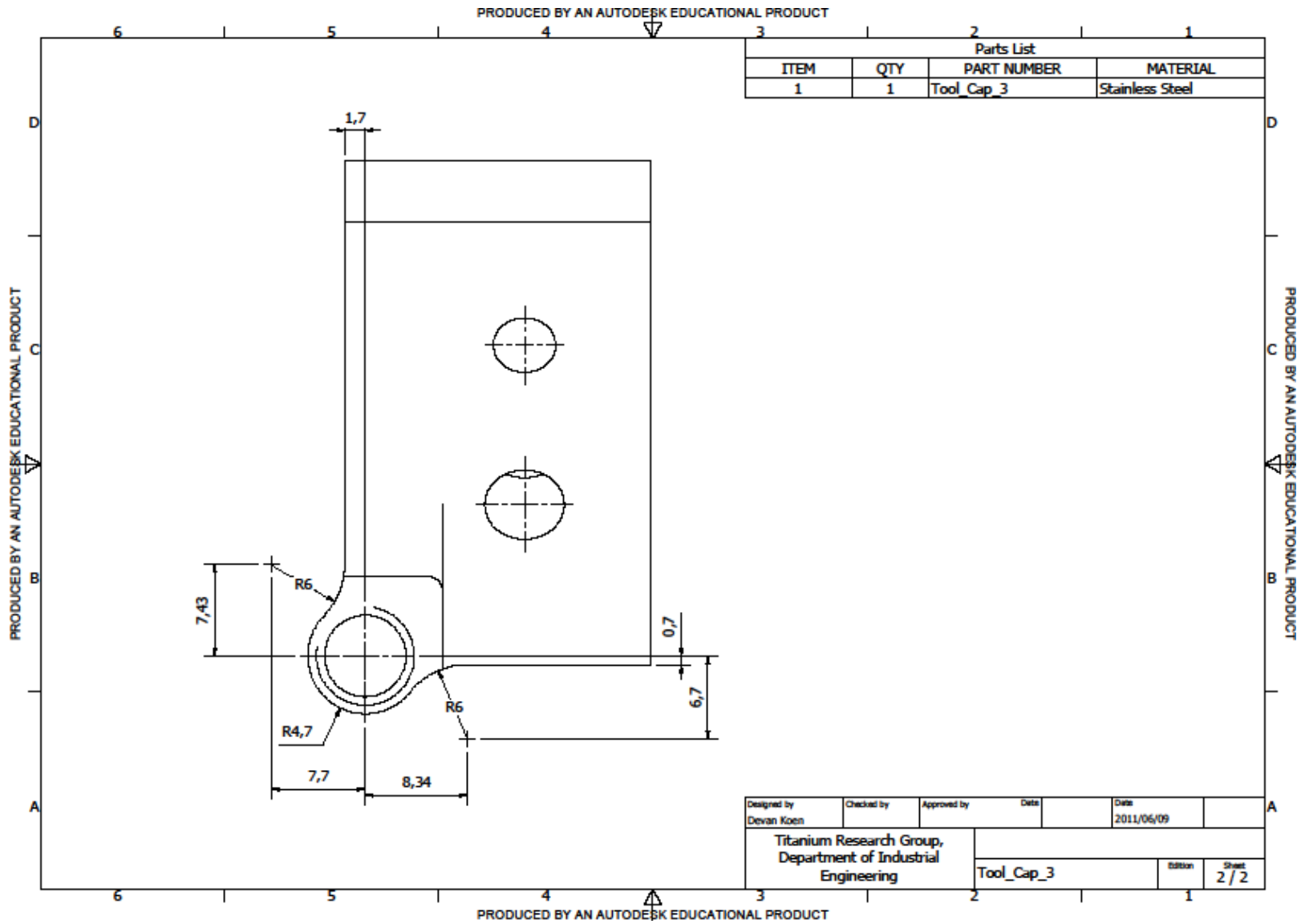
Tool Cap Designs



Tool Cap Design 1



Tool Cap Design 2, Page 1



Appendix 2:

Experiment data capturing sheets

WC TESTS

Ro [mm]	27.5	Vc [m/min]	150.0	f [mm/rev]	0.15			
Ri [mm]	11.3	DOC [mm]	0.250	MRR [mm³/min]	5625.00			
	Cutting Insert	Lubrication Technique	Pass #	Cutting Time	MR [cm³]		VBAvg	VBMax
Parameter Set 1	WC	SO Flood	5	0.00	2.47			
	WC	SO Flood	10	0.00	4.95			
	WC	SO Flood	40	0.00	19.78			
	WC	SO Flood	70	0.01	34.62			
	WC	SO Flood	100	0.01	49.46			
	WC	SO Flood	130	0.01	64.29			
	WC	SO Flood	160	0.01	79.13			
	WC	SO Flood	190	0.02	93.97			
	WC	SO Flood	220	0.02	108.80			
	WC	SO Flood	250	0.02	123.64			
	WC	SO Flood	280	0.02	138.48			
	WC	SO Flood	310	0.03	153.31			
	WC	SO Flood	340	0.03	168.15			

Experimental Data capturing sheet for facing cuts

PCD TESTS

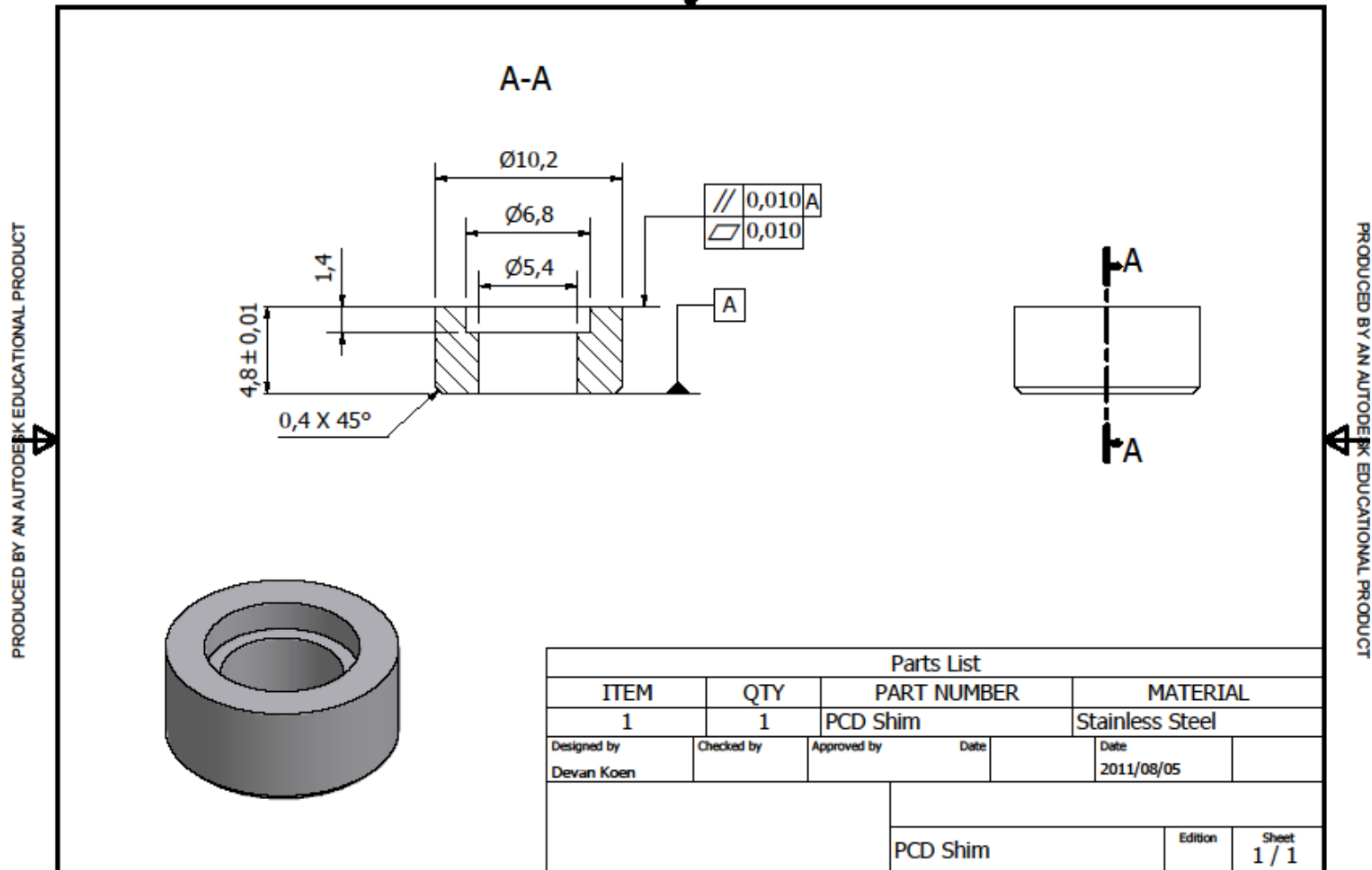
Starting OD [mm]	55.0	Cutting Speed [m/min]	150.0	Feed [mm/rev]	0.15							
Linear Length [mm]	50.0	Depth of Cut [mm]	0.250	MRR [mm³/min]	5625.00							
	Cutting Insert	Lubrication Technique	Run #	Eff OD [mm]	Eff ID [mm]	Tm Cut	Total Tm	MR [mm³]			V_{BMax}	V_{BAvg}
Parameter Set 1	PCD	Flood - Soluble Oil	1									
	PCD	Flood - Soluble Oil	2									
	PCD	Flood - Soluble Oil	3									
	PCD	Flood - Soluble Oil	4									
	PCD	Flood - Soluble Oil	5									
	PCD	Flood - Soluble Oil	6									
	PCD	Flood - Soluble Oil	7									
	PCD	Flood - Soluble Oil	8									
	PCD	Flood - Soluble Oil	9									
	PCD	Flood - Soluble Oil	10									
	PCD	Flood - Soluble Oil	11									
	PCD	Flood - Soluble Oil	12									
	PCD	Flood - Soluble Oil	13									
	PCD	Flood - Soluble Oil	14									
	PCD	Flood - Soluble Oil	15									
	PCD	Flood - Soluble Oil	16									
	PCD	Flood - Soluble Oil	17									
	PCD	Flood - Soluble Oil	18									
	PCD	Flood - Soluble Oil	19									
	PCD	Flood - Soluble Oil	20									

Experimental Data capturing sheet for longitudinal cuts

Appendix 3:

Height correcting spacer for polycrystalline diamond inserts

PRODUCED BY AN AUTODESK EDUCATIONAL PRODUCT

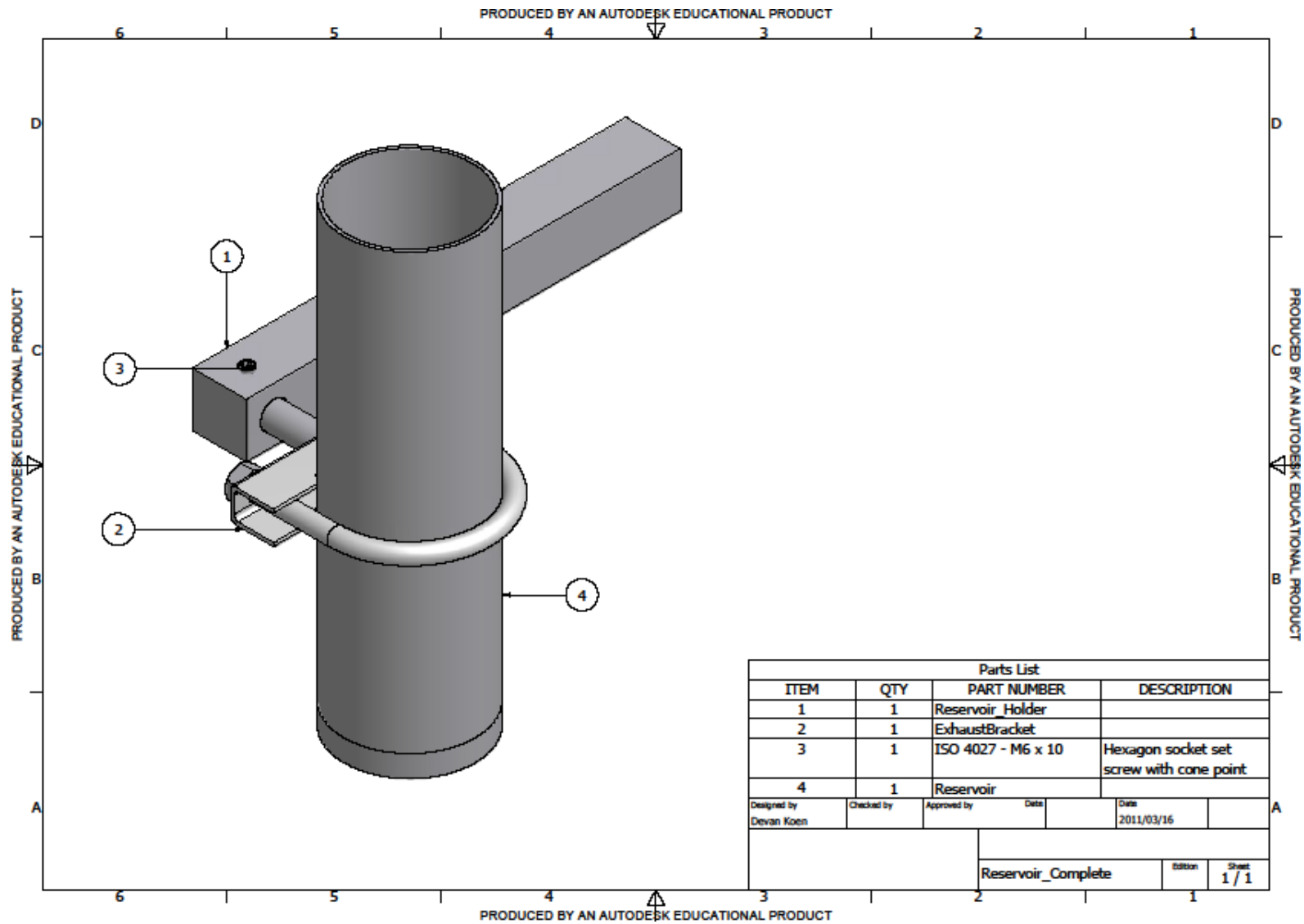


PRODUCED BY AN AUTODESK EDUCATIONAL PRODUCT

Height correcting spacer for polycrystalline diamond inserts

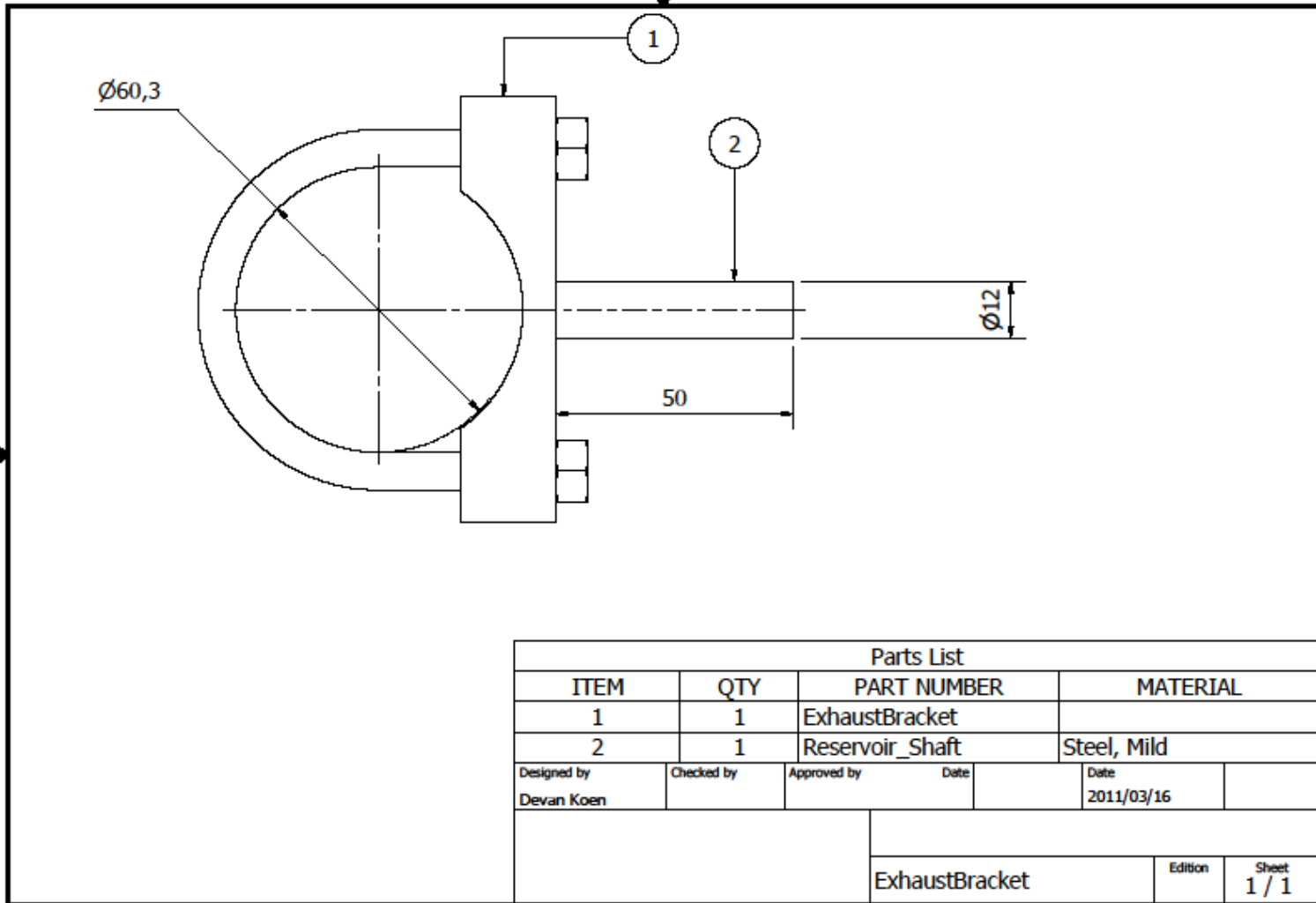
Appendix 4:

Liquid nitrogen supply reservoir



Assembled reservoir system to supply liquid nitrogen

PRODUCED BY AN AUTODESK EDUCATIONAL PRODUCT

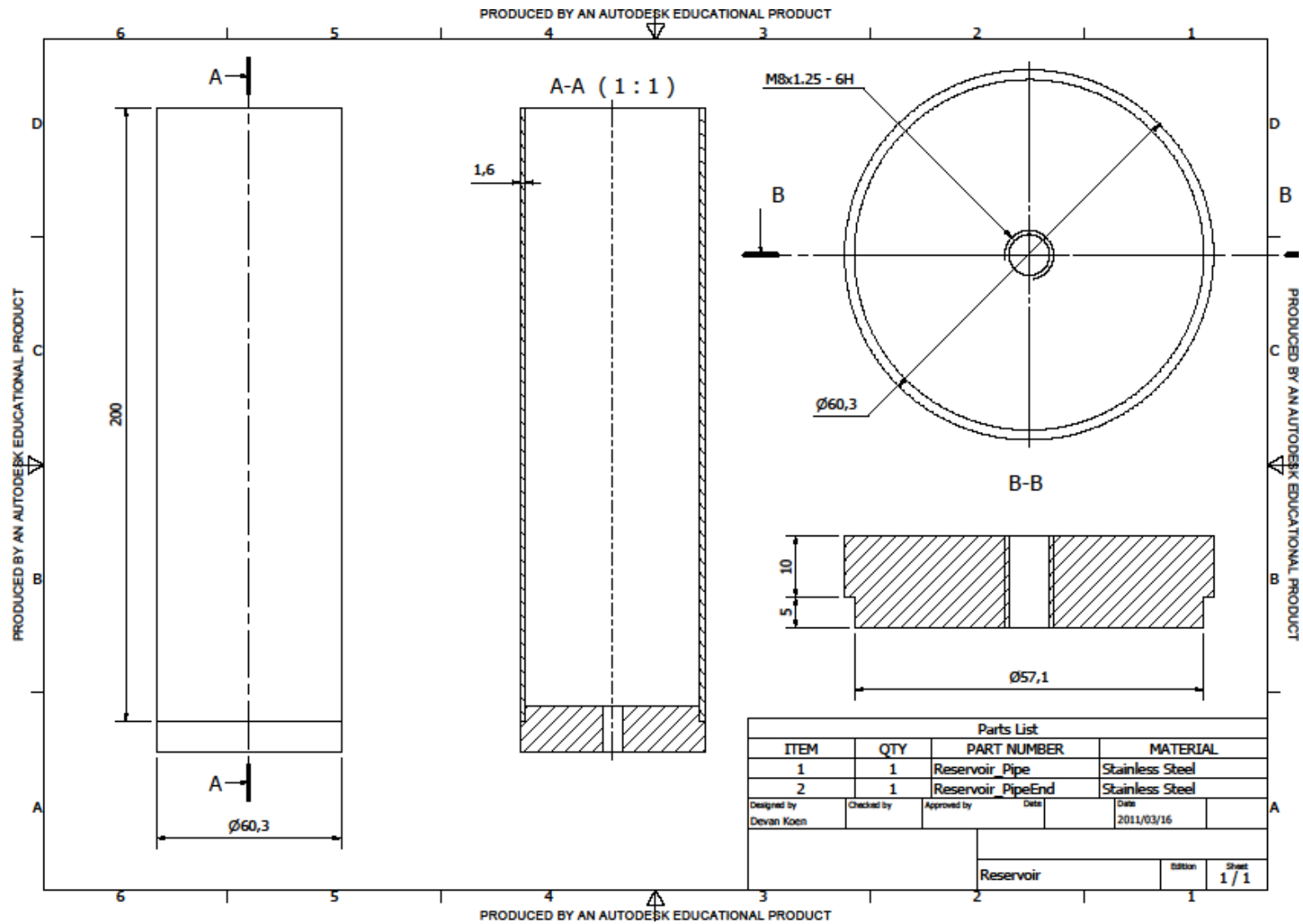


PRODUCED BY AN AUTODESK EDUCATIONAL PRODUCT

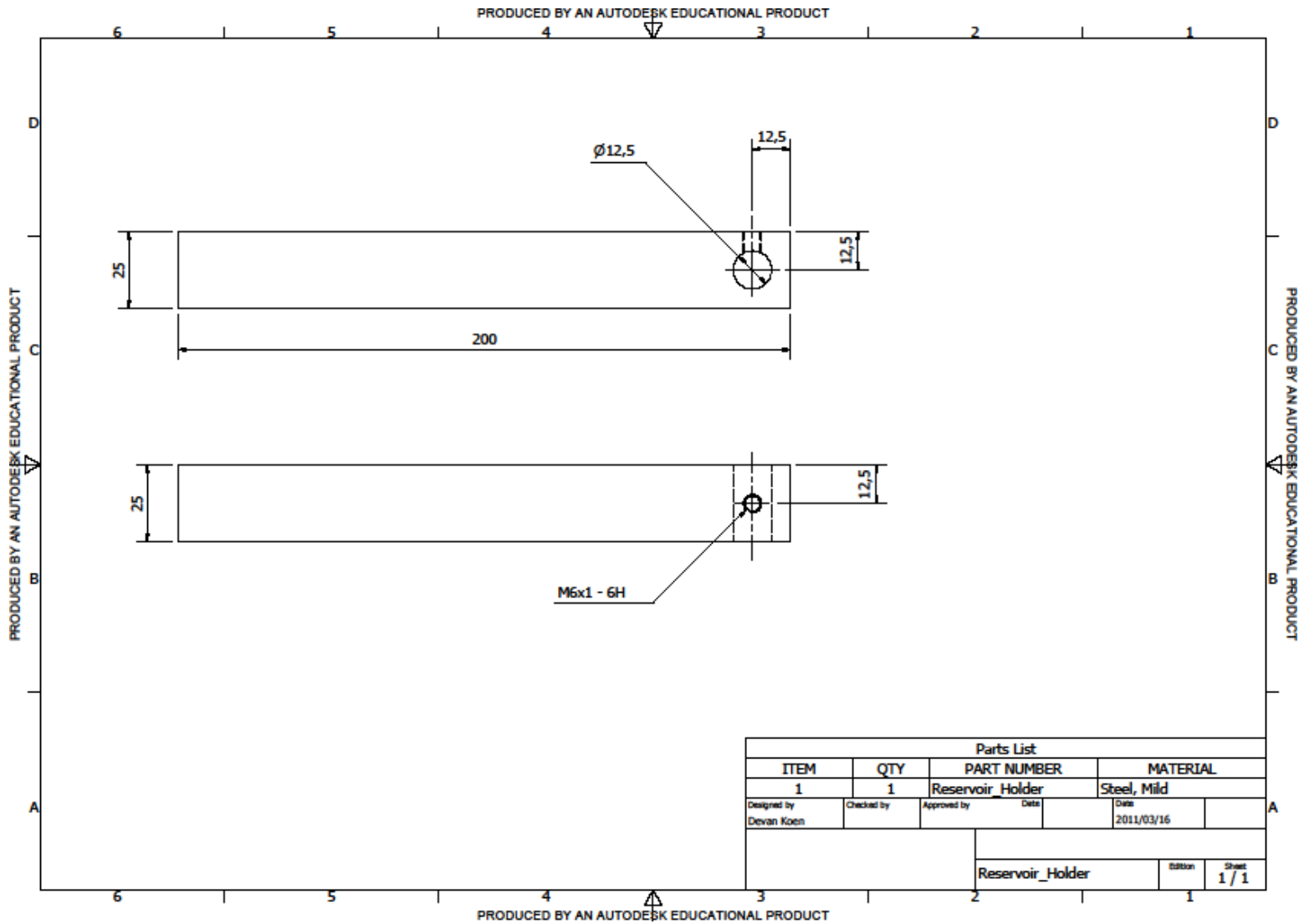
PRODUCED BY AN AUTODESK EDUCATIONAL PRODUCT

PRODUCED BY AN AUTODESK EDUCATIONAL PRODUCT

Modified exhaust clamp to hold reservoir



Reservoir that will contain the liquid nitrogen



Square bar to fit the supply system to the tool turret

Appendix 5:

Conference article

A REVIEW OF NOVEL COOLING METHODS IN TITANIUM MACHINING

A REVIEW OF NOVEL COOLING METHODS IN TITANIUM MACHINING

D. Koen^{1*} and N.F. Treurnicht²

¹Department of Industrial Engineering
University of Stellenbosch, South Africa
devankoen@sun.ac.za

²Department of Industrial Engineering
University of Stellenbosch, South Africa
nicotr@sun.ac.za

ABSTRACT

The utilization of titanium as a high strength to mass ratio structural material for commercial as well as military applications is becoming more significant. The productive and cost effective machining of titanium however continues to be a constraint. A pragmatic approach to development of machining techniques necessarily includes a focus on cooling. This paper reviews cooling methods using liquid nitrogen as cooling medium. Results show that it is paramount to focus the cooling predominantly on the cutting insert. The most promising methods were a closed loop liquid nitrogen jacket and a modified chip breaker configuration.

OPSOMMING

Die benutting van titaan as 'n hoë sterkte tot massa verhouding strukturele materiaal vir kommersiële en militêre toepassings raak al hoe meer prominent. Produktiewe en koste effektiewe masjinerie van titaan is egter steeds 'n beperkende faktor. 'n Pragmatiese benadering tot die ontwikkeling van masjinerie tegnieke sluit noodwendig 'n fokus op verkoeling in. Hierdie referaat bied 'n oorsig oor verkoelings tegnieke wat gebruik maak van vloeibare stikstof as verkoelingsmedium. Die belowendste tegnieke is 'n geslote lus vloeibare stikstof huls en 'n aangepaste spaanderbreker konfigurasie.

¹ The author was enrolled for an MScEng(Industrial) degree at the Department of Industrial Engineering, University of Stellenbosch

² The author was a lecturer in the Department of Industrial Engineering, University Stellenbosch

*Corresponding author

1. INTRODUCTION: TITANIUM MACHINING

Titanium has become increasingly popular in the aviation industry due to its superior material properties to other materials. Typical aerospace titanium has a tensile strength of one and a half times that of typical high carbon steel and its thermal conductivity is half of typical high carbon steel. Together with this, titanium is 44% lighter than high carbon steel and it is highly corrosion resistant without any treatment [3-6]. However, all these material properties also make titanium rather difficult to machine.

When machining titanium, there are a number of wear mechanisms that result from titanium's high temperature strength, low thermal conductivity and high chemical reactivity at high temperatures. Due to these factors, the machining of titanium generates a large amount of heat in the cutting zone. Titanium has an exceptionally small chip-tool interface and due to the low thermal conductivity of the titanium alloys (15 W/mK for Ti-6Al-4V) the titanium does not readily absorb heat [6]. The thermal conductivity of the cutting insert (100 W/mK for H13A tungsten carbide) is usually much higher, which results in about 80% of the heat created being transferred to the cutting insert, more specifically to the cutting edge region [3,6]. The temperatures of the cutting edge can be as high as 1100°C for titanium cutting and at these temperatures most tools tend to fail rather rapidly [3].

As previously stated, titanium is highly chemically reactive at these high temperatures, which also results in wear, namely adhesion and diffusion wear. At these high temperatures, the titanium chips chemically react with the cutting insert, creating a build-up on the tool's rake face. This build-up increases until a chip adheres to the build-up, breaking off from the rake face, removing some of the tool material. As this cycle repeats itself, a crater is formed [2,5].

The tool is also subjected to high mechanical stresses during machining. The effect of the mechanical stress on the tool also increases as the tool heats up, as all tools become softer when heated. Some tools have been developed with this in mind and are selected using high hot hardness as a criterion [6].

One of the theories to improve the machining of titanium is to utilize the thermal softening behaviour of titanium at elevated temperatures. This necessitates the strategy to retain as much of the heat that is generated during the machining process in the work piece. The best way to achieve this would be to maximize the cooling of the insert, while minimizing the cooling of the work piece. It is for this purpose that many researchers have proposed innovative cooling concepts focusing the cooling power predominantly onto the insert. These concepts are referred to as local insert cooling methods [1,4].

2. LOCAL INSERT COOLING METHODS

2.1. Cutting fluids and cryogenic cooling

Cutting fluids can be classified into 3 main categories, namely water soluble fluids, neat cutting oils and gases. Water soluble fluids are mainly used when the cutting speeds are high and the tool pressures are low. When the cutting pressures between the tool and chip are high, neat cutting oils are preferred, especially if the primary consideration is lubrication. Gaseous lubricants, for example liquid nitrogen (LN₂), are the most preferable when problems are experienced with the penetration of the lubrication. In general, the reduction of cutting temperatures results in a lower wear rate and better tool life. When the work piece is cooled, it is possible that the material will harden to such an extent that the tool life is significantly shortened. Research involving LN₂ has mostly been done on turning operations due to the difficulties experienced when used in milling operations [7].

Environmental and health problems are also a reality with conventional cooling. Environmental pollution includes the pollution of water and contamination of soil when the cutting fluid is ultimately disposed. Examples of health problems include dermatological ailments when operators are exposed to fumes and physical contact with the cutting fluid [7]. LN₂ is also abundantly available considering that the earth's atmosphere is composed of 78% of nitrogen. Other advantages are that LN₂ is colourless, odourless, tasteless and non-toxic.

2.2. High pressure liquid nitrogen(LN2) jets

Venugopal et al. tested the effect of LN2 sprayed onto the rake and flank faces by means of specially designed nozzles. The specially designed nozzles were directed at the rake and flank surface of the uncoated microcrystalline K20 tungsten carbide cutting insert. The flow rate and application pressure were determined by means of trial and error to obtain a continuous flow of LN2 while not overcooling the work piece. Tests were conducted at cutting speeds of 70, 100 and 117 m/min with a feed rate of 0.2 mm/rev and a 2 mm depth of cut. These cutting configurations can be considered as high performance conditions as cutting speeds of 20 - 60 m/min are the accepted industry norm, and the feed rate and depth of cut are above the industry norm. A graphic representation of the experimental set-up can be seen in Figure 1.

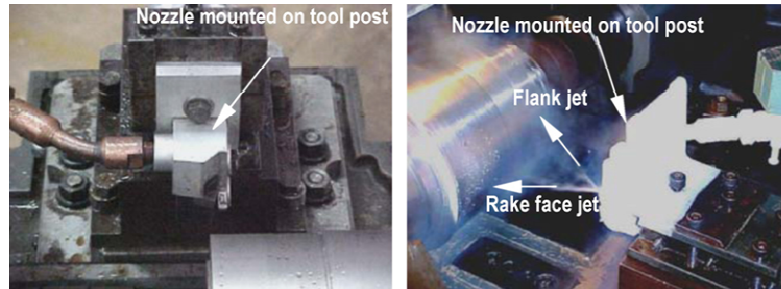


Figure 1 - Liquid nitrogen delivery set-up [5]

The result of this experiment yields a large improvement in the tool life of the cutting insert. At a cutting speed of 70 m/min, machining with LN2 showed a 71% improvement in tool life compared to machining with soluble oil, and a 243% improvement compared to dry machining. As cutting speeds were increased, the effect of the LN2 on the tool life deteriorated, but the improvement was still substantial. It is believed that the reason for the decreased effectiveness is that the LN2 is not able to penetrate to a sufficient depth into the tool-chip interface to cope with the increased heat load caused by the higher cutting speeds. It was also noted that flaking only occurred on the edge of the crater when machining with a coolant. This is interpreted to be the result of thermal shock caused by the rapid rate at which heat is removed. Other wear mechanisms that were observed are crater wear, plastic deformation, micro and macro cracks on the cutting edge and abrasive flank wear [5].

2.3. LN2 cooling using a modified tool holder

In this method, Ahmed et al. modified a standard tool holder so that LN2 could be applied to the mounting surface of the cutting insert. Two different methods of discharging the evaporated gas were tested. The first was to discharge the evaporated LN2 towards the cutting edge of the tool (design 1), and the second was to discharge the evaporated LN2 away from the work piece (design 2). To apply the LN2 to the mounting surface of the cutting insert, a counter bored hole with a diameter of 10 mm and 4 mm deep was made in the surface of the tool holder on which the insert is mounted. A small channel connects the counter bored hole with an intermediate liquid nitrogen holder within the tool holder, which is in turn connected to the LN2 tank by means of a hose. In these experiments the cutting insert used were SNMG 120408-26 carbide inserts on an ANSI 4340 work material.

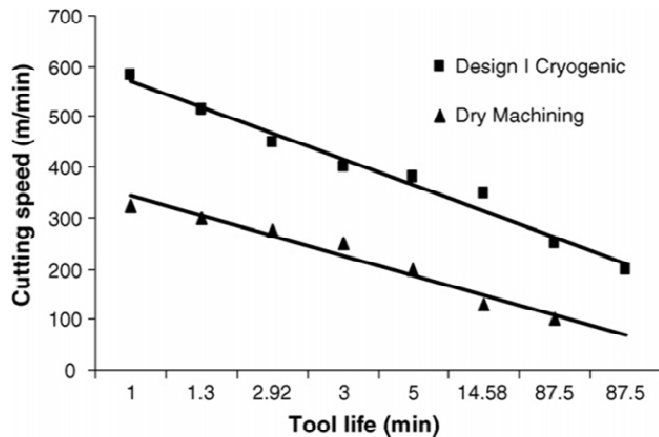


Figure 2 - Natural log-log graph of cutting speed vs. tool life [1]

When the evaporated LN2 is discharged towards the cutting edge of the insert, the tool life of the insert is 30 times longer than dry cutting, as can be seen in Figure 2. The surface finish is however worse than when machining dry. This is an indication that the work piece is being hardened by the evaporating LN2. The wear on the insert when using the design 2 is considerably less. It was measured that after only 3 minutes of machining, the insert from design 1 was worn 13 times more than the insert from design 2. These results can be seen in Figure 3. The surface finish of the work piece after being machined with the second configuration was found to be significantly better [1].

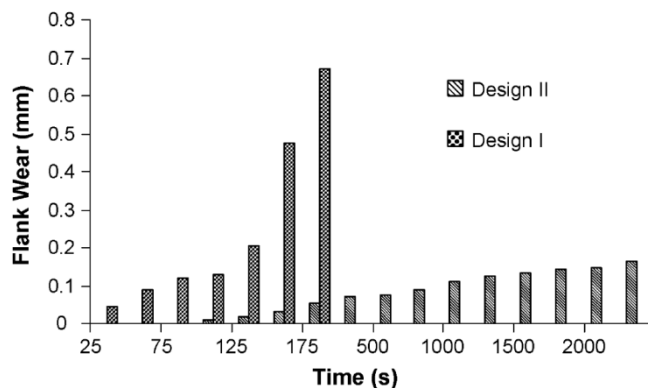


Figure 3 - Flank wear vs. time for cutting speed of 450m/min [1]

2.4. Closed loop LN2 jacket cooling

Wang and Rajurkar attempted to cool the cutting insert by designing a tool cap that circulates LN2 on the surface of the cutting insert while preventing the LN2 to come into contact with the work piece. The tool cap is secured to the tool holder by means of Allen screws. The inlet and outlet for the LN2 is located on the top surface of the tool cap, with the inlet close to the cutting edge. The flow of LN2 is controlled by the LN2 supply cylinder outlet valve and a valve connected to the outlet of the tool cap. The tool cap is located about 5 mm from the tool tip to ensure that the tool cap will not interfere with the machining process.

The experiments were conducted at a cutting speed of 132 m/min, a 1 mm depth of cut and a feed rate of 0.2 mm/rev. To be able to compare results, the cutting operation was done using soluble oil cooling and LN2 cooling. Tool wear was measured at 1.1 mm on the flank after 46 mm of machining with soluble oil, while the tool wear when machining with LN2 was measured at only 0.22 mm. The result is that if LN2 cooling is used, the tool can machine 112 mm before the same amount of wear is recorded compared to when soluble oil cooling is used. This represents a 143% improvement in tool life. It has also been noted that

there was no significant change in cutting forces when machining, indicating that the improvement of tool life is due to the hardness of the tool being maintained and the reduction of the chemical reactivity. The work surface finish of the machined work piece was also examined, and the results are highly significant. The roughness after machining 40 mm with soluble oil cooling was $15\ \mu\text{m}$, while LN2 cooling resulted in a roughness of only $1.9\ \mu\text{m}$ after 108 mm of machining. It can thus be concluded that the use of LN2 cooling by means of this tool cap improves cutting temperatures of the insert resulting in longer tool life and surface finish [6]. Figure 4 shows the tool wear with and without LN2 cooling.

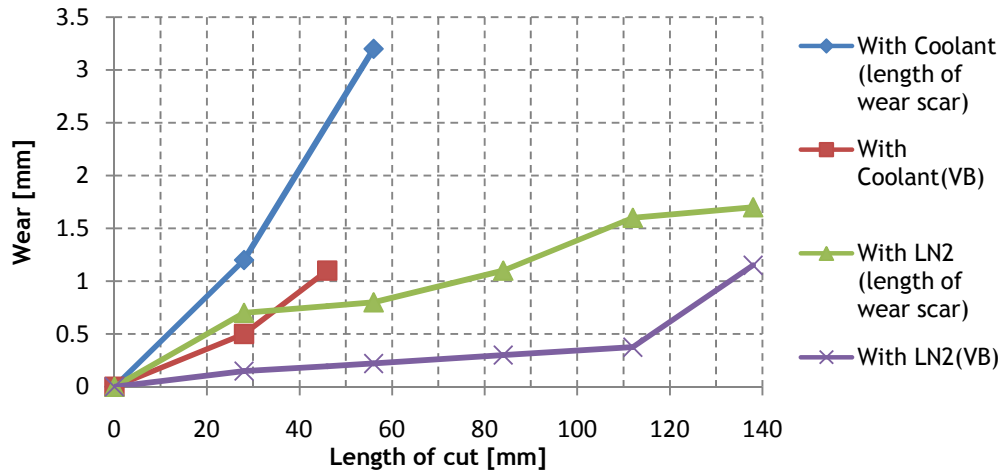


Figure 4 - Tool wear when machining Ti-6Al-4V [6]

2.5. Cooling by means of modified chip breaker

Hong et al. approached the problem by modifying a chip breaker that directs the LN2 to the cutting edge, as can be seen in Figure 5 [4]. The chip breaker lifts the titanium chip so that the LN2 can be forced between the rake face and the chip to penetrate closer to the chip-tool interface. To deliver the LN2 to the cutting zone, channels are etched out on the lower surface of the chip breaker. These channels are directed at the cutting edge where most of the heat is generated. The jets are formed when the chip breaker seals on the cutting insert. An auxiliary jet was added to deliver LN2 to the flank face. A design of the complete cryogenic cooling system can be seen in Figure 6 and Figure 7. The insert that was used for the tests was a CNMA432-K68 manufactured by Kennametal, a carbide insert recommended for titanium machining. For the experiment, the depth of cut was set to 1.27 mm and the feed at 0.254 mm/rev. The cutting speeds for the tests performed were set at 60, 90, 120 and 150 m/s.

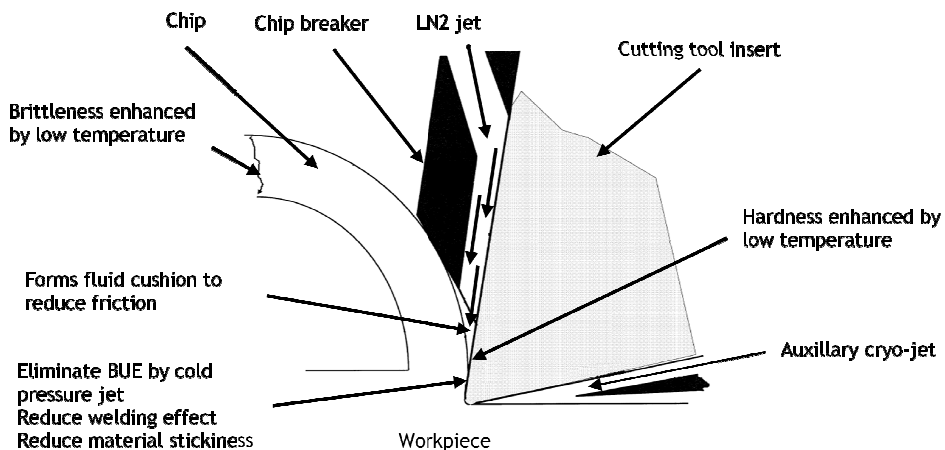


Figure 5 - Schematic drawing of design [4]

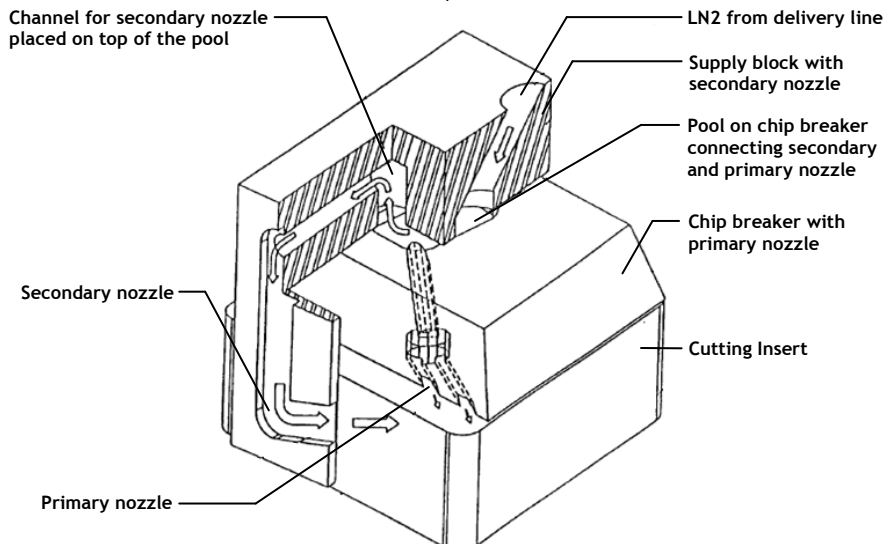


Figure 6 - Design of cryogenic nozzle: Auxiliary nozzle active [4]

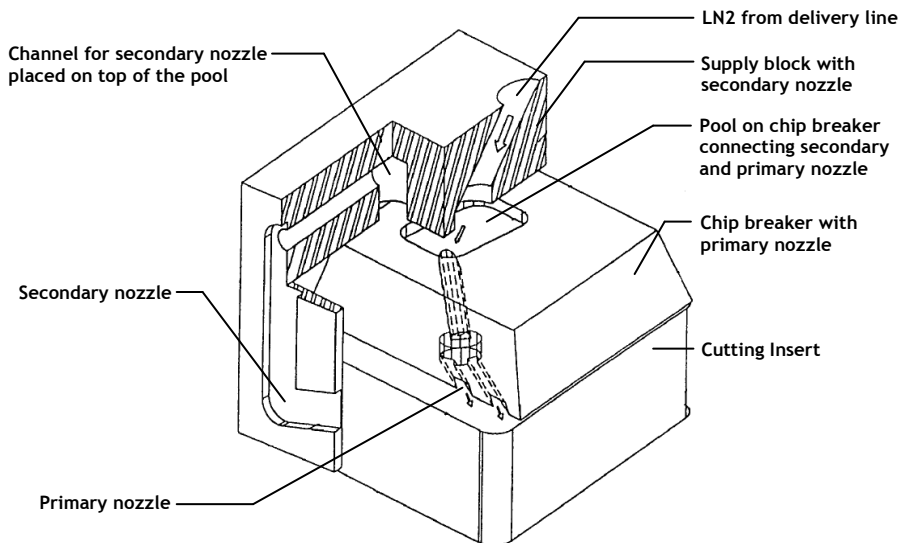


Figure 7 - Design of cryogenic nozzle: Auxiliary nozzle inactive [4]

To establish a baseline, Hong et al. performed their own conventional emulsion cooling test. The results they reported represented a longer tool life than other results found in literature. These results are believed to be state-of-the-art by machining specialists and can be found in Table 1. A variety of cooling configurations using the new generation cooling methods were tested. The following configurations were included in the experiments. Configuration 1 consisted of only a rake face nozzle (primary nozzle). Configuration 2 comprised of the flank face nozzle (secondary nozzle) only. Configuration 3 is defined by using both the primary and secondary nozzles. Another two variables that were tested are the angle of the chip breaker relative to the cutting edge (λ) as well as the distance it is placed from the edge (l) Figure 8. These variables influence the effectiveness of the cooling, and it was found that the best configuration was a λ of 15 degrees and an l of 1.25 mm. It was also noted that if the chip breaker was 1.00 mm or closer to the edge, the primary nozzle tended to block. The tool life using this method was found to be 8 min 51 sec at a cutting speed of 90 m/min, which is a 79% improvement over their conventional emulsion cooling [4].

Cooling Method	Cutting Speed [m/min]			
	60	90	120	150
Conventional Emulsion	1050 s	290 s	158 s	56 s
Primary nozzle ONLY	N/A	547 s	N/A	N/A
Primary and secondary nozzle	1653 s	948 s	437 s	296 s
Percentage improvement over Conventional emulsion				
Primary nozzle ONLY	N/A	89%	N/A	N/A
Primary and secondary nozzle	57%	227%	177%	429%

Table 1 - Experimental results and comparison [4]

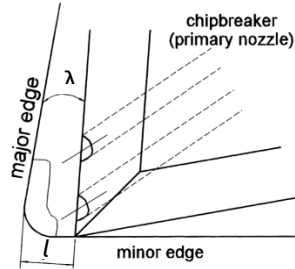


Figure 8 - Chip breaker position [4]

3. EXPERIMENTAL RESULTS

The results in Table 2 have been compiled from literature sources in the field. Because of discrepancies in the wear criterion that was used, not all data is directly comparable.

Method	Author ref.	Cutting speed [m/min]	Feed [mm/rev]	Depth of cut [mm]	MRR [mm ³ /s]	Tool life [sec]	Material removed [mm ³]
Conventional emulsion	[4]	60	0.254	1.27	323	1050	338709
Conventional emulsion	[4]	90	0.254	1.27	484	290	140322
Conventional emulsion	[4]	120	0.254	1.27	645	158	101935
Conventional emulsion	[4]	150	0.254	1.27	806	56	45161
Conventional emulsion	[4]	132	0.2	1.00	440	46 mm	
High pressure LN2 jets	[5]	70	0.2	2.00	467	1440	672000
Closed loop LN2 jacket	[6]	132	0.2	1.00	440	112 mm	
Modified chip breaker	[4]	60	0.254	1.27	323	1653	533225
Modified chip breaker	[4]	90	0.254	1.27	484	948	458709
Modified chip breaker	[4]	120	0.254	1.27	645	437	281935
Modified chip breaker	[4]	150	0.254	1.27	806	296	238709

Table 2 – Comparison of LN2 cooling of Ti-6Al-4V machining with conventional emulsion cooling

In Table 2 the performance of LN2 cooling is reported by displaying the tool life in terms of total material removed as well as in terms of total machining time. The influence of cutting speed, feed, depth of cut as well as material removal rate (MRR) on the tool life achieved is tabled.

The results in Table 2 are shown graphically as follows.

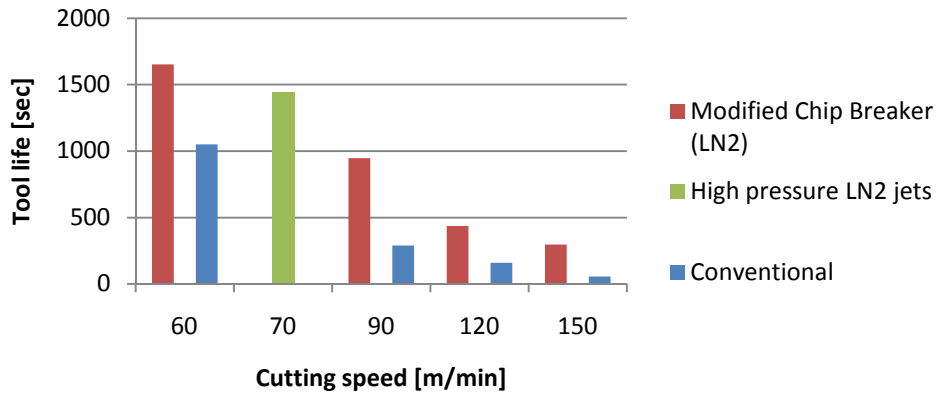


Figure 9 - Tool life expressed as time of investigated cooling methods for different cutting speeds

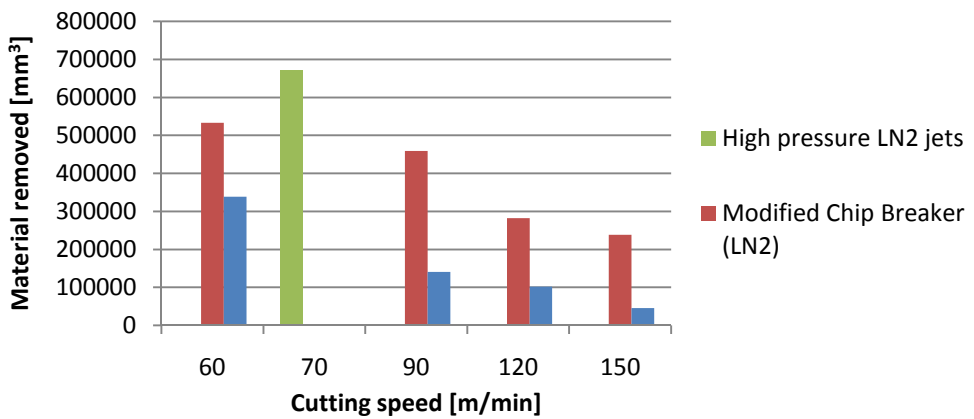


Figure 10 – Tool life in terms of material removed for LN2, compared to conventional cooling

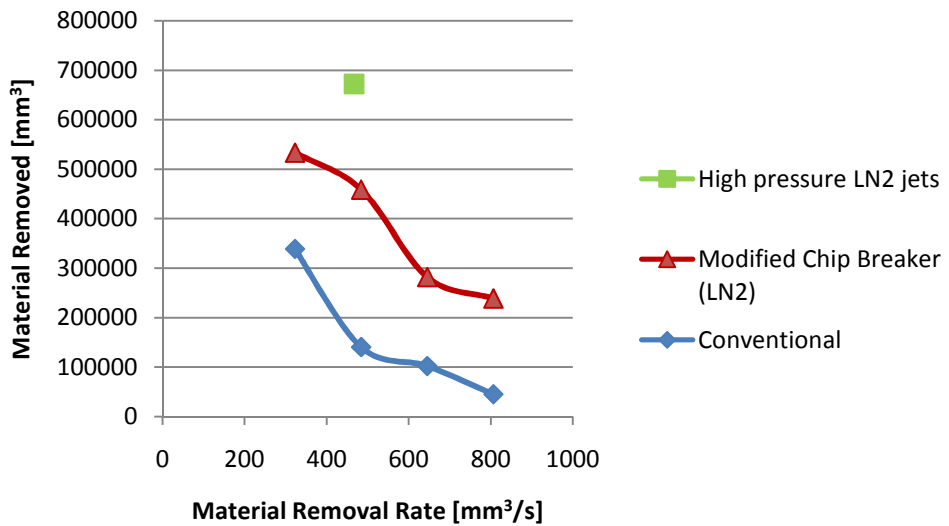


Figure 11 - Tool life in terms of material removed for different rates of material removal

From the graphs it is evident that LN2 cooling consistently yields an improvement in tool life. The tool life is improved regardless of whether tool life is measured in time units or in total volume of material removed per tool. The results show an expected correlation of tool life with cutting speed.

4. CONCLUSION

Authors in the field are unanimous that the high hot strength, low thermal conductivity as well as the high temperature chemical reactivity of titanium requires special machining techniques for high performance.

The softening of titanium at elevated temperatures is a desirable condition for machining. However, the tool requires intensive cooling. To achieve this, a small group of researchers investigated liquid nitrogen (LN2) as cooling medium for its superb penetration of the tool-chip interface, low temperatures and environmental friendliness.

The use of high pressure LN2 jets has shown a 71% improvement on emulsion cooling at cutting speeds of 70 m/min, but as cutting speeds were increased, the tool life decreased. By modifying a tool holder, Ahmed et al. [1] report improvements in tool life of more than 30 times compared to dry cutting. However, most of the cutting parameters are not available. The data is furthermore not directly comparable to the other methods, especially in the light of dry cutting being the control for these experiments.

The use of a closed loop LN2 jacket was proven to be prominently successful yielding a 143% improvement in tool life at high cutting speeds (132 m/min) as well as improving the surface finish of the work piece. The modified chip breaker has also yielded extraordinary results, improving tool life as much as 429% at high cutting speeds (150 m/min), while performing less impressive at lower cutting speeds (177% at 120 m/min).

It can thus be concluded that the closed loop LN2 jacket as well as the modified chip breaker methods were proved to be the most promising of the methods reviewed, especially for the ultimate goal of higher productivity.

5. REFERENCES

- [1] Ahmed, MI; Ismail, AI; Abakr, YA; Nurul Amin, AKM. 2007. Effectiveness of cryogenic machining with modified tool holder, *Journal of materials processing technology*, 185, pp 91-96
- [2] Corduan, N; Himbert, T; Poulachon, G; Dessoly, M; Lambertin, M; Vigneau, J; Payoux, B. 2003. Wear mechanisms of new tool materials for Ti-6Al-4V, *CIRP Annals - Manufacturing Technology*, 52(1), pp 73-76
- [3] Ezugwu, EO; Wang, ZM. 1997. Titanium alloys and their machinability - a review, *Journal of materials processing technology*, 68, pp 262-274
- [4] Hong, SY; Markus, I; Jeong, W. 2001. New cooling approach and tool life improvement in cryogenic machining of titanium alloy Ti-6Al-4V, *International journal of machine tools & manufacture*, 41, pp 2245-2260
- [5] Venugopal, KA; Paul, S; Chattopadhyay, AB. 2007. Growth of tool wear in turning of Ti-6Al-4V alloy under cryogenic cooling, *WEAR*, 262, pp 1071-1078
- [6] Wang, ZY; Rajurkar, KP. 2000. Cryogenic machining of hard-to-cut materials, *WEAR*, 239, pp 168-175
- [7] Yildiz, Y; Nalbant, M. 2008. A review of cryogenic cooling in machining processes, *International journal of machine tools & manufacture*, 48, pp 947-964

Appendix 6:

International conference article:

**Investigating novel cooling methods for titanium
machining**



Investigating novel cooling methods for titanium machining

D. Koen¹, E.J. Herselman¹ G.A. Oosthuizen¹ N.F. Treurnicht¹

¹Department of Industrial Engineering, Stellenbosch University, South Africa

Abstract

Cooling of titanium machining is a major area where the process can be improved. This research reviews novel localised insert cooling using liquid nitrogen (LN2). This could unlock the potential of machining titanium in the thermally softened condition. Several techniques are quantitatively compared and the most promising ones identified. Additionally, gaseous cooling is experimentally investigated to address surface wetting constraints and the reduction of thermal shock. The results show that the configuration tested where emulsion coolant is mixed into a high pressure air stream yields improvements worthwhile of further development.

Keywords

Titanium alloy, Liquid Nitrogen, Gaseous cooling

1 INTRODUCTION

Titanium's high temperature strength and low thermal conductivity cause large amounts of heat to be concentrated in the cutting zone [1]. The thermal conductivity of the cutting insert (100 W/mK for H13A tungsten carbide) is usually much higher than for titanium (7 W/mK), resulting in about 80% of the heat generated being transferred to the cutting insert, more specifically to the cutting edge region [1,2]. The cost of cooling fluids is a major expenditure for any machining operation, amounting to more than 15% as shown in Fig 1.

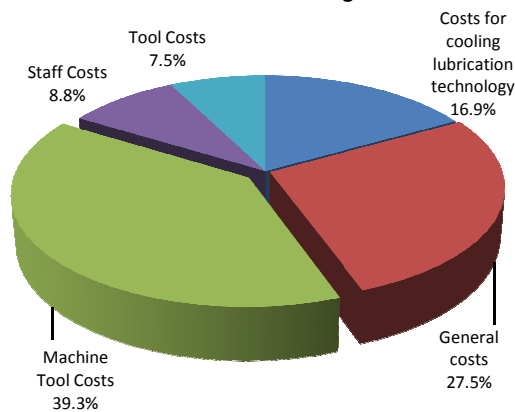


Figure 1 - German car manufacturer's crankshaft manufacturing cost breakdown (adapted from [3])

In order to improve titanium machining, the thermal softening [4] behaviour of titanium at elevated temperatures can be harnessed. For this strategy it is necessary to retain as much of the heat that is generated during the machining process in the work piece. The most practical manner to achieve this objective is to actively cool the insert, while preventing a cooling effect of the work piece. With this strategy in mind, a small group of researchers are investigating novel cooling concepts. For this purpose, liquid nitrogen (LN2) is used. An investigation of this strategy, referred to as local

insert cooling [5,6] is the first objective for this work. Unless otherwise specified, all reviewed article experiments used Ti-6Al-4V work material. In this work, the second objective is to investigate coolant media with better penetration capabilities at high tool temperatures and a reduced tendency to cause thermal cracking. Increasing cooling power with water based coolants yields diminishing returns due to delayed surface wetting constraints and thermal cracking at high tool temperatures [7]. An experimental investigation was done using gaseous cooling.

2 LOCAL INSERT COOLING WITH LN2

2.1 Cutting fluids and cryogenic cooling

Environmental and health problems are also a reality with conventional cooling. Environmental pollution includes the pollution of water and contamination of soil when the cutting fluid is ultimately disposed of. Health problems include dermatological ailments when operators are exposed to fumes and physical contact with the cutting fluid [8]. LN2 is abundantly available considering that the earth's atmosphere is composed of 78% of nitrogen. In addition to this LN2 is colourless, odourless, tasteless and non-toxic.

2.2 High pressure liquid nitrogen (LN2) jets

Venugopal et al [9] designed a high pressure jet system that sprays LN2 onto the rake and flank face of the carbide insert. A continuous flow of LN2 was supplied while taking care not to overcool the work piece. The cutting parameters are shown in Table 1 and the experimental set-up is illustrated in Fig. 2.

Parameter	Value
Depth of cut	2 mm
Feed	0.2 mm/rev
Cutting Speed	70, 100, 117 m/min

Table 1 - Cutting parameters for LN2 jets [9]

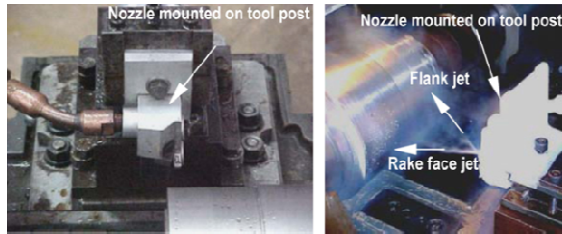


Figure 2 - Liquid nitrogen delivery set-up [9]

The result yields large improvements in the tool life. Tool life with the LN2 jet cooling improved 71% compared to flood cooling, and 243% compared to dry machining. The tool life improvements at relative higher cutting speeds were substantial although the effectiveness of the cooling deteriorated. This is attributed to the decreased ability of the LN2 to penetrate the tool-chip interface and effectively extract the excessive heat generated at the higher cutting speeds. Wear mechanisms that were observed are crater wear, flaking on the edge of the crater, plastic deformation, micro and macro cracks on the cutting edge and abrasive flank wear [9].

2.3 LN2 cooling using a modified tool holder

This cooling technique involves the cooling of the mounting surface of the cutting insert by means of LN2. Ahmed et al [5] tested two different configurations of gas discharge. In the first the gas discharges towards the cutting zone (design 1) and in the second the LN2 gas discharges away from the work piece. The LN2 is fed from a reservoir in the tool holder to a cavity below the insert. The reservoir is hose fed from the LN2 tank. In these experiments, carbide inserts were used on an ANSI 4340 work material. In the case of the evaporated gas being discharged towards the cutting zone (design 1), tool life of the insert is 30 times the life for dry cutting, as can be seen in Fig. 3. The surface finish attained is however inferior to that of dry cutting. It indicates that work hardening occurs just before cutting. In the second configuration (design 2) tool wear is markedly lower. When measuring the tool wear after only 3 minutes of machining, as shown in Fig 4, the insert used in design 1 was worn 13 times more than the insert used in design 2. The results are depicted in Fig. 4. The surface finish achieved with design 2 was significantly better [5].

2.4 Closed loop LN2 jacket cooling

This configuration is where LN2 is circulated through an enclosed cavity over the insert, while at the same time preventing exposure of the work piece to the LN2 [1]. There is a separate inlet and outlet for the LN2 to facilitate circulation and exhaust of gas phase nitrogen.

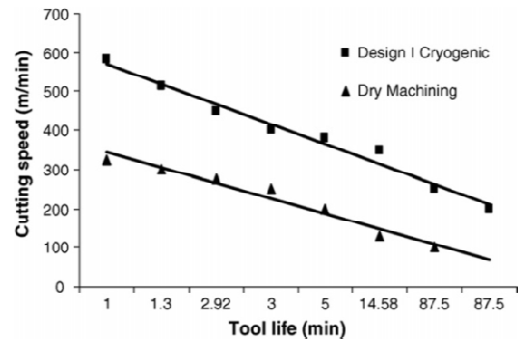


Figure 3 - Natural log-log graph of cutting speed vs. tool life [5]

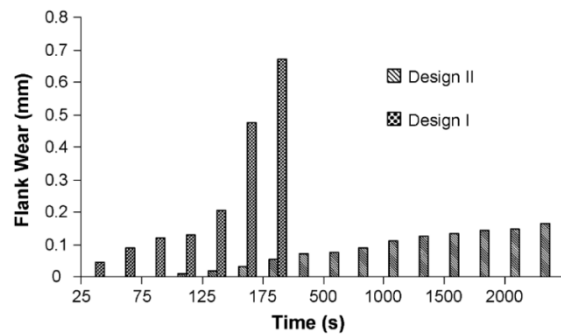


Figure 4 - Flank wear vs. time for cutting speed of 450m/min [5]

A cutting speed of 132 m/min, a 1 mm depth of cut and a feed rate of 0.2 mm/rev was used, with conventional flood cooling as the control treatment. Flank wear amounted to 1.1 mm after 46 mm of machining with flood cooling, while with LN2 it amounted to only 0.22 mm. Further experimentation showed that for the same wear criterion, LN2 machined 112mm in the axial direction. Compared to 20mm for flood cooling this represents a 460% improvement in tool life. Cutting forces remained constant indicating retention of tool hardness. The LN2 treatment resulted in surface finish improvement as well. The conclusion is therefore derived that closed loop LN2 cooling improves tool life and surface finish by means of controlled insert surface temperatures as shown in Fig. 5.

2.5 Cooling by means of modified chip breaker

Hong et al [6] formed two directional jets by etching out channels on the cutting tool surface of a chip breaker, forming jets when it is mounted on the carbide cutting insert. These channels direct the LN2 at the cutting edge, as shown in Fig. 6. The titanium is lifted from the insert by the chip breaker which improves the LN2 penetration of the chip-tool interface. An auxiliary jet was added to deliver LN2 to the flank face. The complete cryogenic cooling system is illustrated in Fig.7 and the cutting parameters are listed in Table 2.

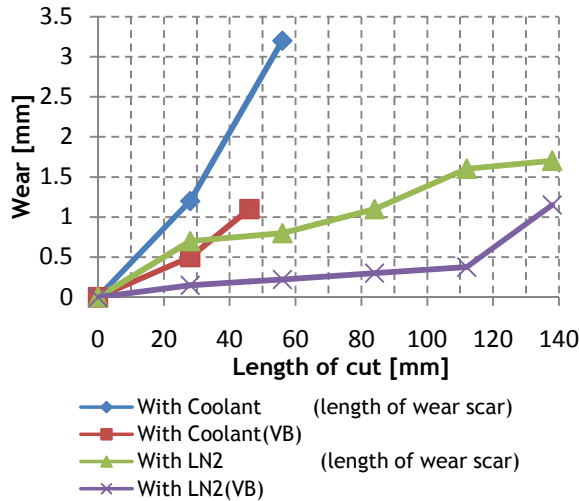


Figure 5 - Tool wear when machining Ti6Al4V [1]

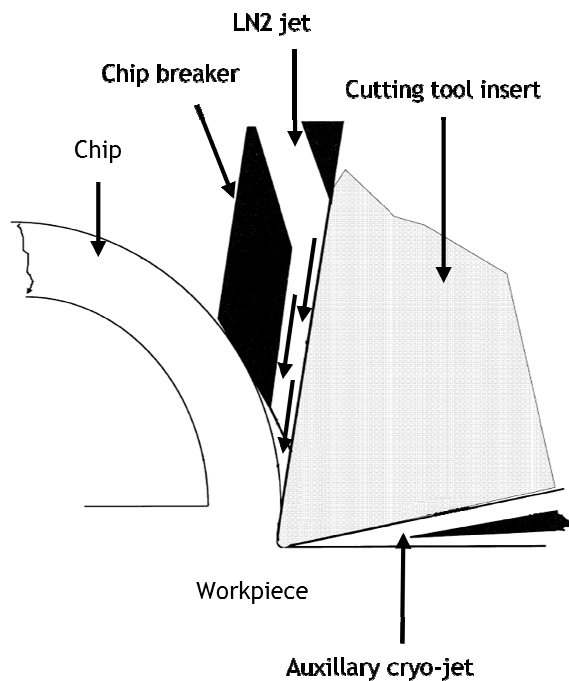


Figure 6 - Modified chip breaker design [6]

Hong et al [6] performed experiments with flood cooling to establish a benchmark. Their findings are shown in Table 3 and are believed to be state-of-the-art by machining specialists. The best position for the chip breaker was determined by trial and error using two variables; the distance (l) from and angle (λ) relative to the cutting edge. A sketch showing these variables is shown in Fig. 8. The optimal values for the values was found to be $\lambda=15^\circ$ and $l=1.25\text{mm}$ [6].

Parameter	Value
Depth of cut	1.27 mm
Feed	0.254 mm/rev
Cutting speed	60, 90, 120, 150 m/min

Table 2 - Modified chip breaker parameters [6]

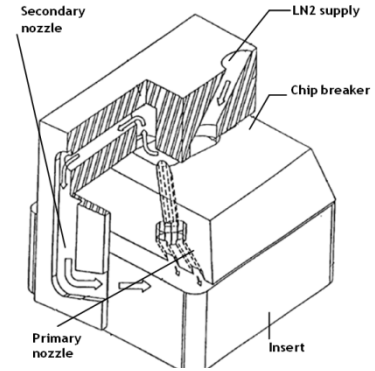


Figure 7 - Design of cryogenic nozzle: Auxiliary nozzle active [6]

Cooling Method	Cutting Speed [m/min]			
	60	90	120	150
Conventional Emulsion	1050 s	290 s	158 s	56 s
Primary nozzle ONLY	N/A	547 s	N/A	N/A
Prim. and sec. nozzle	1653 s	948 s	437 s	296 s
Percentage improvement over Conventional emulsion				
Primary nozzle ONLY	N/A	89%	N/A	N/A
Prim. and sec. nozzle	57%	227%	177%	429%

Table 3 - Tool life and improvements for different cutting conditions [6]

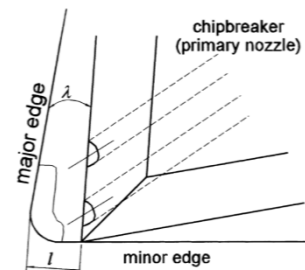


Figure 8 - Chip breaker position [6]

3 GASEOUS LUBRICATION

3.1 Thermal shock

Thermal shock commonly occurs as the predominant failure mechanism when carbide cutting tools are used. Thermal cracking can be defined as the propagation of cracks on the surface of the cutting tool as a result of rapid temperature fluctuations [10]. In the case of interrupted cutting, as experienced in milling, the cutting edges go through a cyclic heating and cooling process as they move in and out of the cut. When cutting speed is increased, the heat load and temperature of the cutting tool is increased. If this is compensated for by means of higher power cooling or an increased stream of coolant, thermal shock becomes predominant. The cracking is believed to lead to thermal fracture, and occurs when the tool exits the work material rather than on entry [11]. Fig. 9 illustrates thermal cracks caused by thermal shock.

Wang et al [1] proposes that thermal crack development is divided into four stages as listed below:

1. Period of comb-type crack development
2. Period of transverse crack development
3. Period of crack crossing
4. Tool fracture

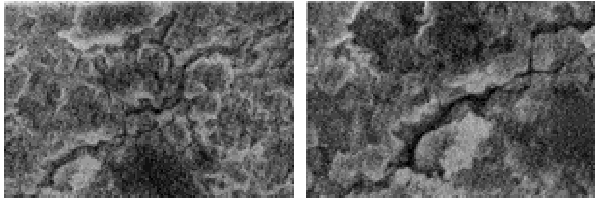


Figure 9 - Thermal cracks caused by thermal shock [11]

3.2 Delayed surface wetting

When machining titanium, temperatures as high as 900°C have been measured at a cutting speed of 75 m/min [12]. At such high tool temperatures, the coolant vaporises on tool contact and creates a vapour layer on the surface of the tool. This creates an insulation boundary layer that significantly reduces the heat dissipation of the tool. To quantify this, the heat transfer coefficient for water is reduced approximately ten times between 380°C to 830 °C. This phenomenon occurs when a two phase coolant such as water is used, also being referred to as coolant jet impingement. With titanium machining cooling is extremely important and this often results in premature tool failure [7].

3.3 Experimental method

In order to simulate milling, a face turning operation was executed on a round bar Ti6Al4V (Grade 5), with a diameter of 56.5mm. The slotted work piece, which was fitted on a CNC lathe, is illustrated in Fig. 10.

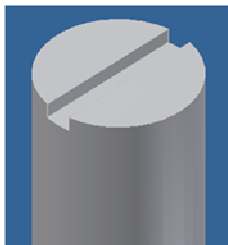


Figure 10 - Configuration of interrupted cut test piece

The programming option to keep cutting speed constant was utilised during the test. The cutting parameters are given in Table 4. An Olympus GX51 inverted optical microscope was used for the analysis.

Parameter	Value
Depth of cut [mm]	1 mm
Feed [mm/rev]	0.1 mm/rev
Cutting speed [m/min]	50, 60, 70, 80, 90, 100
Cutting distance [m]	96

Table 4 - Cutting parameters

In order to reduce thermal shock and at the same time improve the cooling of high temperature cutting tool surfaces, gaseous cooling was employed. A mixer unit using the Venturi principle was used for the experiment. The design principle can be seen in Fig. 11.

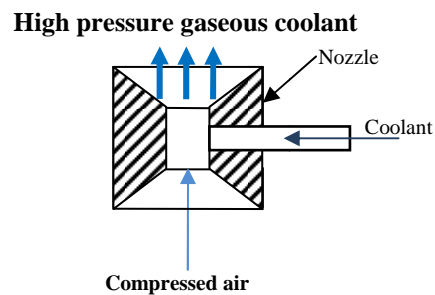


Figure 11 - Venturi principle used in mixer nozzle

The mixer nozzle was tested to deliver 75 litres/hour of emulsion coolant in a 7 bar air stream.

4 EXPERIMENTAL RESULTS

4.1 Local Insert cooling with LN2

Fig. 12 and 13 represent a compilation of the literature sources reviewed [1,2,5,6,9,13]. Because of differences of how wear criteria were reported, data is not identical but adequately comparable. In Fig. 12 the performance of the cooling method is reported by expressing tool life as total material removed, incorporating cutting speed, feed and depth of cut. Fig. 13 shows the tool life against the material removal rate. This shows the productivity of the cooling method. The ideal solution would be situated in the second quadrant. Fig. 12 and Fig. 13 show that LN2 cooling constantly results in improved tool life. The trend reported throughout literature stating that tool life is highly dependent on cutting speed remains applicable.

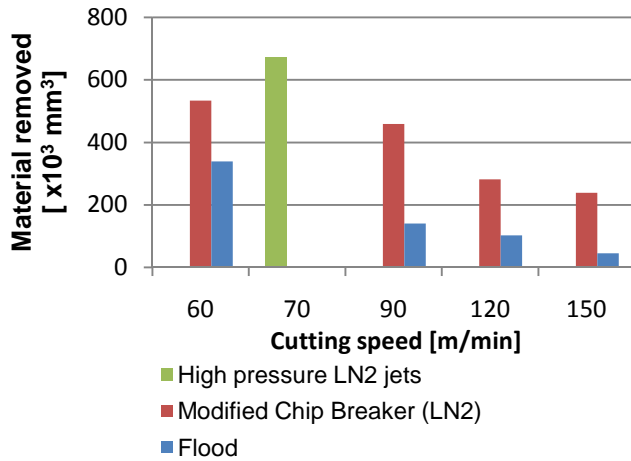


Figure 12 - Tool life in terms of material removed for LN2, compared to conventional cooling

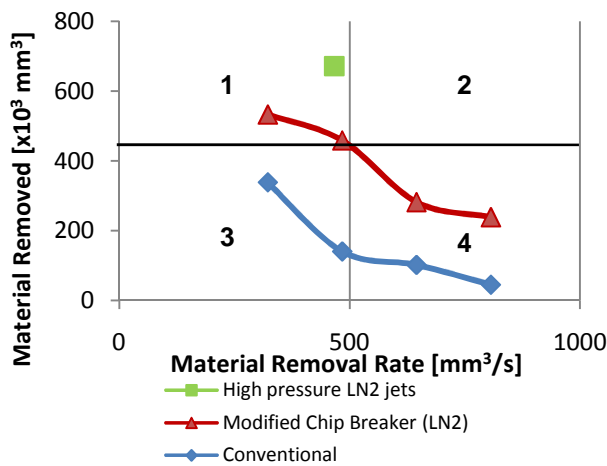


Figure 13 - Tool life in terms of material removed for different rates of material removal

4.2 Gaseous cooling

Several pilot test runs were made where the tool failed as a result of mechanical shock before thermal cracks could be identified. Judicious adjustments of cutting parameters were necessary to identify the cracks in the first two stages of development according to Wang et al [11]. Flood cooling at 50 m/min as shown in Fig. 14(a) clearly shows comb type crack initiation while gaseous cooling (Fig. 14(b)) displays a rake face without cracks.

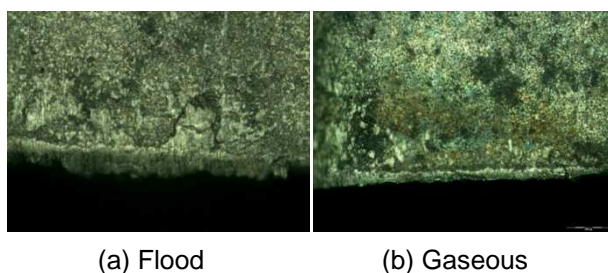
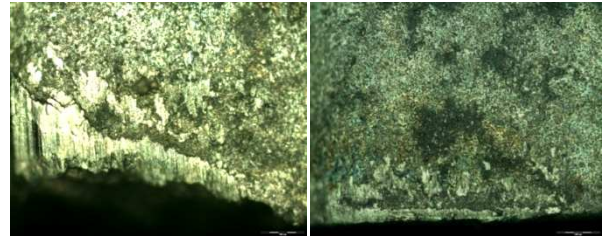


Figure 14 - Cutting speed of 50 m/min (200x)

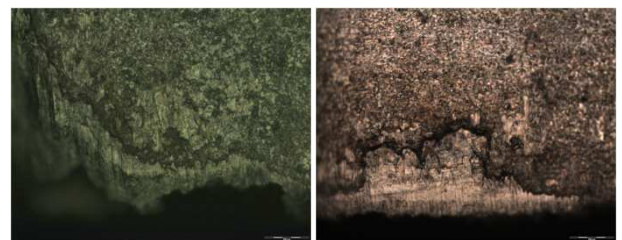
Additionally the cutting edge of the flood cooling already suffers from chipping while the gaseous cooling's cutting edge is intact. As illustrated in Fig. 15, at 60 m/min the flood cooled test specimen has moved through all four stages of thermal cracking with the cutting edge being broken away through transverse cracking.



(a) Flood (b) Gaseous

Figure 15 - Cutting Speed of 60 m/min (200x)

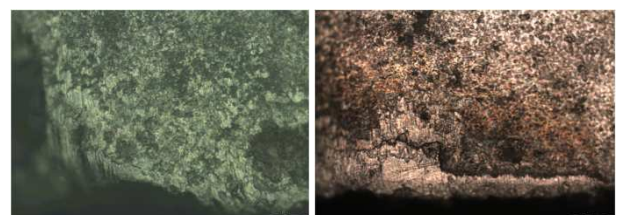
Again the gaseous cooled test specimen does not show any thermal cracking. Fig. 16 clearly shows that the flood cooled specimen has suffered severe tool edge failure; whereas the gaseous cooled specimen's cutting edge is relatively intact.



(a) Flood (b) Gaseous

Figure 16 - Cutting speed of 80 m/min (200x)

Also, as illustrated in Fig. 17, at 100m/min the flood cooled specimen shows a severely compromised cutting edge. The gaseous cooled specimen's cutting edge is intact with early signs of thermal cracking.



(a) Flood (b) Gaseous

Figure 17 - Cutting speed of 100m/min (200x)

5 CONCLUSIONS

The softening of titanium at elevated temperatures is a desirable condition for machining, given that the tool is sufficiently cooled. Therefore this investigation using LN2 to locally cool the insert was undertaken. All the reviewed methods show significant tool life improvements with the use of LN2. The most promising methods were the closed loop LN2 jacket and the modified chip breaker

respectively yielding a 460% improvement at 132 m/min and 177% at 120 m/min.

The gaseous cooling experimentation succeeded to illustrate a significant difference between inserts cooled with flood cooling and gaseous cooling. Comb and transverse type thermal cracks were observed at cutting speeds of 40 and 50 m/min when using flood cooling. Cutting edge fractures could be observed at higher speeds which are known to be the fourth stage of Wang's classification. In contrast gaseous cooling only exhibited signs of thermal cracks at cutting speeds higher than 70 m/min. From these experiments it could therefore be concluded that gaseous cooling is a promising technology to reduce tool failure due to thermal shock induced cracking.

6 REFERENCES

- [1.] Wang ZY, Rajurkar KP. Cryogenic machining of hard-to-cut materials. *WEAR*. 2000; 239: p. 168-175.
- [2.] Ezugwu EO, Wang ZM. Titanium alloys and their machinability - a review. *Journal of Mat. Proc. Tech.* 1997; 68: p. 262-274.
- [3.] Brinksmeier E, Walter A, Janssen R, Diersen P. Aspects of cooling lubrication reduction in machining advanced materials. In *Proceedings of Institution of mechanical engineers*; 1999. p. 769-778.
- [4.] Komanduri R, Hou ZB. On thermoplastic shear instability in the machining of a titanium alloy (Ti-6Al-4V). *Metallurgical and Materials Transactions*. 2002; 33(9): p. 2995-2301.
- [5.] Ahmed MI, Ismail AI, Abakr YA, Nurul Amin AKM. Effectiveness of cryogenic machining with modified tool holder. *Journal of Materials Processing Technology*. 2007; 185: p. 91-96.
- [6.] Hong SY, Markus I, Jeong Wc. New cooling approach and tool life improvement in cryogenic machining of titanium alloy Ti-6Al-4V. *International Journal of Machine Tools & Manufacture*. 2001; 41: p. 2245 - 2260.
- [7.] Barnett-Ritcey DD, Elbestawi MA. Tool performance in high speed finish milling of Ti6Al4V. In *Proceedings of IMECE'02*; 2002. p. 1-9.
- [8.] Yildiz Y, Nalbant M. A review of cryogenic cooling in machining processes. *International Journal of Machine Tools & Manufacture*. 2008; 48: p. 947-964.
- [9.] Venugopal KA, Paul S, Chattopadhyay AB. Growth of tool wear in turning of Ti-6Al-4V under cryogenic cooling. *WEAR*. 2007; 262: p. 1071-1078.
- [10.] Mai YW. Thermal shock resistance and fracture-strength behaviour of two tool carbides. *Journal of the American Ceramic*

Society. 1976; 59: p. 11-12.

- [11.] Wang ZY, Sahay C, Rajurkar KP. Tool temperatures and crack development in milling cutters. *Int. journal for machining tools manufacturing*. 1996; 36(1): p. 129 - 140.
- [12.] Dearnley P, AN G. Evaluation of principal wear mechanisms of cemented carbides and ceramics used for machining Titanium alloy IMI318. *Materials Science and Technology*. 1986; 2(1): p. 47-58.
- [13.] Corduan N, Himbert T, Poulachon G, Dessoly M, Lambertin M, Vigneau J, et al. Wear mechanisms of new tool materials for Ti-6Al-4V high performance machining. *CIRP Annals - Manufacturing Technology*. Unknown; 52(1): p. 73-76.

7 BIOGRAPHY



Devan Koen completed his final year research project in the field of manufacturing for his BEng (Industrial) at Stellenbosch University. Currently he is doing research towards his MScEng as a member of the Titanium Machining Research Group.



Gert Adriaan Oosthuizen holds a MSc.Eng degree in Industrial Engineering from the University of Stellenbosch. He is currently pursuing a PhD in titanium machining and a member of the Titanium Machining Research Group.



Emile Herselman completed his final year research project in the field of machining titanium alloys. Currently he is doing research towards his MScEng in wear characterization of titanium alloys and carbides.



Nico Treurnicht leads the Titanium Machining Research Group. He is member of the steering committee of the AMTS titanium machining research project. He is a full time lecturer and working towards his PhD in titanium machining.